For Reference

NOT TO BE TAKEN FROM THIS ROOM

For Reference

NOT TO BE TAKEN FROM THIS ROOM

Ex libris
universitatis
albertaensis

University of Alberta
Printing Department

Digitized by the Internet Archive
in 2019 with funding from
University of Alberta Libraries

https://archive.org/details/effectofmagnetic00doug

Thesis
1964
#5D

THE UNIVERSITY OF ALBERTA

THE EFFECT OF A MAGNETIC FIELD ON INTERDIFFUSION IN DILUTE ALUMINUM-COPPER SOLID SOLUTIONS

A Thesis

Submitted to the Faculty of Graduate Studies
In Partial Fulfilment of the Requirements
for the Degree of Doctor of Philosophy

DEPARTMENT OF MINING AND METALLURGY

by

DOUGLAS ROY COLTON

EDMONTON, ALBERTA

APRIL, 1964

UNIVERSITY OF ALBERTA

FACULTY OF GRADUATE STUDIES

The undersigned certify that they have read and recommend to the Faculty of Graduate Studies for acceptance, a thesis titled

THE EFFECT OF A MAGNETIC FIELD ON INTERDIFFUSION
IN DILUTE ALUMINUM-COPPER SOLID SOLUTIONS

submitted by DOUGLAS ROY COLTON

in partial fulfilment of the requirements for the degree of Doctor of Philosophy.

ABSTRACT

A study has been made of the interdiffusion of copper from an alpha-solid solution into aluminum in a magnetic field of 30,000 oersteds. Duplicate determinations were made without the magnetic field. The magnetic field applied perpendicular to the direction of diffusion has the effect of reducing the interdiffusion coefficient by 25 per cent compared to the no-field determinations. No effect was found for the field applied parallel to the direction of diffusion. A theory based on the plasma-magnetohydrodynamic properties of the alloy system is developed to explain the results. It is shown that the diffusivity is decreased in the field by a factor of $1/(1+\omega_{ce}^2/\nu_e^2)$ where ω_{ce} and ν_e are the cyclotron and collision frequencies respectively of the diffusion transported electrons. The plasma oscillation screening effect is discussed, and it is shown that the field does not significantly affect the charge screening. It is thus proposed that the diffusivity is decreased through the frequency factor D_o, and not through the activation energy of the jump process.

ACKNOWLEDGEMENTS

The author wishes to express his gratitude to Dr. W. V. Youdelis for his guidance and supervision during the course of this project. He is especially indebted to Dr. Youdelis for his contribution to the theory. The author is also indebted to Dr. J. G. Parr for his counsel and assistance, to Mr. J. R. Cahoon, M. Sc. for help in the construction of the electromagnet and to Professor E. O. Lilge for his considerate departmental supervision. To Mr. Joel Mercier for preparing the many figures and illustrations used in this thesis and to Mrs. F. Klein for her patience and perseverence in typing the manuscript, the author wishes to express his appreciation.

The financial assistance provided by the National Research Council is gratefully acknowledged.

TABLE OF CONTENTS

PAGE

INTRODUCTION 1

HISTORICAL REVIEW 4

- A. INTERDIFFUSION IN DILUTE ALUMINUM-COPPER SOLID SOLUTIONS 4
- B. THE MAGNETIC DIFFUSION EFFECT IN FERROMAGNETIC METALS AND ALLOYS 13
- C. ELECTRICAL ION TRANSPORT 22
- D. THE PLASMA CONCEPT OF A METAL 24

THEORY OF MAGNETIC EFFECTS 26

- A. MAGNETOHYDRODYNAMICS 27
- B. PLASMA DYNAMICS 29
- C. PLASMA OSCILLATIONS AND CHARGE SCREENING 35

EXPERIMENTAL METHODS 44

- A. THE MAGNET 44
- B. PREPARATION OF ALLOYS 44
- C. BONDING METHOD 46
- D. DIFFUSION ANNEALS 51
- E. MEASUREMENTS 59
  - 1. Direct Measurement of the Kirkendall Effect 59
  - 2. Microhardness Measurements 61

TREATMENT OF DATA 67

PAGE

RESULTS 73

DISCUSSION 96

A. DISCUSSION OF ERRORS 96

1. Measurement and Control of Temperature 96

2. Analysis by Microhardness Measurement 102

3. Inhomogeneity of Base Alloys 105

4. Bonding 106

5. Grain Boundary Diffusion 107

6. Computational Errors 107

B. DISCUSSION OF DIFFUSION RESULTS 108

SUMMARY AND CONCLUSIONS 118

BIBLIOGRAPHY 120

APPENDIX A Construction of the Electromagnet 125

APPENDIX B Analysis of Materials 131

LIST OF FIGURES

FIGURE PAGE

1. The magnetic diffusion effect in alpha-iron. 14
2. Mold and capsule assembly used for welding the flat and sandwich couples. 48
3. Mold and capsule assembly used for welding the cylindrical couples. 49
4. Furnace assembly used for the diffusion anneals. 53
5. Measuring thermocouple inserted in well drilled in sample. 57
6. Boltzmann-Matano method of calculating the diffusion coefficient. 71
7. Calibration curve. 74
8. Comparison of penetration curves for sandwich couple S-6 (no-field) and S-7 (field). 78
9. Comparison of penetration curves for cylindrical couples C-1 (field) and C-2 (no-field). 79
10. Comparison of probability plots for couples S-6 and S-7. 80
11. Comparison of probability plots for couples C-1 and C-2. 81
12. Variation of diffusion coefficient with concentration, couples S-6 and S-7 82
13. Matano area versus $(\text{time})^{1/2}$ 83
14. Variation of field and no-field interdiffusion coefficients with temperature 84

FIGURE PAGE

15. Comparison of previous data with the present no-field results. 109

16. Photomicrograph of a weld. 110

17. Photograph of a cylindrical and a flat couple. 110

18. Photograph of the electromagnet. 128

19. Diagram of the electromagnet yoke. 129

20. Field produced by the electromagnet. 130

LIST OF TABLES

TABLE PAGE

I. Summary of previous results on interdiffusion in dilute aluminum-copper solid solutions 12

II. Summary of present results. 75

III. Kirkendall shifts and dimensional changes. 85

IV. Concentration-distance data, couples C-1, C-2 F-1, F-2 86

V. Concentration-distance data, couples C-4, C-7 S-6, S-7 88

VI. Concentration-distance data, couples S-18, S-19, S-20, S-21 90

VII. Concentration-distance data, couples S-24, S-25 S-28, S-29 92

VIII. Concentration-distance data, couple S-32 94

INTRODUCTION

The transport properties of solids in magnetic fields have been extensively studied both theoretically and experimentally, and the results have provided valuable information on the electronic structure of the materials. The effects of the magnetic field arise principally through the Lorentz force exerted on the moving electrons which alters their steady state velocity distribution in any irreversible process. In the case where electron velocities are very high, approaching the Fermi velocity, the Lorentz force in a magnetic field of a few kilogauss will be much greater than the force exerted by any attainable electric field in the solid. Recently, magnetic fields have been applied to the study of the transport of ions in solids. In this work the presence of the magnetic field is of secondary importance in that it is applied in addition to an electric field only to produce the Hall potential, but it would appear vital to a correct interpretation of the latter results to establish the direct effects of the magnetic field alone on the transport properties of the ions.

In recent years a great deal of theoretical and experimental work has also been devoted to the study of plasmas and especially to the problem of diffusion of a plasma in a magnetic field. Control of experimental conditions in the study of plasma behavior in gas discharges is difficult due to the transient and unstable properties of the discharges.[1] Experiments in solids, which utilize the plasma properties of the electron gas, offer the opportunity to observe plasma behavior under more accurately

controlled conditions. Among the many successful experiments of this type are the demonstration of the plasma pinch effect in indium antimonide by Glicksman and Steele[2] and the production of whistler waves in sodium by Bowers.[3] The successful application of experiments in solids to the observation of these and other plasma properties suggests that the approach might also be useful in the study of diffusion of plasmas in a magnetic field.

The present study of the effect of a magnetic field on diffusion in solids is, however, the logical extension of a series of experiments much closer at hand. Studies on the effect of moderately strong magnetic fields on the solidification mechanisms of binary alloy systems by the author,[4] by J. R. Cahoon,[5] and by R. C. Dorward,[6] have established that the presence of the magnetic field appreciably alters the distribution of the solute in unidirectionally solidified ingots. A consideration of the various possible effects of the magnetic field suggested that the change in the solute distribution was effected by the field through inhibition of the diffusion process which accompanies alloy solidification. Accordingly, a study of solid diffusion in a moderately strong magnetic field was undertaken to test the diffusion inhibition hypothesis.

Interdiffusion in dilute aluminum-copper alloys was selected as the particular system to be investigated for several reasons. First among these was its relation to previous work; J. R. Cahoon[5] studied the effect of a magnetic field on the solidification mechanisms of

aluminum(rich)-copper alloys. In addition the solidification phenomena of aluminum(rich)-copper system have been extensively studied under normal (no-field) conditions and this has provided the information essential to the production of sound alloys of completely uniform composition. Also considered was the fact that a method of analysis of the concentration distribution in diffusion couples by microhardness testing had been established for the system by Buckle.[7] The method offered the advantages of reasonable accuracy, rapidity and availability.

HISTORICAL REVIEW

To the authors knowledge, there have been no previous direct investigations on the effect of a magnetic field on diffusion in metals. Therefore, any review of the subject must of necessity be confined to topics which, in their theoretical or experimental aspects, are related indirectly to the present work. The magnetic effects which will be considered are the magnetic diffusion effect in ferromagnetic metals and alloys and the effect of a magnetic field on electrical ion transport in metals. Plasmas will also be briefly discussed in relation to the plasma-like properties of the free electrons of a metal. But first, before entering a discussion of magnetic or plasma effects, consideration will be given to previous work done (in the absence of a magnetic field) on the particular system chosen for this investigation, that is, to a consideration of the experimental methods and the results of previous workers who have studied interdiffusion in dilute aluminum-copper solid solutions.

A. INTERDIFFUSION IN DILUTE ALUMINUM-COPPER SOLID SOLUTIONS

A study of diffusion of solute elements in aluminum is complicated by the tenacious oxide film present on the surface of the metal, and by the limited solid solubilities of the added elements. Accurate determinations of the rates of diffusion require as clean an interface as possible so that no barrier will exist to prevent the transfer of atoms. It is equally important to be able to carry out an accurate analysis for the

solute metal to obtain accurate concentration-penetration curves. In the following review of previous work on interdiffusion in dilute aluminum-copper alloys, an attempt will be made to assess the effectiveness of the bonding methods, and the accuracy and convenience of the analytical techniques employed by the previous workers.

The three common bonding methods which have been employed are plating, clamping, and rolling. Cournot and Perot[8] and also Grube and Haefner[9] studied diffusion in samples prepared by electroplating cylinders of pure aluminum with a layer of copper. The situation was complicated in their work by the appearance of a series of intermediate phases between pure aluminum and pure copper, with the result that acceptable diffusion coefficients were not obtained in either case.

Rolling was used as a bonding method by Mehl, Rhines and von den Steinen,[10] and also by Murphy.[11] In addition, Burkhardt and Sachs,[12] and Buckle and Keil[13] studied diffusion in commercially clad aluminum alloys in which a bond is produced between the pure aluminum cladding and alloy core by a rolling process. The procedure used by Murphy will illustrate the laboratory method; the core material and the pure aluminum cladding were mechanically polished, strapped together, preheated for one hour at 450°C and then hot rolled. The composite sandwich was reduced in thickness approximately 70 per cent by the rolling operation.

Rolling has the advantage that oxide films over the interface are

broken up and distributed over a much larger surface area. There are also disadvantages. Unless the preheating step prior to rolling is carried out in an inert atmosphere it is likely that oxidation of the interface will be increased to such an extent that the advantages gained by breaking up the oxide layer and distributing it over the interface will be more than offset. The interface produced by rolling is also somewhat wavy which could cause serious errors in position determinations if the couples were sectioned for analysis. As Murphy noted " -diffusion couples --- were then cut from a longitudinal central strip of the sandwich where the interface was flattest." There is a third possible disadvantage to the rolling method used by Murphy. He states that the plate and core were mechanically polished prior to being strapped together. Krusensjern and Hentschel[14] have reported that polishing of pure aluminum with loose abrasive results in penetration of the metal by particles of the abrasive to a depth of 6 microns. Imbedded particles of abrasive at the interface would act as barriers to the free movement of the atoms. Some evidence of this effect was noticed during the development of a bonding technique for the present work. Mechanically polished samples which had been finished on cloth laps with loose abrasive were particularly difficult to weld, and failed to produce good bonds even after extensive welding periods at high temperatures and pressures.

Clamping was used as a bonding method by Beerwald,[15] by

Buckle,[7] by Kirkaldy, Mason and Slater,[16] and also by Lundy and Murdoch[17] in a recent determination of the self-diffusion coefficient of aluminum. In the clamping method the samples are prepared in the form of discs which are clamped with C-clamps or assembled in steel capsules before being placed in a furnace for the diffusion anneal. The differential thermal expansion of the aluminum sample and the steel clamp produces pressure which causes the couples to weld at the temperature of the diffusion anneal. The surfaces to be welded are freshly surfaced prior to clamping by electropolishing (Buckle, Lundy) or by machining on a lathe (Kirkaldy). It was found during the present work that unless the discs are also restrained laterally during welding the pressure exerted on the ends may be largely dissipated by sidewise bulging of the discs, and good contact will only be maintained during the very early stages of the welding period.

Oxidation of the interface cannot be completely eliminated in clamped couples even though the surfaces to be welded are freshly prepared, clamped together and then welded in an inert atmosphere. Lundy,[17] who used a particularly sensitive tracer method of analysis to determine the self-diffusion coefficient of aluminum, found a large initial drop in activity near the boundary which he attributes to the presence of a layer of oxide. The effect was not present after diffusion annealing at temperatures above 600°C.

Brick and Phillips[18] used a particulary novel method of bonding in

an attempt to produce an absolutely clean interface. Rods of pure aluminum, preheated to 550°C, were dipped into molten eutectic covered with a layer of flux. The rod was agitated in the eutectic for a few minutes and then the composite specimen (aluminum rod plus eutectic) was chilled and solidified from the bottom. Brick and Phillips report that initial melting and diffusion did not effect the pure aluminum rod to a depth of more than 0.0005 cm. The method was tried in the present work to produce cylindrical couples by dipping rods of alloy into a melt of pure aluminum and solidifying rapidly. The method was abandoned when it was found that severe local melting of the alloy rod could not be overcome.

The methods of analyses used to obtain concentration-distance curves in studies of interdiffusion in dilute aluminum-copper alloys may be classified as follows:

(1) Direct determination of the concentration gradient by removal of thin layers and subsequent analysis by chemical, spectrographic or tracer techniques.

(2) Indirect determination of the concentration gradient by studying the appearance of a second phase after diffusion.

(3) Indirect determination of the concentration gradient by making microhardness traverses across the diffusion zone.

Beerwald[15] used spectrographic analysis of a series of surfaces perpendicular to the direction of diffusion. Successive layers, 0.05 to

0.10 mm. thick, were machined from the diffusion zone parallel to the interface. After each machining operation the new surface was analyzed. The method required repeated mounting of the couple in a lathe which, as Beerwald observed, may have been a source of error as it was difficult to maintain the surfaces exactly parallel to the interface. A standard deviation of 2 or 3 per cent of the content of the constituent, with a lower limit of detection of about 0.0002 per cent are commonly accepted for the precision and sensitivity of spectrographic analysis.[19]

Mehl, Rhines and von den Steinen[10] machined layers from the diffusion zone and analyzed them separately by a combination of chemical and spectrographic methods. The chemical analysis which they used was estimated to have a standard deviation of 0.3 weight per cent copper at higher concentrations (≃6 per cent) and 0.08 per cent at lower concentrations (≃1 per cent).

Murphy[11] also machined layers from the diffusion zone and analyzed them separately. He used a spectrophotometric method for concentrations from 0.50 down to 0.01 weight per cent copper, and activation methods below that. The standard deviation obtained by Murphy for the chemical analysis was 0.003 weight per cent copper. No details were given for the activation analysis, either of the method or of the precision obtained.

Kirkaldy *et al*[16] also used an activation method of analysis. Samples obtained by machining 0.10 to 0.05 mm. layers from the

diffusion zone were irradiated, along with standards, with thermal neutrons in a reactor to produce the isotope ^{64}Cu. The concentration was then determined by measuring the residual x-ray activity of the samples and comparing it to that of the standards. The standard deviation obtained was 1.5 per cent of the content.

Brick and Phillips[18] used an approximate metallographic method of obtaining concentration distance data. The method depends on the decrease with temperature of the solid solubility of copper in aluminum. The diffusion couples were reheated for short times below the actual diffusion temperatures, whereupon $CuAl_2$ was precipitated in areas where the solute exceeded the solubility saturation value. The edge of the precipitated zone furthest from the eutectic was taken to be at the saturation concentration limit c . The distance from the original interface to the edge of the precipitate gave the corresponding x value. Repetition of the procedure for a series of temperatures gave a series of c-x values from which a portion of the diffusion curve could be plotted. The shape of the portions of the diffusion curves obtained in this way are anomalous in that they are straight lines and not portions of S-curves asymptotic to the distance axis. It must be concluded that the method of analysis used by Brick and Phillips is only a useful approximation.

Buckle[7] developed the microhardness technique to study diffusion in thin zones between pure aluminum and an aluminum-copper alloy (4 weight per cent). In this method microhardness measurements are

made across the diffusion zone on a plane parallel to the diffusion direction and the microhardness readings converted to composition by means of a calibration curve. The method has considerable advantage in the precision with which the distances may be measured as this is limited only by the resolving power of the microscope. It also has the advantage that it is rapid and non-destructive. This makes it possible to make a very large number of measurements on a couple and thereby increase the precision of the concentration-distance data. Buckle estimated the precision of measurement to be between one and two per cent of the content for indentations 15 microns in diagonal. Buckle and Keil[13] compared the microhardness technique with local spectroscopic analysis in the determination of diffusion in the pure aluminum cladding of "Vedal" (Al-4%Cu-1.5%Mg). The diffusion curves obtained by the two methods were in complete coincidence, with the microhardness curve showing less scatter.

Table I records collectively the previous quantitative work on interdiffusion in dilute aluminum-copper alloys. It is evident that, at a given temperature, the results are well within an order of magnitude of each other. This is much better agreement than different investigators have obtained in some other systems. For example, the diffusion results for zinc in alpha brass show agreement only within three orders of magnitude.[20] A further discussion of the results of previous work will be given in a following section in connection with the discussion of the results of the present work.

TABLE I

DIFFUSION OF COPPER IN ALUMINUM

Author(s)	Purity of Aluminum Used	Initial Core Conc. (Wt. %)	Temp. (^oC)	D (cm^2/sec)	Applicable Conc. Level (Wt. %)	D_o (cm^2/sec)	Activation Energy, Q (k. cal./g. atom)
Beerwald[15]	99.998	2	457	0.85×10^{-10}	-	0.084	32.6
			497	2.50×10^{-10}			
			515	5.1×10^{-10}			
			565	14.0×10^{-10}			
		0.4	565	13.0×10^{-10}			
Brick and Phillips[18]	Pure Al	Eutectic	440	0.57×10^{-10}	-	-	31.5
			490	2.4×10^{-10}			31.4
			540	14.0×10^{-10}			31.4
Buckle[7]	99.998	4	500	2.1×10^{-10}	0.5	-	41.9
			515	4.8×10^{-10}			
			550	12.7×10^{-10}			
Buckle and Keil[13]	Pure Al	5.2	505	6.7×10^{-10}	0.2	-	-
			505	4.6×10^{-10}	0.5		
			505	2.9×10^{-10}	1.0		
			505	2.3×10^{-10}	1.5		
Mehl, Rhines and von den Steinen[10]	99.998	6.96	400	0.10×10^{-10}	2.0	-	33.9
			448	1.2×10^{-10}			
			504	5.2×10^{-10}			
Murphy[11]	99.997	0.50	540	13.0×10^{-10}	0-0.50	0.29	31.1
Kirkaldy, Mason and Slater[16]	99.99	3.90	556	18.0×10^{-10}	0-3.90	-	-

B. THE MAGNETIC DIFFUSION EFFECT IN FERROMAGNETIC METALS AND ALLOYS

Investigation on diffusion of a variety of elements (iron, nickel and cobalt) in iron, and on diffusion in cobalt-nickel alloys has indicated that the diffusivity below the ferromagnetic Curie temperature is lower than that expected from an extrapolation of the data obtained above the Curie temperature. The departure of the measured values from the extrapolation amounts to a reduction in the diffusion coefficient by a factor of three for self diffusion in alpha-iron at temperatures 50°C below the Curie temperature. Fig. 1 for the diffusion of ^{55}Fe in alpha-iron which has been replotted from the data of Borg and Birchenall,[21] illustrates the effect. It is manifested as a non-linear negative deviation of the diffusivities in a transition region which extends approximately 30°C on either side of the Curie temperature. Below the transition temperature the diffusivities again appear to follow an Arrhenius plot but with a slightly higher activation energy.

The magnetic diffusion effect, by which the retardation of diffusion in the ferromagnetic state is commonly known, has two features that are common to the present work. First, in the ferromagnetic state, diffusion takes place in a magnetic field. This is true because, although the ferromagnetic body may not exhibit any external magnetic effects, it is made up of a very large number of randomly oriented domains or regions which are strongly magnetized even in the absence of an applied magnetic field.

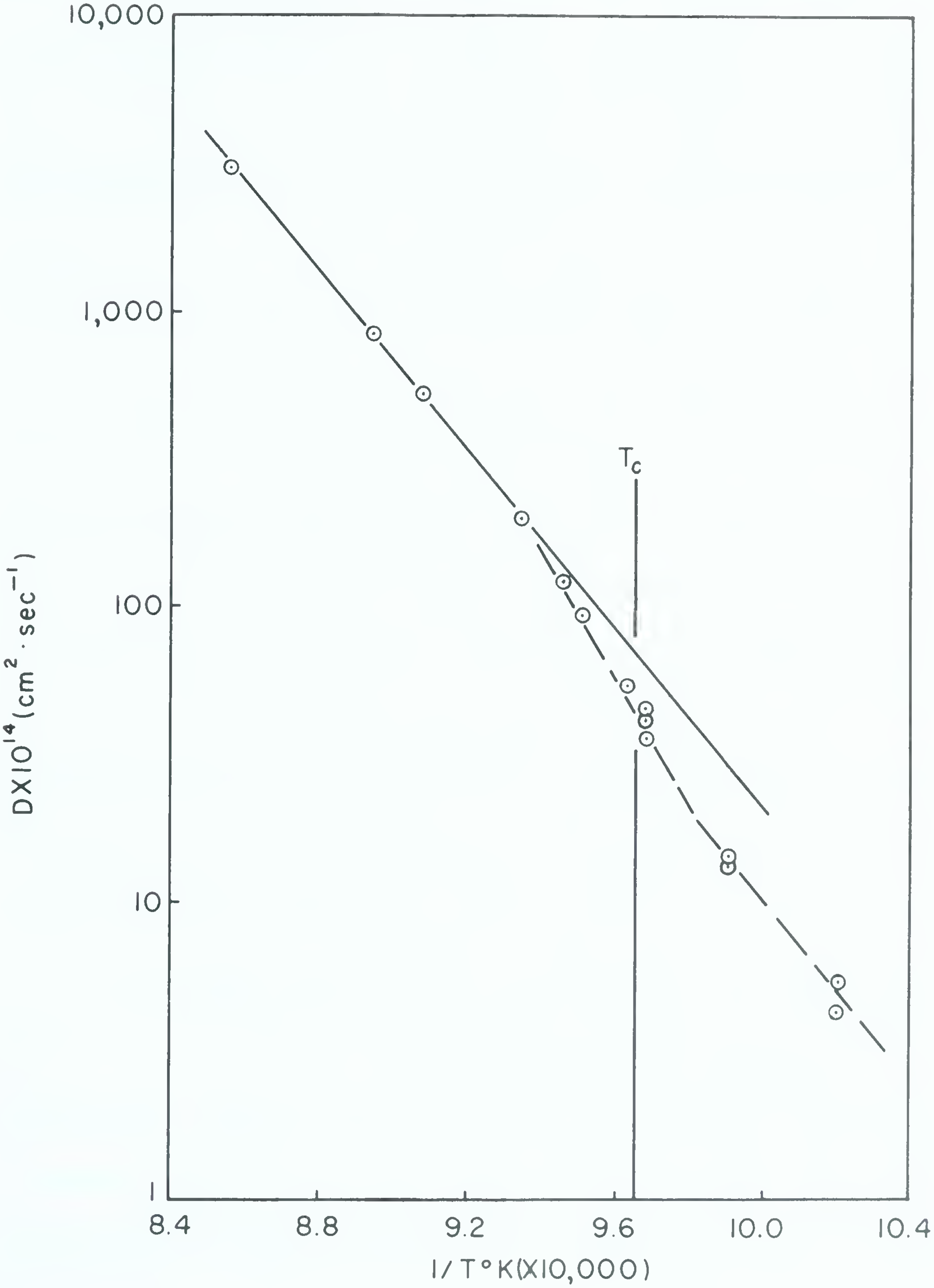

Figure 1 - The magnetic diffusion effect in alpha-iron. (After Borg and Birchenall[21].)

Second, the results are comparable in that in both cases the diffusion rate is found to be reduced by the presence of magnetic fields. In addition, the factors which are discussed in the theories advanced to explain the magnetic diffusion effect in ferromagnetic materials may have some application in the development of a theory to explain the results of the present work on the weakly paramagnetic aluminum (rich)-copper system.

A possible effect of the onset of ferromagnetism upon the diffusivity in alpha-iron was first reported by Birchenall[22] in 1958. However, the self diffusion coefficients determined for alpha-iron up to that time were not sufficiently precise to establish accurate correlation between low values for the diffusion coefficient below the Curie temperature and the magnetic transformation. In 1960, Borg and Birchenall[21] redetermined the self-diffusion coefficients for iron between 980 and 1167°K using ^{55}Fe as a tracer and an improved counting procedure to increase the precision of the results.

The results obtained by Borg and Birchenall are reproduced in Fig. 1 in which the effect of the magnetic transformation is clearly discernible. They attributed the anomalous decrease in diffusivity on transformation from the paramagnetic state to the ferromagnetic state primarily to a decrease in the number of vacancies, and estimated that a decrease in vacancy concentration by a factor of about two could account for the magnetic effect on the diffusion coefficient.

At about the same time as Borg and Birchenall were conducting

their experiments on self-diffusion in alpha-iron, Stanley and Wert[23] measured the diffusion constants of iron-vanadium alloys over a wide temperature range by a combination of tracer and anelastic methods. Above the ferromagnetic Curie temperature, for an alloy containing eighteen weight per cent vanadium, they obtained

$$D(^{48}V) = 3.9 \exp(-58{,}500/RT) \text{ cm. sec.}^{-1}$$

while in the ferromagnetic state below 823°C they obtained

$$D = 0.25 \exp(-61{,}900/RT) \text{ cm. sec.}^{-1}$$

Their results indicate that a very large reduction in diffusion occurs when the alloy orders magnetically. Diffusion in the magnetic state at a temperature about 300°C below the Curie temperature is about 100 times slower than one would expect from an extrapolation of the results in the paramagnetic state. The effect is divided into two parts, a tenfold reduction in D_o and another tenfold reduction due to the increase in the activation energy of approximately 3,400 calories per mole. The increase in activation energy was attributed to an increase in the energy of formation of vacancies, or to an increase in their motional energy or both. Stanley and Wert attempted to account for the observed decrease in D_o by postulating a change in the entropy of motion of vacancies. Applying a theory developed earlier by Zener,[24] that for the reversible motion of an atom from its equilibrium position, x_o, to the saddle point, x', much of the work goes into elastically straining the lattice around the saddle point, and the work ΔG_m may be approximately calculated from

the elastic strain set up in the lattice upon moving the diffusing atom from x_o to x_1, thus

$$\Delta G_m = \int_{x=0}^{x_1} f dx \simeq \mu \mathcal{E}_o^2 \quad , \qquad (1)$$

where $\mathcal{E}_o$ is some representative strain for the matrix when the atom is in the saddle point and μ is the elastic modulus for the solvent. If ΔG_m is assumed to be a Gibbs free energy it follows that

$$\Delta S_m = - \left(\frac{d \Delta G_m}{dt} \right)_p \qquad (2)$$

If $\mathcal{E}_o$ is assumed to be independent of temperature then ΔS_m, and therefore D_o, are proportional to the temperature derivative of μ. Stanley and Wert point out that Sato and Alers[25] have presented evidence for a change in $d\mu/dt$ near the Curie temperature of ferromagnetic materials. The effect was assessed by Stanley and Wert to be in the right direction but of much smaller magnitude than required to explain their results.

In 1961, Buffington, Hirano and Cohen[26] reported on the measurement of the self diffusion of iron by tracer methods. Their results are as follows:

Alpha-iron (paramagnetic)

$$D = 1.9 \exp \; (-57,200/RT) \text{ cm. sec.}^{-1}$$

Alpha-iron (ferromagnetic), below 750°C,

$$D = 2.0 \exp \; (-60,000/RT) \text{ cm. sec.}^{-1}$$

The anomaly in diffusivity associated with the magnetic change of alpha-iron is manifested almost entirely in the increase of 2,800 calories per mole in the heat of activation, there being no appreciable change in the frequency factor, D_o. Buffington et al point out that if the observed magnetic effects were attributed entirely to a variation in D_o, the latter would have to be lowered by 3 or 4 orders of magnitude, and the corresponding changes in vibrational frequency, lattice spacing, and activation entropy would be unlikely. They reason that the change in activation energy below the Curie temperature should be attributed to an increase in the energy required to form a vacancy in the ferromagnetic state.

Also in 1961, Hirano, Cohen and Averbach[27] reported on the diffusion of nickel into iron in which the magnetic effect was again clearly present. Their results are:

Alpha-iron(paramagnetic) above 800°C,

$$D(^{63}Ni) = 1.3 \exp(-56,000/RT) \text{ cm. sec.}^{-1}$$

Alpha-iron (ferromagnetic) below 680°C,

$$D(^{63}Ni) = 1.4 \exp(-58,700/RT) \text{ cm. sec.}^{-1}$$

The magnetic anomaly also appears in these results as an increase in activation energy with no significant decrease in the frequency factor, D_o. The authors attribute the change to an increase in the formation energies of vacancies in the ferromagnetic state. They obtain a quantitative correlation by equating the energy of magnetization to the increase in activation energy in the ferromagnetic state.

In 1962 Hirano, Agarwala, Averbach and Cohen[28] reported on the self-diffusivities of Co and Ni in cobalt-nickel solid solution alloys. Their results show a greater difference in D_o between the ferromagnetic and paramagnetic states than reported for α-iron, with the values in the ferromagnetic state being generally larger than those in the paramagnetic state. For pure cobalt in the ferromagnetic region between 772 and 1048°C they obtained:

$$D(^{60}Co) \simeq 0.50 \exp(-65,400/RT) \text{ cm. sec.}^{-1}$$

$$D(^{63}Ni) \simeq 0.34 \exp(-64,300/RT) \text{ cm. sec.}^{-1}$$

For the paramagnetic region between 1192 and 1297°C:

$$D(^{60}Co) \simeq 0.17 \exp(-62,200/RT) \text{ cm. sec.}^{-1}$$

$$D(^{63}Ni) \simeq 0.10 \exp(-60,200/RT) \text{ cm. sec.}^{-1}$$

These results show an increase in D_o of over 100 per cent, and an increase in the activation energy of over 3,000 calories per mole in passing from the paramagnetic to the ferromagnetic state in pure cobalt.

The change in the cobalt-nickel alloy containing 51 atomic per cent nickel was somewhat less. They report for the ferromagnetic range (701-819°C)

$$D(^{60}Co) \simeq 0.096 \exp(-61,500/RT) \text{ cm. sec.}^{-1}$$

$$D(^{63}Ni) \simeq 0.36 \exp(-63,600/RT) \text{ cm. sec.}^{-1}$$

and for the paramagnetic range (899-1192°C)

$$D(^{60}Co) \simeq 0.12 \exp(-60,200/RT) \text{ cm. sec.}^{-1}$$

$$D(^{63}Ni) \simeq 0.21 \exp(-60,600/RT) \text{ cm. sec.}^{-1}$$

Hirano et al concluded that the difference in activation energy between the paramagnetic and ferromagnetic states decreased with decreasing Curie temperature. They attributed the observed magnetic effect to the additional energy of formation of a vacancy in the ferromagnetic state.

In 1963 Borg[29] published his comments on the work of Hirano et al on diffusion in cobalt-nickel alloys in which he is very critical both of the results and of the vacancy theory which was used to interpret the results. Borg pointed out that Hirano et al determined activation energies in the paramagnetic and ferromagnetic regions of each alloy by analyzing the measurements above the Curie temperature separately from those obtained below it. Borg made a least squares analysis of all the points obtained by Hirano et al for ^{60}Co diffusing into pure Co and obtained

$$D \approx 0.51 \exp(-65,500/RT) \text{ cm. sec.}^{-1},$$

which is very nearly identical with the value

$$D \approx 0.50 \exp(-65,400/RT) \text{ cm. sec.}^{-1}$$

reported by Hirano et al for only the ferromagnetic region. Borg also replotted the diffusion coefficients obtained by Hirano et al for ^{60}Co and ^{63}Ni diffusing into pure Co on a logD versus $1/T^{o}K$ plot and obtained what appeared to be perfectly straight lines throughout the para- and ferromagnetic regions, with no suggestion of a discontinuity in the vicinity of the Curie point. Borg then states that "the total absence of the magnetic effect is obvious".

These criticisms do not appear to be completely justified. A careful plot of the same data produced lines with a slight discontinuity at the Curie temperature much as Hirano et al had shown in their paper. In addition, in the least mean squares analysis of all the points, Borg apparently included the points at 1048°C and 1090°C which Hirano et al did not include in their calculations because they fall in the transition region. With six of the nine points which Borg plotted in the ferromagnetic or transition regions it is not surprising that the over all best fit line coincided quite closely with that of Hirano et al in the ferromagnetic region.

In support of Borg's contention that the data has been incorrectly interpreted, it should be pointed out that, although the plots of lnD versus 1/T°K by Hirano et al clearly indicate a greater magnetic effect in the alloy containing 50 atomic per cent nickel than in pure cobalt, their least squares analysis indicates that the reverse is true. It is probably safe to conclude that the magnetic diffusion effects obtained by Hirano et al are represented more accurately by their Arrhenius plots than by their calculated values of D_o and Q.

A point which seems to have been missed in the controversy over the presence or absence of the magnetic effect in pure cobalt is that there may be more involved than just a para- to ferromagnetic transition in cobalt at 1120°C. Several investigators have presented evidence that there is a second transformation in cobalt (f. c. c. to h. c. p. at or

near the Curie temperature.[30, 31] The occurence of such a phase transformation might mask the magnetic diffusion effect in pure cobalt.

Borg also criticizes the use of the vacancy decrease hypothesis used by Hirano _et al_ in interpreting their results. (Borg and Birchenall[21] originated this theory to explain their results for self-diffusion in alpha-iron). He concludes by stating that the vacancy decrease hypothesis is inadequate and that an alternative explanation based upon the influence of magnetism upon the elastic constants forms the basis of a paper then in preparation. (The paper has not appeared in print to date.)

C. ELECTRICAL ION TRANSPORT

If an alloy is heated and an electric current is passed through it, the combined effect of the electric field and the electric current will produce a migration of the solute ions toward either the anode or the cathode. Experiments of this type on the electrical transport of ions in metals yield data from which the solute ion charge may be calculated. The situation is complicated, however, by the existence of not only the electric field force on the ion, F_1, but also of a force, F_2, due to the "electron-wind". Electrons, which are being accelerated toward the anode by the electric field, are scattered by the ions which are in an activated state. The momentum transferred from the electrons to the ions by the scattering process produces the electron wind force which is directed toward the anode. Fiks[32] has evaluated the net force on the

ions as

$$F = F_1 - F_2 = eE(Z - nl\rho)$$

where E is the electric field intensity, n and l are the concentration and free path length respectively of the conduction electrons, ρ is the scattering cross section of the activated ions and Ze is the ion charge.

The ion charge cannot be determined directly by measurements of electrical transport since the quantities n, l and ρ are not determined by the experiments. Reference must be made to other experiments on the properties of conduction electrons such as resistance measurements or cyclotron resonance. Such data as are available may not be applicable to the conditions of the transport experiment. To avoid this difficulty Miller[33] proposed and carried out ion charge determinations based on the investigation of electrical transport of ions in a transverse Hall electric field. In this arrangement there is no momentum transfer to the diffusing ions from the electron current, assuming a spherically symmetrical Fermi surface exists for the metal. Theoretically, the positive ions which are moving longitudinally under the action of the electric field and electron wind should also experience a Lorentz force and migrate transversely to create a Hall potential. Miller and Gurov[34] have shown, however, that because of the very low mobility of the ions compared to that of the electrons, the Hall field due to the ion current is negligible and may be neglected in calculations.

A theoretical and experimental investigation of ion transport in liquid alloys has been undertaken by a number of investigators including Angus, Verhoeven and Hucke,[35] and Mangelsdorf.[41] As in the case for ion transport in solids, the interpretation of the results for charge determination is complicated by the "electron wind" factor. V. B. Fiks[37] discussed the theoretical aspects of ion migration in liquid metals due to the Hall electric field. An experiment (of which Fiks was apparently unaware) had been carried out earlier by Knof[38] who studied the movement of gold perpendicular to crossed electric and magnetic fields in liquid gold amalgams. Knof was apparently successful in obtaining a migration due to the Hall field. However, the results of his experiments may have been complicated by segregation during solidification after completion of the runs, because a further discussion of his experiments, which was promised, never appeared in print.

In experiments on transport of ions in a Hall electric field, a magnetic field is applied only to produce the Hall potential and any direct effects of the magnetic field upon the ion mobility are neglected. It would appear desirable to test this assumption by experiment.

D. THE PLASMA CONCEPT OF A METAL

In its original and narrower sense the term plasma is applied to a highly ionized gas, having a nearly equal number of positive and

negative charges, so that the state of the whole is nearly field free. In a much broader sense the term plasma is taken to mean a gas of charges embedded in a region of charges of opposite sign to maintain electrical neutrality. Thus a solid or liquid metal may be considered to have plasma-like properties by virtue of the presence of free or nearly free conduction electrons.

There are many phenomena in solids which can be considered as manifestations of plasma effects. One such phenomenon, which had previously been known to exist only in gaseous plasmas but which has recently been demonstrated by Glicksman and Steele[2] in the electron-hole plasma of a semi-conductor, is the plasma "pinch" effect. The effect is produced when a large current is passed through the plasma. The current creates a magnetic field in the form of circular field lines around the current. The current carriers moving in this magnetic field experience a Lorentz force which pinches them into a thin stream.

The theory of plasmas and their behaviour in magnetic fields has been extensively developed by numerous authors and for a comprehensive review the reader is referred to a recent paper by Golant.[1] The concepts and equations which are considered relevant to the present work, particularly those which are concerned with diffusion of a plasma in a constant magnetic field, will be introduced in the theory section as needed.

THEORY OF MAGNETIC EFFECTS

A detailed discussion of the effect of a magnetic field on the thermodynamic quantities of a weakly paramagnetic or diamagnetic metal will not be given here.for in the simple diffusion process in a solid solution alloy no phase changes are involved where one might expect the field to have some effect. Generally, the effect of the field on the thermodynamic functions will be of the order of the ratio of the magnetic energy induced to the total energy of the system. The magnetic energy is given by $1/2\chi H^2$, where χ is the specific magnetic susceptibility and H is the magnetic field*. For weakly paramagnetic and diamagnetic alloys in a magnetic field of 10,000 oersteds the magnetic energy is of the order of 10^{-6} calories per gram, which is negligible in comparison with the specific heat of the alloy. Consequently we look for the effect of the magnetic field on diffusion through its effect on the kinetics of motion of the diffusing component.

The study of the interaction between electromagnetic fields and moving conducting fluids is known as magnetohydrodynamics or plasma dynamics, depending on whether the fluid can be described in terms of conventional continuum theory, or kinetic theory in the absence of the continuum property. In a plasma (ionized gas) of very low density, the classical magnetohydrodynamic equations cannot be applied, and it is necessary to go to the Boltzmann equation directly to derive more precise relationships between the macroscopic quantities. A metal, by

---

* e.m.u. and c.g.s. units are used throughout this thesis unless otherwise specified.

virtue of the presence of the free (conduction) electrons, will under certain circumstances exhibit phenomena amenable to a classical magnetohydrodynamic description, while under other circumstances certain phenomena are best described using the equations of plasma dynamics.

A. MAGNETOHYDRODYNAMICS

The magnetohydrodynamic equation of motion is the ordinary hydrodynamic equation modified by Maxwell's electromagnetic equations to take account of the interaction between motion and the magnetic field. If $\vec{v}$ is the macroscopic velocity of the fluid of density ρ, permeability μ and kinematic viscosity ν, then the equation of motion is given by[39]

$$\rho\dot{\vec{v}} + \rho(\vec{v}\cdot\vec{\nabla})\vec{v} = -\vec{\nabla}p + \rho\vec{g} + \nu\rho\nabla^2\vec{v} + \mu\vec{j} \times \vec{H}, \tag{3}$$

where p is the pressure, $\vec{g}$ the gravitational acceleration, and $\vec{H}$ the field strength. $\vec{j}$ is the macroscopic current defined by

$$\vec{j} = \sigma(\vec{E} + \mu\vec{v} \times \vec{H}), \tag{4}$$

where σ is the electrical conductivity of the fluid and $\vec{E}$ the electric field. Along with Eq. (3), which is derived from the Boltzman Equation[40] and Eq.(4), Maxwell's equations relating the electric and magnetic fields are required for a complete description of the system. However, for the case considered here, where the fluid (or solid) has a finite resistivity and the external fields are constant, Eq. (3) and (4) suffice to describe the behaviour of the system.

The body force $\mu \vec{j} \times \vec{H}$ in **Eq.** (3) is of electromagnetic origin and is sometimes referred to as the pondermotive force. Its direction is such as to impede movement of the fluid across the magnetic lines of force. Using **Eq.** (4) we get for the pondermotive force

$$\mu \vec{j} \times \vec{H} = \mu\sigma(\vec{E}_\perp \times \vec{H} - \mu H^2 \vec{v}_\perp), \qquad (5)$$

where $\vec{E}_\perp$ and $\vec{v}_\perp$ are the components of $\vec{E}$ and $\vec{v}$ perpendicular to the field. The quantity $\mu^2 \sigma H^2 v_\perp$ is the induction drag tending to destroy motion across the lines of force, and may be regarded as a magnetic viscosity. The ordinary viscous force is comparable with $\rho \nu v l^{-2}$, and the non-linear inertia (convective) term $\rho (\vec{v} \vec{\nabla}) \vec{v}$ is comparable with $\rho v^2 l^{-1}$ (cf. Eq. 3), where l is a characteristic length of the system. A comparison of these forces shows that the magnetic viscous force will dominate over the ordinary viscous and convective forces only when the respective parameters $\mu^2 H^2 l^2 \sigma (\rho\nu)^{-1}$ and $\mu^2 H^2 l \sigma (\rho v)^{-1}$ are large compared with unity. For systems of large dimensions and for strong fields the magnetic viscous force will dominate, so that in this latter case it is possible to neglect the second order viscous and convective terms to linearize the equation of motion.

The magnetic viscous (macroscopic) force will inhibit diffusion perpendicular to the field to the extent that there is a density change associated with a concentration change, and hence bulk motion of the fluid or solid. However, for solid or liquid metal systems diffusion is relatively slow and density changes small, so that the magnetic viscous force will be

negligible. For example, for diffusion in mercury ($\sigma \sim 10^{-5}$ emu, $\rho\nu \sim 10^{-2}$ g cm.$^{-1}$ sec.$^{-1}$) across a field of 10^4 oersteds, $\mu^2 H^2 l^2 \sigma (\rho\nu)^{-1} << 1$ for a gradient length $\gtrsim 10^{-3}$ cm. Thus the magnetic viscous force is smaller than the ordinary viscous force, which itself would be negligible if density changes accompanying diffusion were small. We expect, therefore, that magnetic viscosity will play a negligible part in diffusion inhibition in solid or liquid metal systems.

B. PLASMA DYNAMICS

The macroscopic magnetohydrodynamic viscous force experienced by the diffusing system represents the sum total of the magnetic forces experienced by the individual particles, i.e. the electrons and the positively charged ion cores. And, although the macroscopic force may be negligible (when density changes and hence bulk motion during diffusion are small), the magnetic forces on the individual particles are still present and will tend to inhibit their relative motion or diffusion. The Lorentz force will cause the particles to gyrate in the magnetic field with a frequency $\omega_{ce} = eH/m$, which is called the cyclotron frequency. Eqs.(3) and (4) are valid only when the gyration radius of the electron ($r_e = v_e/\omega_{ce}$) is much larger than its mean free path, or equivalently, when the collision frequency ν_e greatly exceeds the gyration frequency, i.e. $\omega_{ce}/\nu_e << 1$. If the field strength is such that the gyration radius is of the order of the mean free path or smaller, the classical description of the transport properties breaks down, and recourse to the fundamental Boltzmann

equation is necessary to describe the two-fluid system in which Ohm's law is no longer assumed valid.

A concentration gradient in an alloy will give rise to a corresponding free electron gradient if the electron densities differ for the various components.[41] The free electron gradient is analogous to an electron plasma under a density or pressure gradient, and an interaction of the magnetic field with the gradient will cause the plasma to drift. In the absence of electron-ion collisions the drift of the electrons and ions will be perpendicular to both $\vec{H}$ and $\vec{\nabla}p$, while collisions between electrons and ions result in a diffusion flow component parallel to $\vec{\nabla}p$. Spitzer gives for the transverse velocity of the plasma in a magnetic field (ref. 40, p. 24) ; (where $p = p_e + p_i$).

$$\vec{v}_\perp = \frac{\vec{H}}{\mu H^2} \times \left(-\vec{E} + \frac{\vec{\nabla} p_i}{e n_e} \right) - \left(\frac{1}{\nabla \mu^2 H^2} \right) \vec{\nabla} p \,, \qquad (6)$$

where n_e is the volume density of electrons and the subscript (i) refers to the ions. For the case of negligible resistivity (infinite conductivity) there is no mass flow parallel to the pressure gradient (this corresponds to the situation $\omega_{ce}/\nu_e \gg 1$, for which Eqs. (3) and (4) are no longer valid). The plasma is said to be confined, the confining force being equal to a 'magnetic pressure' $\mu H^2/8\pi$ *. The component of $\vec{v}_\perp$ parallel to $\vec{\nabla}p$ represents a net outward drift of the confined plasma. This is

---

*The magnetic pressure $\mu H^2/8\pi$ is obtained using Maxwell's equation $4\pi j \doteq \text{curl } \vec{H}$ to define the current in the pondermotive force $\mu \vec{j} \times \vec{H}$, which is equal to the pressure gradient for the linearized steady state case (cf. Eq. 3).

[illegible]

[illegible]

$$[illegible]$$

[illegible]

[illegible]

predominantly due to the electron-ion collisions, since the resistivity term $1/\sigma$ is related to the rate of momentum transfer to the ions by the electrons. In low density plasmas, where the gyration frequency greatly exceeds the collision frequency, the encounters between identical particles do not, to a first approximation, alter their density distribution. This is a result of the peculiar shift of the guiding centra (orbital centers of the gyrating particles) of the two interacting particles by equal and opposite amounts.[42]

It is not possible to compare the components of flow velocity along $\vec{\nabla} p$ in Eq. (6) to normal diffusion velocities in metals because of their essentially different natures. The pressure gradient in (6) results from the field itself, and the 'diffusion' is flow resulting from the motion of ions and electrons together (ambipolar diffusion), not movement of one species relative to another. Eq. (6) does however show the nature of diffusion inhibition. The mass transfer associated with the density gradient is divided into two components, one perpendicular to the gradient (Hall current) and one parallel to it, the extent of parallel flow or 'diffusion' being inversely proportional to H^2. Thus for very high field strengths flow along the density gradient vanishes.

It is possible to obtain more useful expressions which relate to the currents (and hence mass transfers) in the alloy, viewed basically as a two-fluid plasma of ions and electrons, if the effect of the field on the motion of the electrons only is considered. The affected motion of the

electrons will in turn determine the ion motion through the attempt of the system to maintain electrical neutrality. This is a physically reasonable assumption, since in the non-steady state the effect of the magnetic field on the motion of the electrons relative to the ions is of the order of ω_{ce}/ω_{ci} (equivalent to the inverse ratio of their masses), i.e. $\sim 10^5$. Thus in the above view the forces responsible for ion motion are essentially electrical, deriving from the slight deviation from electrical neutrality as the electrons tend to drift away and hold back from the diffusing ions when under the influence of the magnetic field. The extent to which the charge distribution within a plasma can deviate from the equilibrium distribution is the Debye distance

$$h_D = \left(\frac{\kappa T}{4 \pi n_e e^2} \right)^{1/2} \tag{7}$$

If for metals we assume the thermal energy κT can be replaced by the Fermi energy E_F,* the extent to which appreciable charge separation can occur is only of the order of an angstrom unit, or less than one interatomic spacing.

The assumption that electron motion determines the ion motion in this particular consideration is not a contradiction of the well known fact that plasma diffusion is controlled by ion phenomena. As a consequence of the mass differences the ions diffuse much slower than the highly mobile electrons, and the ion control is expressed by the ambipolar diffusion constant which is approximately twice the ion

---

*A useful approximation for evaluating h_D by which order of magnitude agreement is obtained with more refined theories (see Eq. 14).

diffusion constant, i. e. $D_a \sim 2D_i$. The plasma diffusion constant is twice the ion diffusion constant by virtue of the effect of the much faster diffusing electrons. In the presence of a magnetic field the electron diffusion constant is severely reduced, thus decreasing the diffusion constant of the plasma as a whole.

The electron current transverse to the magnetic field obtained by solving the equation of motion for the electron gas (ref. 39, p. 103) is*

$$j_e = \frac{\sigma}{(1 + \omega_{ce}^2 / \nu_e^2)} \left[\vec{E}' + \vec{E}'' \frac{-\omega_{ce}}{\nu_e H} (\vec{E}' + \vec{E}'') \times \vec{H} \right], \qquad (8)$$

where $E' = \vec{E} + \vec{v} \times \vec{H}$ and $E'' = \vec{\nabla} p_e / n_e e$. In the latter the electron pressure gradient is viewed as an effective electric field. $\vec{\nabla} p_e$ is related to the electron density gradient and thus to the chemical potential of the electrons (which is equal to the Fermi energy for the free electrons in a solid), so that we may write instead, $E'' = (\partial E_F / \partial n_e) \dfrac{\vec{\nabla} n_e}{n_e e}$ (for $\vec{\nabla} T = 0$). In the absence of an external electric field, the electron currents are due to diffusion only. For the electron drift velocities involved in diffusion $E'' >> E'$, so that the electron diffusion currents along and perpendicular to the density gradient are respectively (cf. Eq. 8):

$$j_{e_x} = \frac{\sigma}{(1 + \omega_{ce}^2 / \nu_e^2)} \left[\frac{1}{n_e e} \cdot \frac{\partial E_F}{\partial n_e} \cdot \frac{\partial n_e}{\partial x} \right], \qquad (9)$$

---

*In adapting this equation to the present purposes we are making use of a treatment which views the plasma as being in a region where $\omega_{ce}/\nu \gg 1$, and where the so called "free spiraling approximation" applies. This is also a classical description of a plasma which is admittedly a simplification because we have here to deal with a degenerate electron gas.

and

$$j_{e_y} = \frac{\nabla}{(1+\omega^2_{ce}/\nu_e^2)} \cdot \frac{\omega_{ce}}{\nu_e} \left[\frac{1}{n_e e} \frac{\partial E_F}{\partial n_e} \cdot \frac{\partial n_e}{\partial x} \right] . \tag{10}$$

Eq. (9) shows that the electron diffusion flux along the density gradient is reduced by the factor $1/(1 + \omega^2_{ce}/\nu^2_e)$ by the magnetic field. Thus chemical diffusion (i.e. the ambipolar diffusion of the ion cores) is also reduced by this same amount, and we may write for chemical diffusion perpendicular to the field

$$J_{\perp} = D \quad (\nabla c)_{\perp} \tag{11}$$

The diffusivity transverse to the magnetic field, D, is defined by

$$D_{\perp} = D/(1 + \omega^2_{ce}/\nu^2_e) \tag{12}$$

where D is the normal diffusion constant in the absence of a magnetic field. Eq. (10) gives the magnitude of the Hall current, however, there is no corresponding ion current in the Hall direction, since the electron density distribution is not altered by the Hall current. The medium is here assumed infinite in extent, so that no charge accumulation against surfaces is possible. In finite samples, where bounding surfaces are present, the Hall currents must close to prevent charge accumulation with its resultant Hall potential; otherwise, the Hall field will cancel (to the first order) the Lorentz force of the magnetic field. However, even for the latter case an effect of the magnetic field remains, which is due to the component of transverse

magnetoresistance arising from the (actual) non-spherical symmetry of the Fermi surface.[43] For most metals this effect is small even at temperatures near absolute zero, and becomes vanishingly small as room temperature is approached.[44]

Eq. (11) implies that the extent of chemical diffusion inhibition is independent of the magnitude of the free electron gradient. This is valid as long as there exists a finite (though small) difference in the free electron densities of the interdiffusing components. Thus, even for an electron concentration difference of only 10^{-2} the distance over which charge separation can occur is only $\sim 10^{-7}$ cm (cf. Eq. 7). Eq.(11) also suggests that diffusion inhibition is independent of the diffusion velocity, and therefore is of the same degree in both solid and liquid systems. This is a physically reasonable conclusion since an increase in the diffusion velocity would increase the cross drift velocity proportionately.

C. PLASMA OSCILLATIONS AND CHARGE SCREENING

It remains to investigate the effect of a magnetic field on charge screening in a metal, for any change in the effective potential of the ion will affect its diffusion rate. The potential of an impurity ion, calculated using the Thomas-Fermi approximation, is given by[45] (e in e.s.u.)

$$V_{(r)} \simeq \alpha \left(\frac{Ze}{r} \right) e^{-qr} \qquad (13)$$

α is a constant depending only on the charge Z, and q is the screening

parameter defined by

$$q = \left(4 \pi e^2 \; N(E_F) \right)^{1/2} , \qquad (14)$$

where $N(E_F)$ is the energy level density near the Fermi surface. Current theories[46] on the vacancy mechanism of impurity diffusion assume that the diffusion activation energy is to a large degree comprised of the electrostatic interaction energy between the diffusing ion and the vacancy. The vacancy is assumed to have an effective negative charge equal to the charge of the solvent ion, while the impurity ion is assumed to have a charge equal to the charge difference between the solvent and solute ions, and therefore may be positive or negative. Any effect of the magnetic field on the screening parameter q will be reflected in the diffusion rate through the change in V(r) and hence the activation energy.

Screening and organized oscillations of an electron gas are related manifestations of the collective behaviour of the electrons. The theory of the collective motion of electrons has been extensively developed by Bohm and Pines in a series of published papers.[47-50] The oscillation of the electron gas arises from the long range coulomb force between the electrons. If for some reason a hole or excess charge appears in the electron gas, the whole electron gas contracts or expands collectively in an attempt to maintain a uniform charge density. In so doing it will overshoot the mark creating opposite polarization, and an oscillation of the gas will set in. Thus the potential

energy of the electric field of a defect is converted to the kinetic energy of oscillation of the surrounding electron gas. The basic plasma frequency can be easily obtained using simple classical arguments (ref. 43, p. 161). It is

$$\omega_p = \left(\frac{4\pi n_e e^2}{m}\right)^{1/2} \tag{15}$$

which for the electron density in metals is $\sim 10^{16}/\text{sec}$. From the view of the collective interaction of the electrons, it is this collective oscillation of the electrons which is the basis for the mechanism of their charge screening. Comparing Eq. (14) and (15) the screening parameter q is related to the basic plasma frequency ωp thus:

$$q = \omega_p \left(\frac{m}{n_e} N(E_F)\right)^{1/2} \tag{16}$$

More fundamentally, the plasma oscillation frequency ω is a function of the wave number k, the two being related through the plasma dispersion relation. Bohm and Pines have shown that there is a maximum wave number for an organized collective mode (corresponds to a minimum wave length) beyond which collective interaction ceases, and the short range two-particle interaction forces dominate. The critical

---

-Oscillations arising through the coulomb force are longitudinal as distinguished from transverse oscillations which also occur in plasmas. The latter are electromagnetic waves, which in the presence of an external magnetic field will couple with the longitudinal waves. For $kc \gg \omega_p, \omega_{ce}$, where c is the velocity of light, the effect of the transverse waves is small and may be neglected. This situation exists for the problem of screening in metals, where wave numbers of the order of 10^7 to 10^8 cm.^{-1} are of importance.

wave number k_c turns out to be the same order of magnitude as the screening parameter q in the Thomas-Fermi approximation of the potential of the charge. Thus screening is shown to be a collective electron interaction phenomenon, and the screening parameter relates to the minimum wave length possible for collective oscillation and therefore screening. For a classical (non-degenerate) plasma k_c is shown to be $1/h_D$, the reciprocal of the Debye distance. For larger wave numbers the plasma oscillations are strongly damped as first shown by Landau.[51] The damping factor (Landau damping decrement) is the imaginary part β of the oscillation frequency expressed as a complex function, $\omega = \omega_r + i\beta$.

In the treatment of Bohm and Pines and others (see below), the ions are assumed smeared out into a positive background (random phase approximation). This neglects the perturbation and damping of the oscillations resulting from electron-ion collisions. Bohm and Pines[49] have discussed collisional damping of plasma oscillations in metals, and have shown that it is negligible in comparison to the Landau (collisionless) damping.

The behaviour of a non-degenerate electron plasma in a constant magnetic field has been investigated by Bonch-Bruevich and Mironov[52] by a different but equivalent method using Green's functions. This method has the advantage that it can treat the problem of damping and screening more effectively than the collective 'surplus variables' method

of Bohm and Pines. The plasma oscillations are considered to be polarization waves in a dielectric medium (electron gas), and the plasma spectrum and screening law are obtained from the polarization operator. Their results will be discussed briefly because of their applicability to the systems of conductivity electrons or holes in semiconductors, where the charge carrier density is low, so that the classical statistics apply. Bonch-Bruevich and Mironov have derived an expression for the effective potential of a charge, which shows explicitly the magnetic field contribution to the screening parameter. Only the general form of the solutions for the potential will be given here, which differ for the two limiting cases $r \gg h_D$ and $r \ll h_D$.* They are (for $\hbar\,\omega_{ce}/\kappa\,T \ll 1$)

$$\Phi(r)_{r \gg h_D} = \frac{Ze}{r}\exp\left[\frac{-r(1+\gamma'\sin^2\theta)}{h_D}\right] \qquad (17a)$$

and

$$\Phi(r)_{r \ll h_D} = \frac{Ze}{r}\left\{\exp\left[-\alpha r\,(1-\delta'\sin^2\theta)\right]\right\}\cos\alpha\,r(1+\delta'\,\sin^2\theta) \qquad (17b)$$

where $\alpha = \sqrt{2}\,(\pi n_e m_e e^2/\epsilon\hbar^2)^{1/4}$, ($\epsilon$ is the lattice permittivity), γ' and δ' are parameters (>0) representing the contributions of the magnetic field, and θ is the angle between the vectors $\vec{k}$ and $\vec{H}$. It is

---

*The parameter of importance determining the asymptotic solutions is $r\,\xi \lesssim 1$, where ξ is not h_D^{-1} as used here but is of the same order of magnitude.

interesting to note that for distances greater than the Debye distance screening is increased, while for distances less it is decreased (cf. Eq. 17). It can easily be shown that this is due to the increase in the Landau damping decrement by the field for the oscillations $k > h_D^{-1}$. Furthermore the field effect is anisotropic, disappearing for wave propagation parallel to the field ($\Theta = 0$). This is to be expected in the classical case since for $\Theta = 0$ the Lorentz force is absent. For germanium ($T = 300^{\circ}K$, $n_e \sim 10^{17}/cm^3$, $\epsilon = 16$) $\gamma' \sim 10^{-3}$ and $\delta' \sim 10^{-2}$ (cf. ref. 52) for a field strength of 10^5 oersteds and $\Theta = \pi/_2$. This field effect is negligible on the potential (cf. Eqs. 17) and therefore on the interaction energy of charges. Thus we conclude that for diffusion in semiconductors, moderate fields ($\leq 10^5$ oersteds) will have little or no effect on the diffusion rate via the screening mechanism.

To the knowledge of the author, the screened potential of a charge in a fully degenerate plasma, such as is approximated by the system of conduction electrons in a metal, has not heretofore been obtained. In the following a less rigorous but valid argument is presented to show that a magnetic field of $< 10^7$ oersteds will have negligible effect on screening of charges in metals. Recalling that the screening parameter q in the Thomas-Fermi approximation is related to the plasma oscillation frequency ω through Eq. (14) (to a first order of approximation), the effect of a magnetic field on q will be determined through its effect on ω and $N(E_F)$. The latter we neglect since the magnetic field does

not change the average density of the energy levels, even though it does alter their detailed distribution.[53] Any change in the detailed distribution of the energy levels will affect ω, and so will be taken into account in considering the field effect on ω.

The effect of a magnetic field on the plasma oscillations of a degenerate gas has been treated in detail by Stephen[54] (in the random phase approximation) using the Green's function technique. Stephen gives for the oscillation frequency parallel to the field (for the case of long wave lengths and low fields, and for the zero temperature limit)

$$\omega_{\parallel}^2 = \omega_p^2 + \frac{6k^2 E_F}{5\,m}\left\{1 + \frac{5}{16}\left[\left(\frac{\hbar\omega_{ce}}{E_F}\right)^2 - \frac{1}{3}\left(\frac{\hbar\omega_{ce}}{E_F}\right)^2\right]\right\}. \qquad (18)$$

The contribution of the magnetic field is given by the two terms in the square brackets, the first due to spin and the second due to orbital motion of the electrons. The field contribution is independent of k and becomes significant only at fields of 10^7 - 10^8 oersteds (cf. Eq. 18), where $\hbar\omega_{ce} \sim E_F$. For large k values (for which Eq. 18 is no longer valid), the imaginary part of the dispersion relation becomes significant indicating Landau damping of the oscillations.

The case of oscillation perpendicular to the magnetic field is complicated by the occurrence of gaps in the frequency spectrum at multiples of the cyclotron frequency. The existence and the nature of the frequency gaps has been discussed in detail by Gross[55] and Saltpeter[56]. They are comparable to the forbidden energy bands for an electron in a

solid. Wave propogation in a plasma perpendicular to a magnetic field is thus in some respects similar to the propogation of an electron-wave in a solid, in that there exists gaps at selective frequency (energy) intervals for which no wave propogation is possible. For the electron densities in metals, the frequency gaps are small and have a negligible effect on the average frequency distribution spectrum. However, for very strong fields such that $\hbar\omega_{ce} \geq E_F$, the gaps are of the order of $E_F/\hbar$ and result in the complete absence of plasma waves perpendicular to the field (see Zyranov[57]). Corresponding to Eq. (18), Stephen gives for the oscillation frequency perpendicular to the field

$$\omega_{\perp}^2 = \omega_p^2 + \omega_{ce}^2 + \frac{6k^2 E_F}{5m} \frac{\omega_p^2}{\omega_p^2 - 3\omega_{ce}^2} \left\{ 1 + \frac{5}{16} \left[\left(\frac{\hbar\omega_{ce}}{E_F} \right)^2 + \frac{2}{3} \left(\frac{\hbar\omega_{ce}}{E_F} \right)^2 \right] \right\} . \qquad (19)$$

Unlike the case for parallel propogation, there is a further field contribution besides the terms in the square brackets, which is the addition of the cyclotron frequency and the modification of the electronic energy contribution by the factor $\omega_p^2/(\omega_p^2 - 3\,\omega_{ce}^2)$. For very strong fields where $\omega_{ce} > \omega_p$ ($\sim 10^8$ oersteds), the right hand side of Eq. (19) becomes negative corresponding to the absence of oscillations. For the case of moderate fields ($< 10^5$ oersteds) and for the large k values important in charge screening in solids ($\sim 10^7 - 10^8$ cm.$^{-1}$), damping

of the oscillations results as in the field free case, but the field contribution to $\omega_\perp$ still remains $\sim\omega_{ce}$ (cf. Eq. 19). For the field strengths used in the present study (3×10^4 oersteds), $\omega_{ce} < 10^{-4}\omega_p$; so that the field effect on the charge screening parameter q and hence the activation energy may be considered negligibly small.

From the above discussion we conclude that the effect of the magnetic field on diffusion in metal alloys will be largely via the plasma-magnetohydrodynamic forces, expressed quantitatively in chemical diffusion by Eq. (11) and (12), and charge screening in the field will play a very small, if not negligible role. This requires that any field change in the diffusivity will be manifested through a change in the frequency factor D_o, and not through a change in the activation energy Q, when the diffusivity is expressed by the Arrhenius law expression $D = D_o e^{-Q/RT}$.

In summary, it should be emphasized that the theory which has been presented is not free from difficulties, particularly in the assumptions made in regarding a metal as a two-fluid plasma of ions and electrons, and applying magnetohydrodynamic and plasma dynamic equations to describe its behavior. The degree of the validity of the assumptions made in the theory will, of course, be determined by the extent to which theory and experiment agree in the present investigation and in further more refined experiments.

EXPERIMENTAL METHODS

A. THE MAGNET

The magnetic field for the diffusion experiments was obtained using a water cooled, iron-clad electromagnet which was constructed for the project from a design based on those of Dreyfus,[76] Bitter[77] and Bowen.[78] The details of the design are given in Appendix A. The magnet features a high field strength for a given power input, a property which is inherent in the iron-clad design, and efficient cooling which permits operation at high power levels without excessive heating. It is equipped with soft iron pole pieces which have a face diameter of 4 inches and gap of 1.5 inches. Power is supplied by a thirty-six kilowatt, direct current, constant voltage generator. The magnet is capable of continuous operation at field strengths in excess of 30,000 oersteds.

B. PREPARATION OF ALLOYS

The alloys were prepared from super-purity aluminum (99.98 per cent) supplied by The Aluminum Co. of Canada Ltd., and high-purity copper (99.999 per cent) supplied by Johnson, Matthey & Co. Ltd. A detailed analysis of these materials is given in Appendix B. The aluminum was in the form of an ingot which had to be cut up into small blocks to facilitate handling. After cutting in a bandsaw the aluminum was degreased in carbon tetrachloride and then thoroughly cleaned by immersion in dilute aqua-regia. The copper was supplied as small rods from

which pieces of the required size were cut with a hacksaw and then cleaned in nitric acid.

The technique of unidirectional solidification was used to obtain ingots with a known distribution of copper along the length from which the ends could be cropped to leave a section of macroscopically uniform composition.[58] The melts were made up in 200 gram lots by first melting a weighed quantity of aluminum and then adding the required amount of copper in the form of a freshly cleaned pellet. Graphite crucibles machined from National AGSX grade graphite were used to contain the melts in an open electric muffle furnace. The melts were mixed by pouring back and forth between two crucibles a total of ten times, degassed by bubbling with argon, skimmed to remove the thin oxide layer which formed on top, and then poured into a preheated graphite mold mounted on a steel base-plate. Cold water was immediately impinged on the base-plate to solidify the melt from the base upward. The ingots were then removed from the mold and cropped to remove macroscopic segregation. Each cropped ingot was further divided into two alloy pieces. The alloys were hot worked, homogenized for one week at 545°C, hot worked again and then solution annealed and quenched into cold water. In the hot working steps the alloys were reduced approximately fifty per cent in two directions, first across the diameter and then along the length. After quenching the alloys were machined on a lathe to produce uniform cylinders free from surface contamination.

The casting and cropping technique was intended to remove macroscopic segregation, and the homogenization anneal was employed to remove interdendritic segregation. The hot working steps were designed to weld up any porosity which might be present due to gas evolution during solidification. All alloys were made up to a nominal copper content of 3.0 weight per cent. Samples for analysis were obtained by machining layers from each end of the cylinders. The samples from each end were analyzed separately for copper using the iodide method[59] and in all cases excellent agreement was obtained between the two analyses indicating that the casting technique had produced alloys which were macroscopically uniform in composition. Good agreement was also obtained between the analysis and the "weighed-in" composition of the alloys, indicating that losses incurred by oxidation of the melts were negligible. The alloys were mechanically and chemically polished and examined for porosity under the microscope and also by making microhardness traverses across the faces. None of the alloys used to make diffusion couples showed any evidence of porosity.

C. BONDING METHOD

The sandwich couples consisted of a disc of alloy welded between two discs of pure aluminum. The disc composites were welded by holding at a high temperature (550°C) and pressure (sufficient to extrude pure aluminum) for a period of fifteen minutes. A diagram of the

welding unit is given in Figure 2. It consisted essentially of a stainless steel capsule, which contained the sample, restrained within a thick-walled, hollow, stainless steel cylinder by two tightly fitting end pistons. Heat was supplied by an induction coil surrounding the central portion of the cylinder. Pressure was generated by the thermal expansion of the sample and pistons against the restraining force of a heavy steel clamp. To prevent oxidation the unit was flooded with argon before assembly; the argon atmosphere was then maintained in the unit throughout the welding period by the tightly fitting end pistons. After repeated use the interior parts of the mold showed only a slight tarnish indicating that the welding atmosphere was reasonably inert.

The disc sandwiches were assembled for welding in stainless steel capsules consisting of a sleeve with tightly fitting end pieces. The use of disposable, tightly fitting capsules eliminated two problems encountered while trying to arrive at a satisfactory welding procedure. First, the welding pressure was sufficient to extrude the pure aluminum through any available opening. Second, the discs became bonded not only to each other but also to the stainless steel where there was contact during the welding operation. After welding, the stainless steel capsules were easily removed from the mold and machined away from the welded couples.

The thermocouple which was inserted into the side of the mold was used only to control the welding temperature; it did not directly indicate

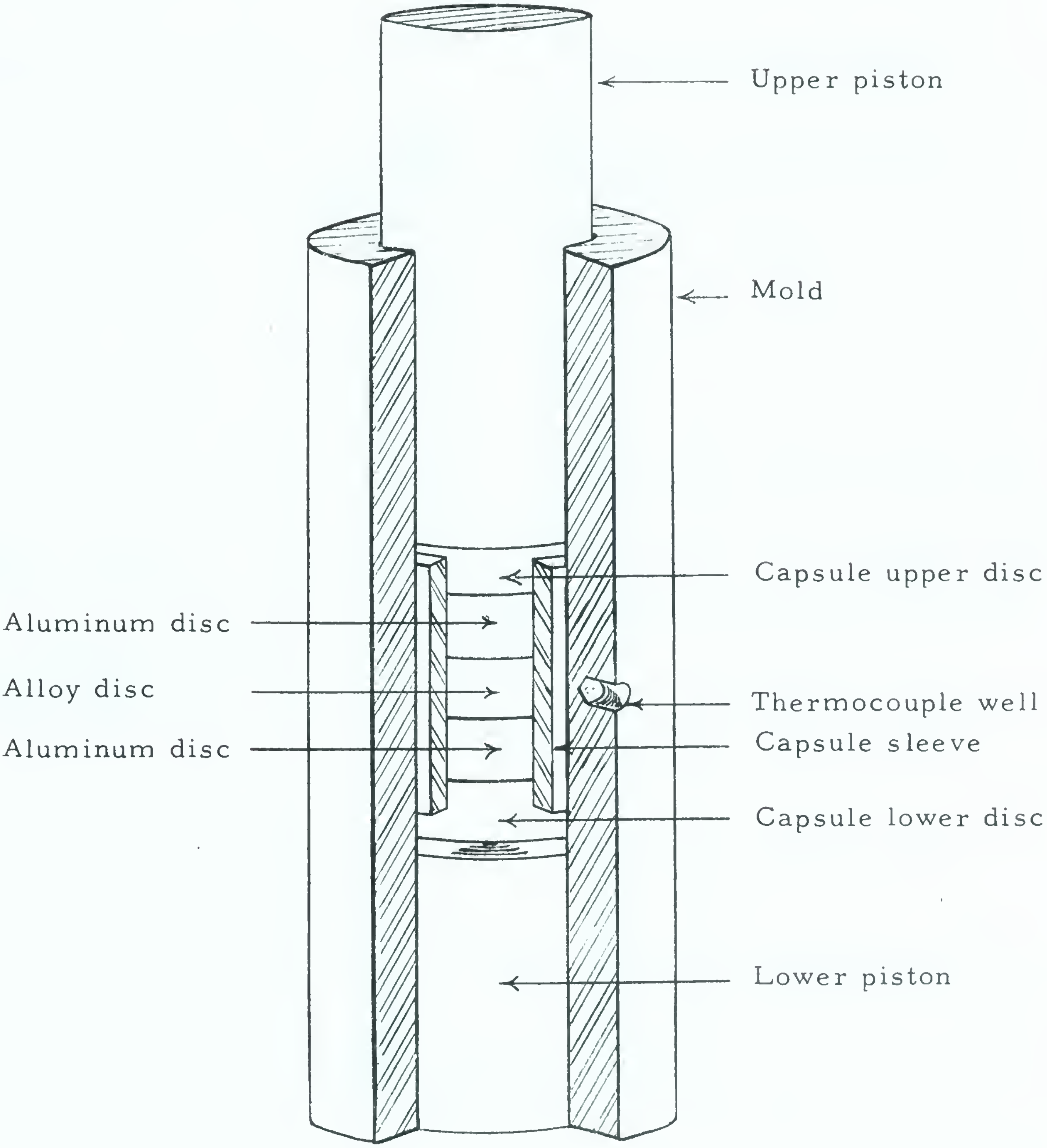

Figure 2. The stainless steel mold and capsule assembly used to weld the flat and sandwich couples.

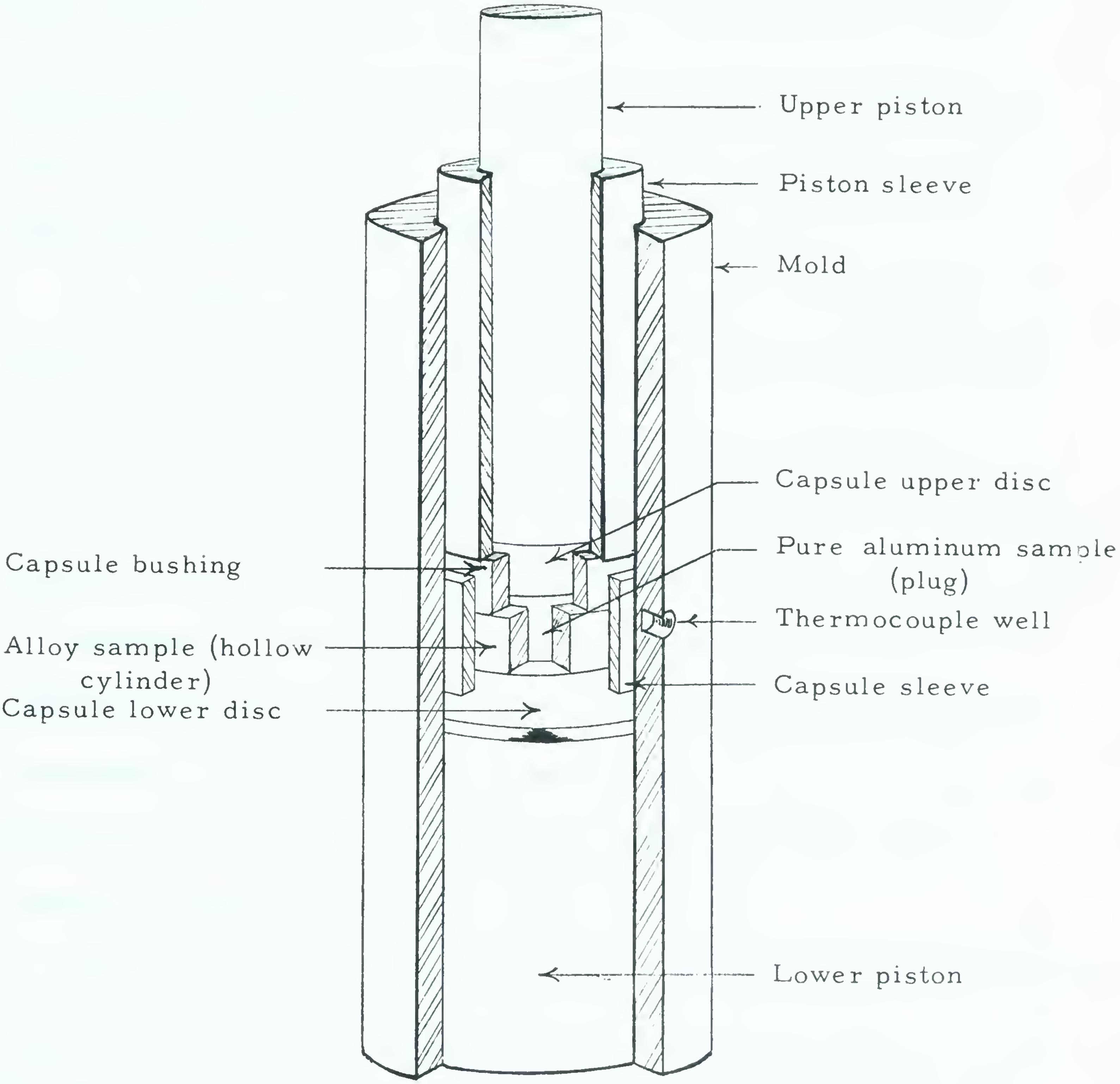

Figure 3. The stainless steel mold and capsule assembly used to weld the cylindrical couples.

the welding temperature of the diffusion couple. The relationship between the temperature of the mold wall, as indicated by the control thermocouple, and the temperature of the sample being welded was obtained by calibration using a drilled base piston through which a thermocouple was inserted into the center of a trial sample.

For cylindrical couples a sample for welding was assembled in the form of a plug of pure aluminum inserted into a hollow cylinder of alloy. Pressure generated during the welding procedure caused the pure aluminum plug to expand outward and weld to the alloy. The mold and capsule assembly used to weld the cylindrical couples is shown in Figure 3. It differed from the unit used to weld the sandwich couples in the design of the upper piston and capsule which were intended to constrain the cylinder of alloy on all sides while pressing the pure aluminum plug against its inner surface. After welding it was again necessary to machine the stainless capsule away from the couple.

The following welding procedure was used for the sandwich couples:* two pure aluminum discs and one alloy disc were first cleaned by washing thoroughly with soap and water and then rinsing with alcohol and finally with acetone. After cleaning the discs were handled only with tongs or with rubber gloves. The discs were freshly faced on a precision lathe at high speed using a diamond tool and immediately assembled in a

---

* The welding procedure for the cylindrical couples differed only in the details of the machining steps.

capsule. The capsule was placed in the mold which was flooded with argon for three minutes. The top piston was inserted and the clamp placed in position and tightened as firmly as possible. Power was applied to the induction heating unit at a rate sufficient to reach welding temperature within five minutes. The welding temperature of 550°C was maintained for fifteen minutes after which the power was shut off and the mold quickly quenched into cold water. The stainless steel capsule was then machined away from the welded couple. Considerable care was exercised during the machining operation to ensure that the weld interfaces were exactly parallel to the sides of the finished couples.

In most cases the welded disc composites were cut in half lengthwise to make a matching pair of couples (one for the field run and one for the corresponding no-field run). These couples are designated as "pair" in the table of results.

After machining, the couples were mechanically and chemically polished and then etched and examined under the microscope for soundness of weld. Any couples showing defects along the weld interface were rejected.

D. DIFFUSION ANNEALS

Duplicate couples were wrapped in aluminum foil and annealed in thin-walled tube furnaces under controlled atmosphere and temperature for periods which were calculated using published activation energy

data[11] to give approximately the same amount of diffusion at the following temperatures: 520, 540, 560 and 580°C. The basic time of four days at 540°C was chosen to give sufficient penetration to facilitate accurate analysis without requiring unduly long runs on the magnet. Additional anneals of nine days duration were made at 540°C for two corresponding pairs of field and no-field couples. All anneals were made in duplicate, one with and one without the magnetic field.

The couples were annealed under an argon atmosphere maintained at a positive pressure of a few inches of mercury. Before each diffusion anneal the furnace was purged with flowing argon for fifteen minutes. The flow was continued, at a reduced rate, during the heating-up period. The furnace was also briefly purged at 24 hour intervals during the diffusion anneal. Very little oxidation of the foil wrapper or of the couples was evident after completion of an anneal.

A diagram of the furnace assembly is given in Figure 4. The furnace consisted of a thin-walled silica tube, 18 inches long, with Kanthal A ribbon heating element wound uniformly around the central 9 inches of its length. The element was embedded in Saureisen zirconia base cement by applying a coating of cement to the tube, winding on the element in a lathe, and then applying another coating of cement. The ends of the element were secured with a few turns of Kanthal A wire which also served as terminals. The furnace was insulated by wrapping with two layers of asbestos tape secured with a layer of asbestos cement. The completed

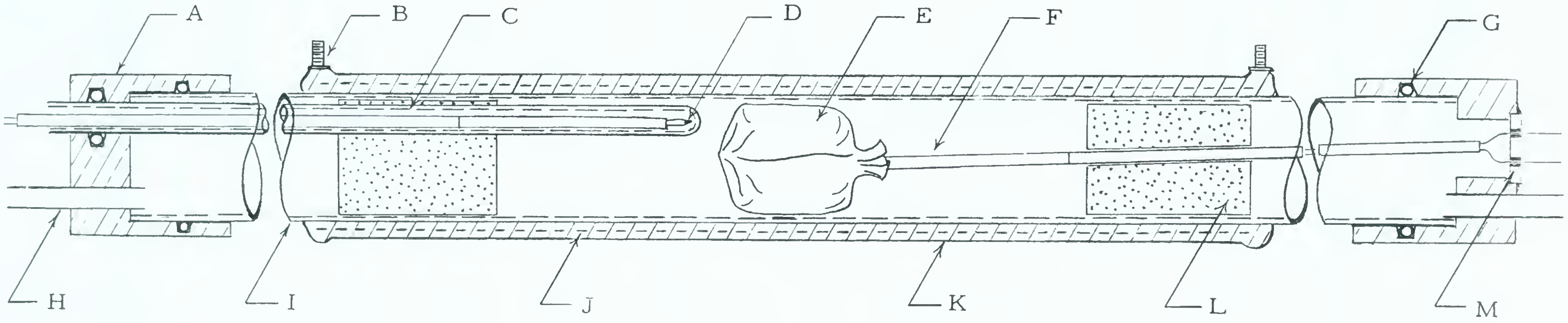

Figure 4. Furnace used for the diffusion anneals. A, brass end piece; B, terminal; C, control thermocouple shield (silica tube), D, control thermocouple; E, sample wrapped in aluminum foil; F, measuring thermocouple; G, 'o'-ring seal on end piece; H, gas inlet tube; I, silica furnace tube; J, Kanthal A winding; K, insulation; L, porous plug; M, Stupakoff insulator.

furnaces could contain samples up to one inch in diameter although the furnaces themselves had an external diameter of less than 1.5 inches. Two furnaces were constructed, each of which was used for more than 700 hours at temperatures above 500°C without failure.

The porous plugs placed at each end of the hot zone served to reduce the temperature gradients along the length of the furnaces. The temperature distribution in the central section of a furnace was obtained by embedding a thermocouple in an aluminum block and advancing the block an inch at a time through the hot zone. A ten minute stabilization interval was allowed at each position. The temperature was uniform to within one or two degrees throughout the central three inches of the hot zone in which the samples were located.

The furnace temperatures were controlled by automatic temperature controllers with on-off action controlling "high-low" power supplies. Two different kinds of controllers were used: a Wheelco Capacitrol Model 252P and a Thermo Electronic Model 80025. It might be well to emphasize at this point that in all cases the corresponding field and no-field diffusion anneals were controlled with the same instrument.

The Wheelco is a millivoltmeter type of instrument which uses a Chromel-P-Alumel thermocouple as a primary sensing element. It is sensitive to approximately a 2°C change of temperature. The control thermocouple, however, was shielded by only a thin silica tube and was very sensitive to changes in the power input to the furnace. As a result

the fluctuation in sample temperature produced by the control action of the Wheelco took place over a range of less than 0.25°C.

The Thermo Electronic Model 80025 controller is a potentiometer type instrument which also uses a Chromel-P-Alumel thermocouple as a primary sensing element. This instrument is sensitive to a one microvolt input change. In terms of temperature this is approximately equivalent to 0.03°C. The high sensitivity of this controller resulted in some control chatter during operation but the fluctuation in sample temperature produced by the control action was too small to be detected.

The "high-low" power supply consisted essentially of two variable transformers and a relay. One transformer was set to apply sufficient power to the furnace to maintain the temperature a few degrees below the set point; the other was adjusted to maintain the temperature a few degrees above the set point. The automatic controller selected power from the "high or "low" transformer by means of the relay. The power differential between the "high" and "low" settings was adjusted to approximately 50 watts.

The furnace had to be supplied with direct current power when located in the magnetic field. Alternating current produced severe vibration which very quickly disrupted the windings. Direct current power was obtained by passing the output of the "high-low" power supply through a full-wave bridge rectifier and a simple low pass filter.

Chromel-P-Alumel thermocouples (28 gauge) were used for both

control and measurement of the temperature of diffusion. The choice of this type of thermocouple was largely based on its relatively high thermoelectric power; the thermoelectric power of type-P thermocouples is about 40 μV/°C at 500°C compared to approximately 4.5 μV/°C for type-R platinum-platinum-rhodium thermocouples. The available potentiometer which was capable of sensing a change in e.m.f. of only a few microvolts could only be used for spot checks and it was possible in that case that significant temperature variations could pass without detection. It appeared desirable, therefore, to use Chromel-P-Alumel thermocouples and obtain a continuous record of the sample temperature in which fluctuations of the order of 1°C would be plainly discernible. The sensitivity of the Brown-Honeywell recorder used in these experiments (given by the manufacturer as 0.019 millivolts), was sufficient to detect and record temperature fluctuations of approximately one degree when using Chromel-P-Alumel thermocouples as the primary sensing elements.

The measuring thermocouple was insulated along its length inside the furnace with two-hole alumina insulators. The insulators were 0.125 inches in diameter and 3.0 inches long. The measuring thermocouple was inserted into one end of the diffusion couple to a depth of 0.375 inches in a hole which was drilled as shown (see Figure 5) to avoid contact between the thermocouple bead and the aluminum diffusion couple. A tight fit between the end of the thermocouple insulator and the hole in the diffusion couple served to anchor the measuring thermocouple in

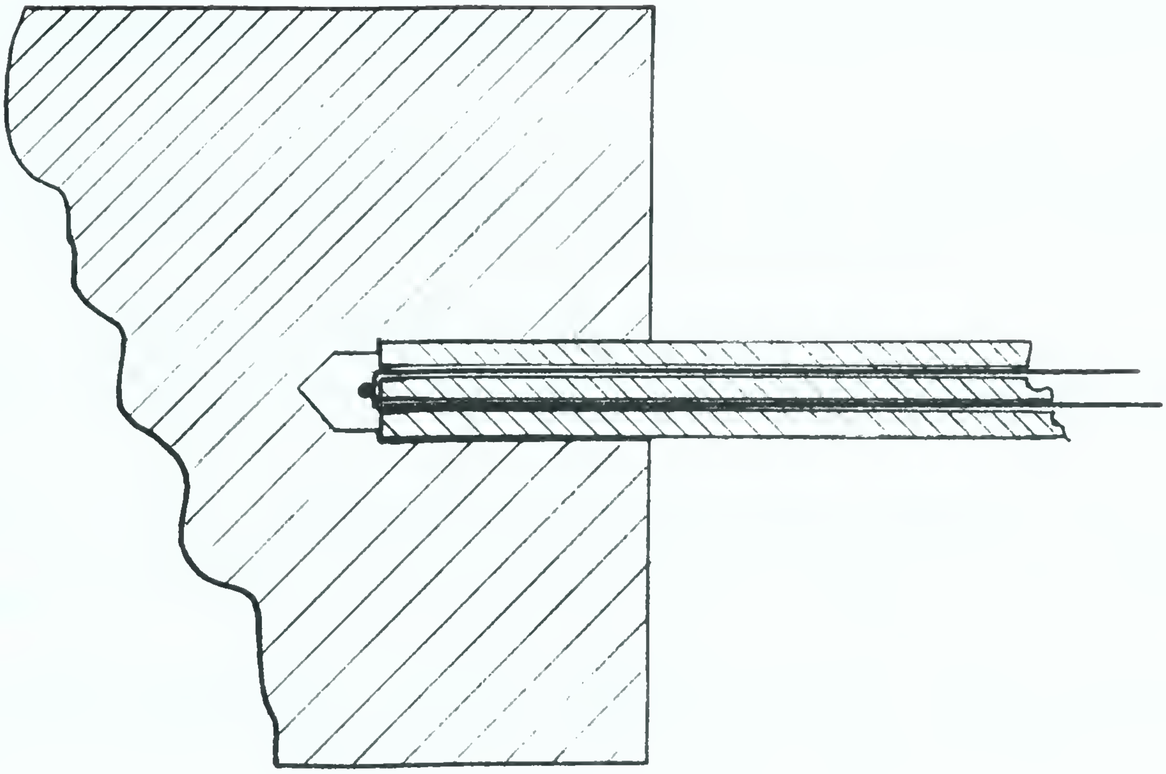

Figure 5. Measuring thermocouple inserted in well drilled in diffusion couple so as to avoid contact between the thermocouple and the sample. Scale, 3'' = 1''.

position. The measuring thermocouple wires were passed out of the furnace through a Stupakoff insulator which was soldered into the brass end piece. The thermocouple wires were connected directly to either the recorder or to the potentiometer leads immersed in the ice bath. No intervening connecting leads of copper or other materials were used. Outside of the furnace the thermocouple wires were insulated with plastic spaghetti. The thermocouples, when mounted for field runs, were placed so that the loop areas were as nearly perpendicular as possible to the direction of the magnetic field to minimize the occurrence of induced e.m.fs due to magnetic field fluctuations.

The measuring thermocouples were calibrated before and after each run in situ by comparison with a laboratory standard which was calibrated by the National Research Council. The accuracy of the calibration of the laboratory standard was given as 1°C. The furnace assembly used for calibration was the same as that used for the diffusion anneals except that the diffusion couple was replaced with an aluminum block drilled to accept the standard thermocouple close to the measuring thermocouple which was mounted in the usual way. This type of calibration was used to take into account the errors that are produced when inhomogeneities in the thermocouple wire are placed in large temperature gradients. In addition, the thermocouples when made up from the stock spools of wire were calibrated against the melting points of pure (99.9999%) aluminum and of pure antimony (99.999%). The temperature

of each furnace was checked and recorded several times each day using a Tinsley Model 3184D potentiometer and $0^{o}C$ reference junction. Between the spot checks a continuous record of the sample temperature was kept on a Brown-Honeywell Electronik multipoint recorder. The ice bath was not used for a reference junction temperature when the measuring thermocouple was connected to the recorder as the instrument has a built-in room temperature compensator. After the completion of each diffusion run the two temperature records were carefully examined and any periods of drift away from the set point were allowed for by taking a weighted average of the annealing temperature. This was done by estimating the time at which the furnace was within each one degree interval of temperature, calculating the equivalent time at the set point using published activation energy data, and adding the corrected times to obtain the total time for the diffusion anneal.

The multipoint recorder was also used to keep a continuous record of the current to the magnet. The signal for this purpose was obtained from a 1200 ampere, 50 millivolt shunt which was built into the generator. The variation in magnetic field intensity produced by fluctuations in line voltage to the generator or to other causes was less than two per cent.

E. MEASUREMENTS

1. Direct Measurement of the Kirkendall Effect

The Kirkendall shift was measured in the sandwich couples by

determining the distance between the welds before and after diffusion. Two of the couples, S-3 and S-4, had 0.003 inch diameter tungsten wires welded into the interface. For the other couples the welds themselves were used as markers.[71]

The measurements of the inter-weld distance were made on a Reichert Universal Camera Microscope, Model MEF, equipped with a round rotary mechanical stage. The stage is displacable in two directions at right angles by means of micrometer screws. The scales on the micrometer screws are marked with 0.01 mm. divisions and by interpolation it is possible to reproduce measurements with a precision of better than ±0.002 mm.

The sandwich couples were carefully positioned on the microscope with the weld interfaces parallel to one direction of travel of the stage. Thirty-five measurements were made of the distance between the welds at 0.1 mm. intervals across a central portion of the alloy core of the couples. The position of each couple on the microscope was marked so that the measurements could be made across the same area of the alloy core after the diffusion anneal.

The distance across the pure aluminum core was measured on two of the cylindrical couples. In this case twenty-five measurements were equally distributed radially across the core.

After diffusion the couples were first machined on a lathe to remove surface effects. A 0.05 mm. layer was removed from the face of each

couple using a diamond tool, high speed, and ample lubrication to obtain as smooth and strain-free a surface as possible. The couples were ground down on emery paper and chemically polished to reveal the welds after which the measurements of the inter-weld distance were repeated.

The length and width of the couples were also measured with micrometers before and after diffusion to detect any changes in overall dimensions which might take place during the diffusion anneals.

2. Microhardness Traverses across the Diffusion Zones

The method of using microhardness measurements to obtain the concentration versus distance profile of a diffusion couple, and thereby avoid sectioning, was first used extensively by Buckle[7] on aluminum alloys, and the procedure used here was largely an adaptation of his work.

The Reichert Model MIHEP-2760 microhardness tester was employed for all hardness measurements. Precise positioning of the impression is realized on this instrument by the use of a common mount for the front lens of the objective and the Vickers test diamond. Complete details of the structure and use of the hardness tester are available in the literature[60, 61] and for this reason a full description is not given here. The hardness tester was mounted on the Reichert Model MEF microscope.

Concentration versus distance data were obtained across the

diffusion zone of the couples by measuring microhardness as a function of position, and converting the microhardness readings to concentration by means of a calibration curve. The calibration curve related concentration to microhardness for a constant load of 26.3 grams.

It is usually necessary, when comparing hardness values, to use results which are based on indentations of the same diameter. This involves the determination of a complete curve of hardness as a function of indentation size and requires a completely homogeneous field on which to place a large number of hardness impressions. The usual procedure is therefore not suitable for the determination of concentration gradients in diffusion couples and recourse must be made to a method of comparing the hardness readings on the basis of constant load.

To determine the dependence of hardness on concentration a series of four standard alloys ranging from one to four weight per cent copper was prepared from super-purity aluminum and high-purity copper. The melts were made up by induction melting in recrystallized alumina crucibles, otherwise the procedure was the same as described under "Preparation of Alloys".

To obtain consistent hardness values on dilute aluminum-copper alloys it is necessary to carefully control first, the amount of age hardening which has taken place and second, the surface condition of the samples. To attain this goal, Bückle used the following technique:

the alloys were mechanically polished, solution annealed, electrolytically polished and then allowed to age harden for five days at room temperature before the hardness measurements were taken. Following Bückle, the standard alloys prepared for the present work (including a sample of pure aluminum) were mechanically polished, solution annealed, quenched and electrolytically polished. Microhardness determinations were made immediately after the electrolytic polish and at intervals of 3, 6, 24, 48, 72, 96 and 120 hours after the quench. In each determination 50 measurements were taken across the face of each of the standard alloys. After repeating the series of determinations several times it became apparent that the hardness measurements which were taken within a six hour period after the quench were the most reliable. An age-hardening period of less than six hours was therefore adopted as standard for the microhardness measurements.

An additional modification was made to Bückle's technique due to the difficulty experienced in obtaining a clean surface by electropolishing. Following a suggestion by Choi,[79] the following chemical polishing solution was prepared:

80 ml. orthophosphoric acid
12 ml. sulfuric acid
8 ml. nitric acid

The acids were all used in concentrated form. The solution was heated to 90°C and the samples immersed, face down, for a three minute period.

The solution produced a smooth polish, and the deposit which formed on the alloys was easily removed with running water.

The procedure used in preparing the diffusion couples for the microhardness measurements was as follows: A couple was first resurfaced on a lathe, using a very sharp diamond tool, to a depth of 2 mm. to remove all surface effects. Next, the couple was mechanically polished by grinding down through 240, 320, 400 and 600 grit emery paper and finishing on a nylon lap with levigated alumina. The emery papers and the lap were kept well lubricated with soap to obtain a bright surface as free as possible from embedded particles of abrasive. The couple was then given a solution anneal for 15 minutes at 545°C in a bath of molten sodium nitrate. A salt bath was used for solution annealing in order to remove the uncertainty in time introduced by the heating-up portion of an anneal carried out in an ordinary furnace. The couple was quenched out of the salt bath into water at a temperature of 25°C. After chemical polishing for three minutes at 90°C the couple was ready for the microhardness measurements which were started immediately.

The first step in making the microhardness measurements on a sandwich couple was to align the couple on the microscope with the weld interfaces exactly parallel to one direction of stage travel. The hardness indentations were accurately placed in rows perpendicular to the welds by traversing along the other direction of travel, which was mechanically aligned perpendicular to the first, by means of a

micrometer screw.

The cylindrical couples presented a different problem in alignment; the centre of the pure aluminum core had to be accurately located and marked. The rows of identations radiated out across the diffusion zone from this central point.

Three indentations were placed at each 0.05 mm. interval across the diffusion zone using the welds as reference lines for accurate positionsing. For the sandwich couples the indentations were distributed among twelve rows, six across each of the diffusion zones; the distribution was such that the mean of the three readings at each 0.05 mm. interval included readings from each of the two diffusion zones. The spacing between individual indentations in each row was 0.200 mm. For the flat couples the rows of indentations were distributed across the single diffusion zone, for the cylindrical couples the rows were radially distributed at equal intervals around the diffusion zone.

The length of the rows of hardness indentations varied with the duration of the diffusion anneal. For couples which were given a diffusion anneal of 4 days at 540°C or an equivalent time at a different temperature, the rows of indentations extended out from the weld for a distance of 1.05 mm. into the alloy and for a distance of 1.50 mm. into the pure aluminum. For couples which had been given a diffusion anneal of nine days at 540°C the rows extended 1.50 mm. into the alloy and 2.50 mm. into the pure aluminum.

In addition to the rows across the diffusion zone fifty indentations were made both in the alloy and in the pure aluminum. These indentations were placed in areas adjacent to the diffusion zones, usually as an extension to the other rows.

The complete series of indentations was made in as short a time as possible without stopping to make any measurements. The indentations were usually completed three hours after the couple was quenched. The series of measurements made on the standard alloys had revealed no detectable increase in hardness due to aging at room temperature for up to six hours after quenching. The hardness indentations made on the alloy portion of the diffusion couples were well distributed throughout the three hour period in which the traverses were completed and no systematic hardening of the alloy was indicated by the measurement of these indentations in any of the couples.

TREATMENT OF DATA

The hardness value, H_m, corresponding to the length of the indentation diagonal, d, is given by[60]

$$H_m = \frac{VP}{d^2} \text{ kg/mm}^2 \quad , \qquad (20)$$

where V is a constant which depends on the geometry of the indenter, and P is the load which was also held constant for this work. Eq. (20) was combined with the linear relationship between hardness and composition (determined by calibration) to give the following simple expression from which concentration was calculated from the diagonal length of the indentations:

$$\frac{c_x}{c_o} = \frac{\dfrac{1}{(d_x)^2} - \dfrac{1}{(d_{Al})^2}}{\dfrac{1}{(d^2{}_{Ay}} - \dfrac{1}{(d_{Al})^2}} \quad , \qquad (21)$$

where c_o = core concentration in atomic per cent copper

c_x = concentration at distance x from the weld

d_x = indentation diagonal at point x

d_{Al} = indentation diagonal of pure aluminum

d_{Ay} = indentation diagonal of the alloy core

The value used for d_x was the mean diagonal length for the three indentations made at a distance x from the weld. The diagonals d_{Al} and d_{Ay} were each the mean values for fifty indentations made in areas of the pure aluminum and of the alloy core adjacent to the zone of diffusion. The concentration at each indentation position was calculated

in this manner instead of being read directly from the calibration curve to improve the accuracy of the data. The calculation of the concentration - distance profile for a couple then assumed a linear relationship for concentration and hardness between the hardness readings on the pure aluminum and on the alloy as determined for that particular couple. While the readings on the pure aluminum and on the alloy always agreed within one or two per cent of the standard values, plots of the concentration - distance data on probability paper were improved, especially near the ends of the ranges, by allowing for slight variations in the condition of the individual couples.

The concentration ratios c/c_o versus distance from the weld interface were plotted on probability paper and a best fit line drawn through the points. This line then served as a basis from which the concentration-penetration curve was plotted which most accurately represented the experimental data.

Probability paper as used in statistics permits the plot of a cumulative normal (or Gaussian) distribution as a straight line. This is accomplished by using a special ruling of the ordinate axis, viz. a scale where the values of the error function $\Phi(u)$ are plotted instead of the values of the argument u. This scale has one disadvantage in that it is difficult to interpolate between the lines. An equivalent plot of diffusion data may be made on ordinary graph paper as follows: Calculate the values of $A = 2(c/c_o - 0.5)$ for each point. Obtain from

tables the values of the argument u for the error function corresponding to each function value A. Plot the u values as ordinate, with the zero line in the center, against the position coordinate x as abscissa. In this way a probability plot may be made of diffusion data on ordinary graph paper to any scale desired. If the data plots as a straight line a regression line may be calculated by the method of least squares. This technique was applied to obtain the probability plots for couples C-1 and C-2. The regression line for each couple was obtained for the concentration range 0 - 1.0 atomic per cent copper over which the data plotted as a straight line.

If the diffusion coefficient D is not a function of position, Fick's second law of diffusion becomes,

$$\frac{\partial c}{\partial t} = D \frac{\partial^2 c}{\partial x^2} , \qquad (22)$$

where x is the distance, c is the concentration of the diffusing substance, and t is the time. The boundary conditions appropriate to the present problem for which a solution is desired are:

$c = 0$ for $x < 0$ at $t = 0$

$c = 0$ for $x \rightarrow -\infty$, all t

$c = c_o$ for $x > 0$ at $t = 0$

$c = c_o$ for $x \rightarrow +\infty$, all t

where c_o is a constant representing the initial concentration of the alloy side of the interface. The solution of Eq. (22) for the given

boundary conditions is given by[62]

$$\frac{c}{c_o} = 1/2 \left[1 + \phi\left(\frac{x}{2\sqrt{Dt}}\right) \right] , \qquad (23)$$

where

$$\phi\left(\frac{x}{2\sqrt{Dt}}\right) = \frac{2}{\sqrt{\pi}} \int_o^{x/2\sqrt{Dt}} e^{-\omega^2} d\omega \qquad (24)$$

in the Gauss error function.

On probability paper, any data accurately satisfying Eq. (23) will plot as a straight line, the slope of which depends only on the product Dt. The plot on probability paper furnishes an accurate test of the constancy of D with composition, for if D varies with composition the line will curve. In this case a concentration dependent solution must be found from

$$\frac{\partial c}{\partial t} = \frac{\partial}{\partial x} \left(\frac{D \partial c}{\partial x} \right) . \qquad (25)$$

Providing the initial conditions can be described in terms of the one variable $\eta = x/\sqrt{t}$, c is a function only of η and Eq. (23) can be transformed into the ordinary homogeneous differential equation

$$- \frac{\eta}{2} \frac{dc}{d\eta} = \frac{d}{d\eta}\left(D \frac{dc}{d\eta}\right) \qquad (26)$$

The solution obtained for D by integration of the ordinary differential equation Eq. (26) is[63]

$$D (c) = \frac{1}{2t} \left(\frac{dx}{dc}\right)_{c=c_1} \int_o^{c_1} x dc , \qquad (27)$$

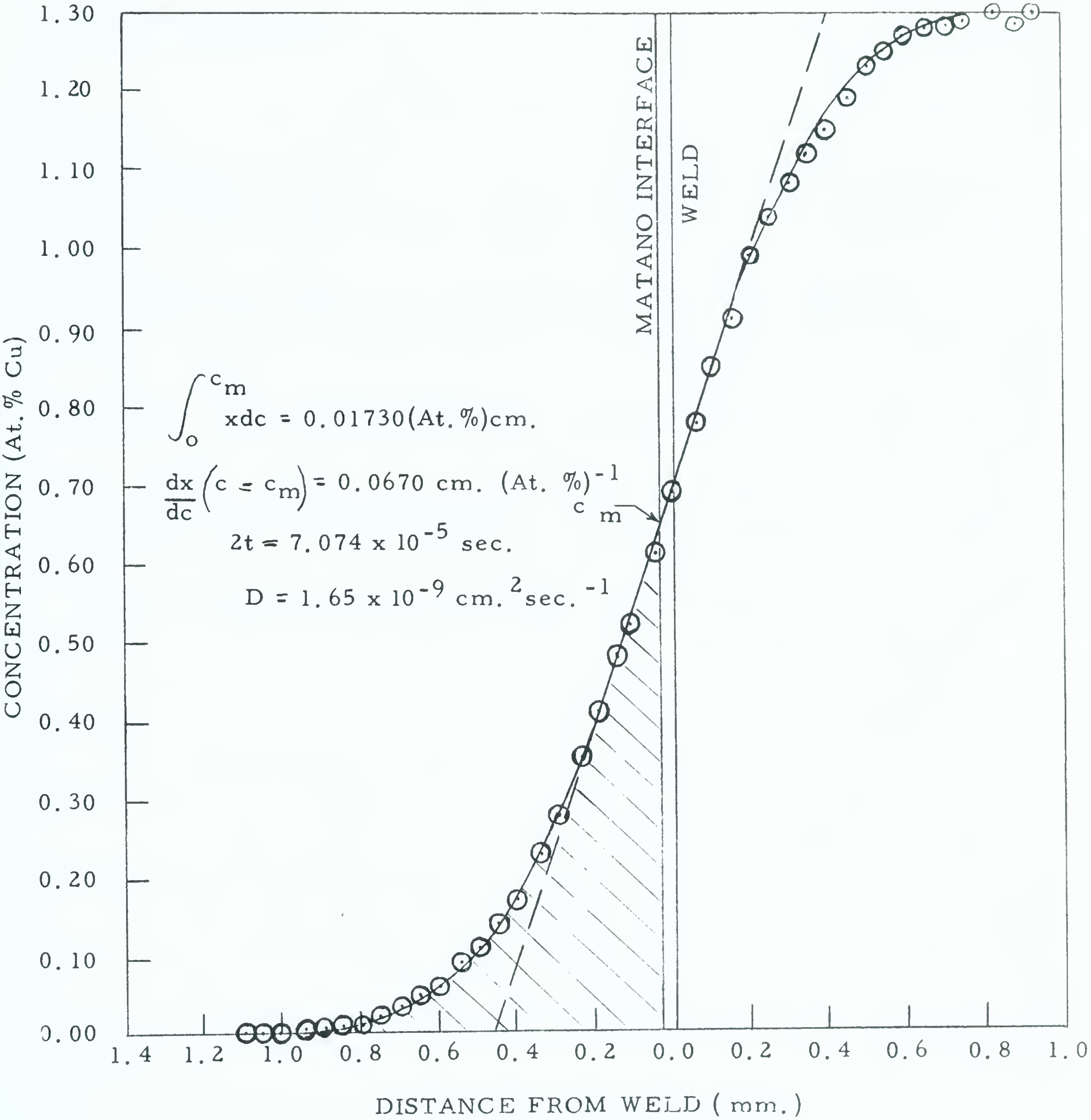

Figure 6. Calculation of the interdiffusion coefficient for couple S-6 at the position of the Matano interface.

with the condition that

$$\int_{0}^{c_o} x\,dc = 0 \qquad (28)$$

which defines the plane at x = 0. Eq. (27) is the well known Boltzmann-Matano solution of the diffusion equation for D = D(c). To obtain values of the diffusion coefficient D by the Boltzmann-Matano method the terms of Eq. (27) are evaluated graphically from the concentration-penetration curve. The method, which is illustrated in Figure 6 for couple S-6, was used to obtain the diffusion coefficients for the present work. To minimize errors in the measurement of slopes the diffusion coefficients were all evaluated at the position of the Matano interface.

RESULTS

The calibration curve of composition (atomic per cent copper) versus hardness (diamond pyramid units) is given in Figure 7. The curve for alloys of the present work and that determined by Buckle are given for comparison. The important feature of the curves is that they both indicate a linear relationship between composition and microhardness. Buckles hardness values, however, are slightly higher. This could be attributed to a number of factors but more probably to the degree of age hardening and the indentation load used.

A summary of the diffusion results of 17 diffusion couples is given in Table II. For each diffusion couple annealed in the magnetic field, there is a corresponding no-field couple for direct comparison of the results. For 7 pairs of couples both the field and no-field couples came from the same welded composite, and these couples have been designated in the table as 'pair'. The procedure of 'pairing' the field and no-field diffusion couples was used to eliminate differences which might arise from welding or from the composition of the base alloys. The diffusion couples have been further designated by the letters S, F, or C in column 2, and by F, NF, and PF in column 3, corresponding respectively to sandwich, flat, or cylindrical couples, and field, no-field and parallel field anneals. All the field anneals were carried out in fields of 30 kilo-oersteds except for couple S-32 which was annealed in a field of 20 kilo-oersteds. The diffusivities given in column 8 were

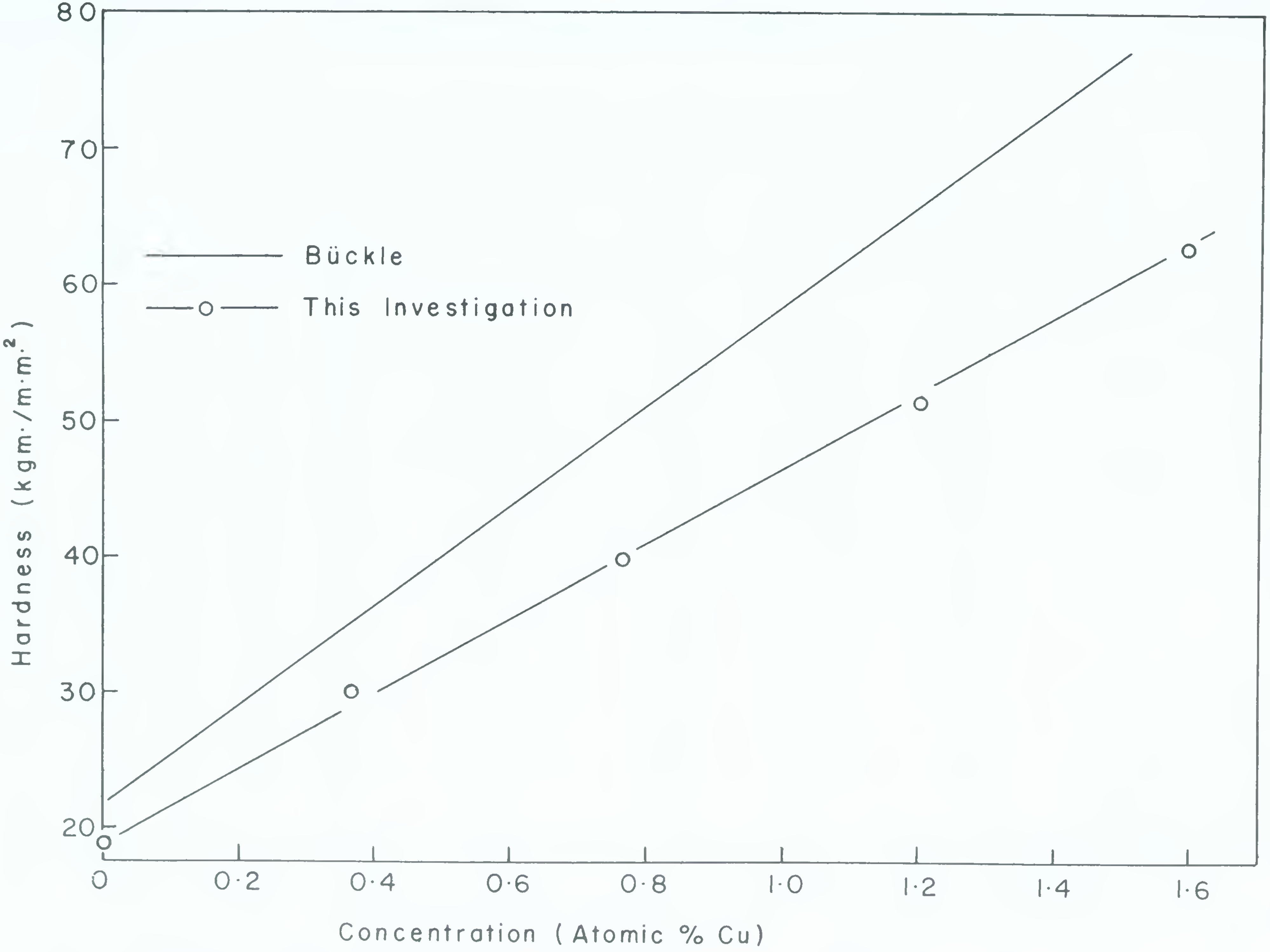

Figure 7 - Calibration curve of microhardness versus concentration for dilute aluminum-copper alloys. The curve for the present work represents measurements made with a constant load of 26.3 grams on alloys aged for less than six hours at room temperature. Buckle's(7) curve (load not given) for alloys aged for five days is given for comparison.

TABLE II

SUMMARY OF DIFFUSION RESULTS

Couple Designation			Temp. (°C)	Time (sec. x 10^{-5})	Core at % Cu	Matano Area cm. at % Cu x 102	D cm^2/sec. x10^9	$\frac{D_F}{D_{NF}}$	$\frac{A_F^2}{A_{NF}^2}$
pair	C-1	F*	540	7.767	1.41	2.510	1.35	0.75	0.78
	C-2	NF	540	7.776	1.41	2.840	1.80		
	C-4	F	540	3.524	1.18	1.445	1.35	0.79	0.79[‡]
	C-7	NF	540	3.534	1.26	1.710	1.70		
	F-1	F	540	7.803	1.26	2.220	1.25	0.74	0.78
	F-2	NF	540	7.812	1.26	2.520	1.70		
	S-7	F	540	3.537	1.30	1.520	1.25	0.76	0.77
	S-6	NF	540	3.492	1.30	1.730	1.65		
pair	S-18	NF	540	3.618	1.27	1.835	1.75	0.97	0.97
	S-19	PF	540	3.606	1.27	1.810	1.80		
pair	S-20	F	520	5.722	1.26	1.550	0.85	0.74	0.73
	S-21	NF	520	5.732	1.26	1.810	1.15		
pair	S-24	F	560	2.192	1.26	1.580	2.20	0.73	0.76
	S-25	NF	560	2.214	1.26	1.810	3.00		
pair	S-28	F	580	1.418	1.26	1.560	3.35	0.76	0.74
	S-29	NF	580	1.416	1.26	1.815	4.40		
	S-32	F	540	3.526	1.25	1.620	1.50	0.87	0.88[†]

*H - 30 kilo-oersteds for all couples except S-32 for which H - 20 kilo-oersteds.

[‡] Matano area of C-7 corrected to 1.18% core concentration for comparison.

[†] Compared to mean value of Matano areas for C-7, S-6 and S-18, corrected to 1.25% core concentration.

calculated from the diffusion penetration curves, using the Boltzmann-Matano method, for the concentrations at the Matano interfaces. Typical penetration curves for the field and no-field anneals are shown in Figures 8 and 9 for the sandwich (S-7, S-6) and cylindrical (C-1, C-2) couples respectively. The penetration curves were plotted from points taken from the composition ratio (c/c_o) versus distance (from the weld interface) curves plotted on probability paper. The probability plots corresponding to the diffusion penetration curves of Figures 8 and 9 are shown in Figures 10 and 11 respectively. The method of plotting the initial diffusion results on probability paper and then replotting the penetration curves was used to obtain the most accurate curves, since any anomalous points are smoothed out on the probability plots. The effect on the Matano areas is negligible but the accuracy and consistency of slope measurements is considerably improved. The probability plots are linear except at the extreme high alloy end of the diffusion couples indicating that diffusivity is independent of concentration over most of the concentration range. The relationship between diffusivity and concentration is illustrated more directly in Figure 12 where the diffusion coefficients are plotted as a function of concentration for couples S-6 and S-7. In column 9 of Table II the ratios of the field to no-field diffusivities are given, calculated from the D values in the previous column. This ratio is again given in the last column, but it is calculated from the ratio squared of the Matano areas (total

area under the concentration curve and the Matano interface). It is assumed that this latter method gives the most accurate determination of the field effect on D, since no slope determinations are required as in the former case. It can be shown by integration of the diffusion equation that for the case of no concentration dependence the diffusivity is proportional to the square of the Matano area. In Figure 13 the curves of the variation of the Matano area versus $(\text{time})^{1/2}$ are given for the cylindrical no-field and field diffusion couples C-1, 2, 4 and 7. Figure 14 gives the Arrhenius plots for the no-field and field results from which the activation energies for the diffusion process may be obtained. Table III lists the results for the direct measurements of the Kirkendall shift and the over-all dimensional changes of the couples during the diffusion anneals. Tables IV to VIII give the concentration - distance data from which the interdiffusion coefficients were calculated.

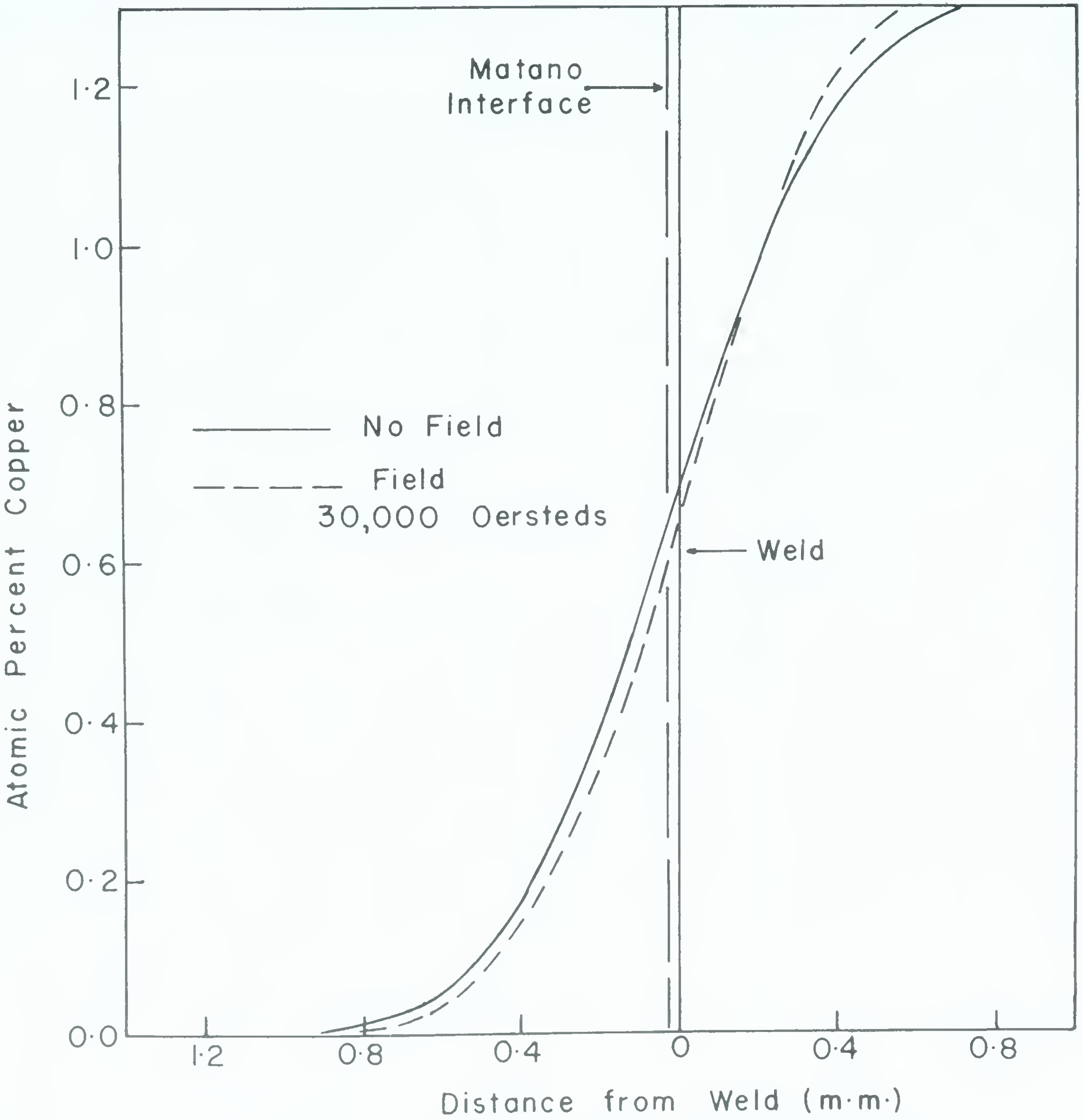

Figure 8 - Comparison of penetration curves for sandwich couples S-6 (no-field) and S-7 (field) annealed for four days at 540°C.

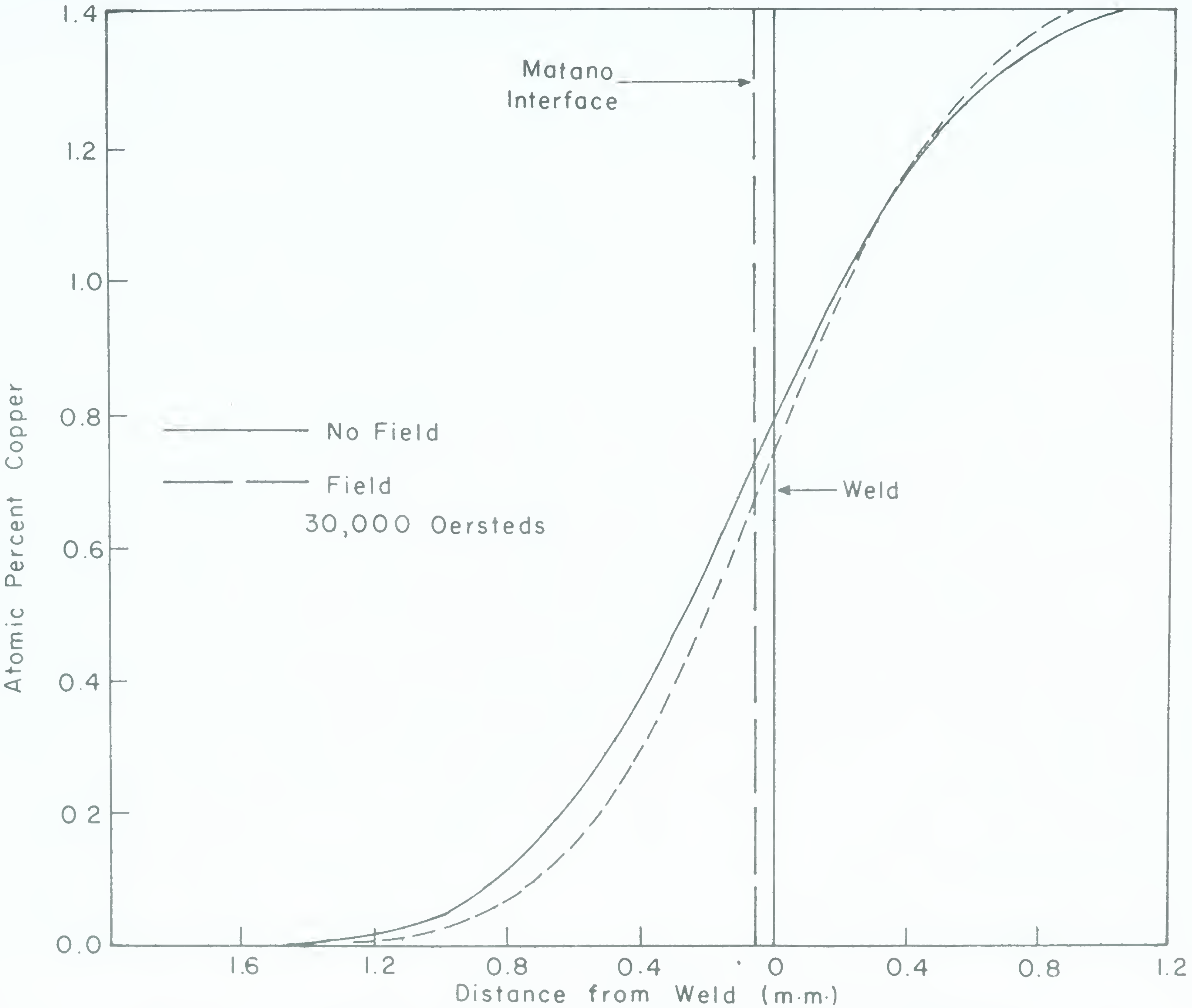

Figure 9 - Comparison of penetration curves for cylindrical couples C-1 (field) and C-2 (no-field) annealed for nine days at 540°C.

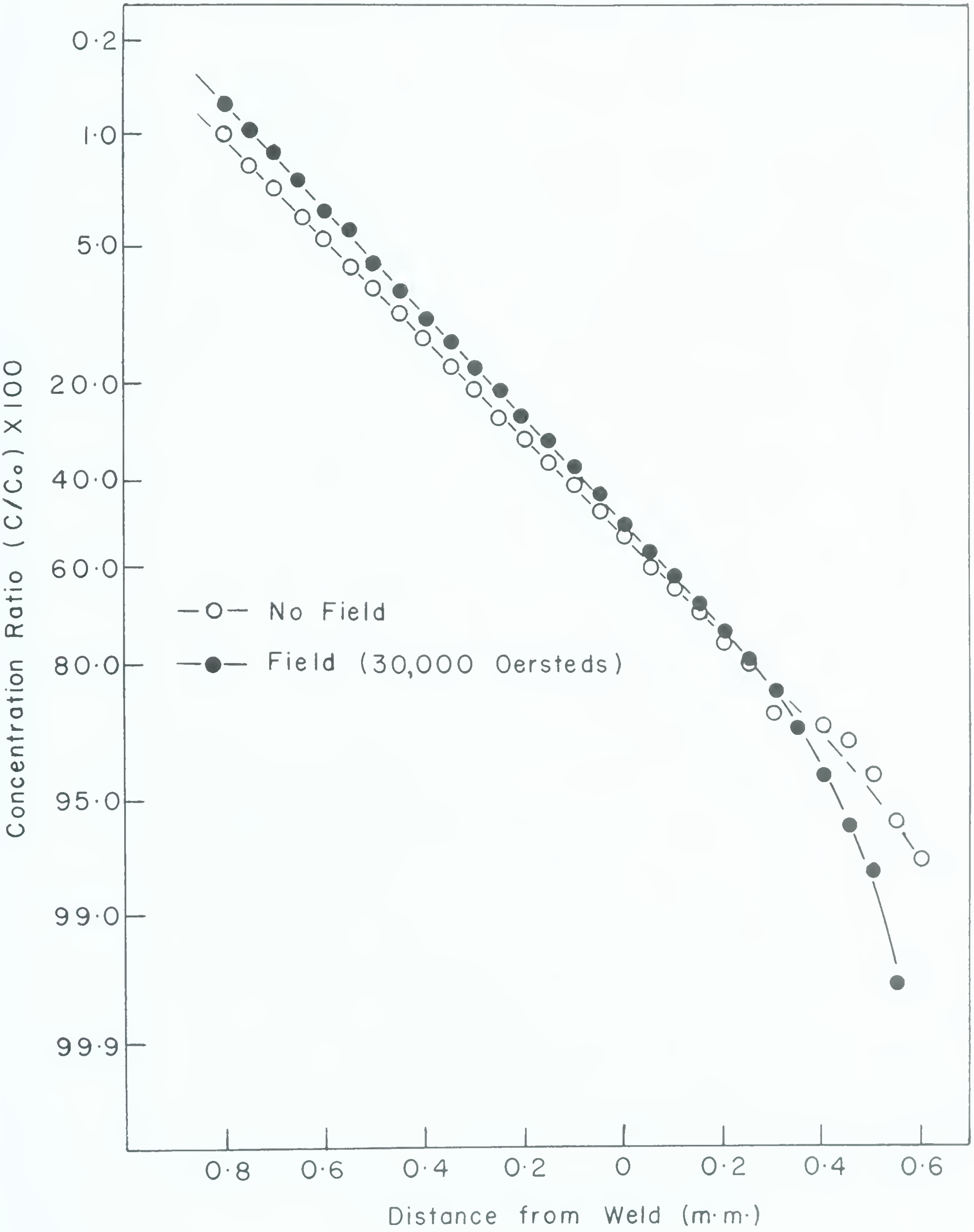

Figure 10 - Comparison of probability plots for sandwich couples S-6 (no-field) and S-7 (field) annealed for four days at 540°C.

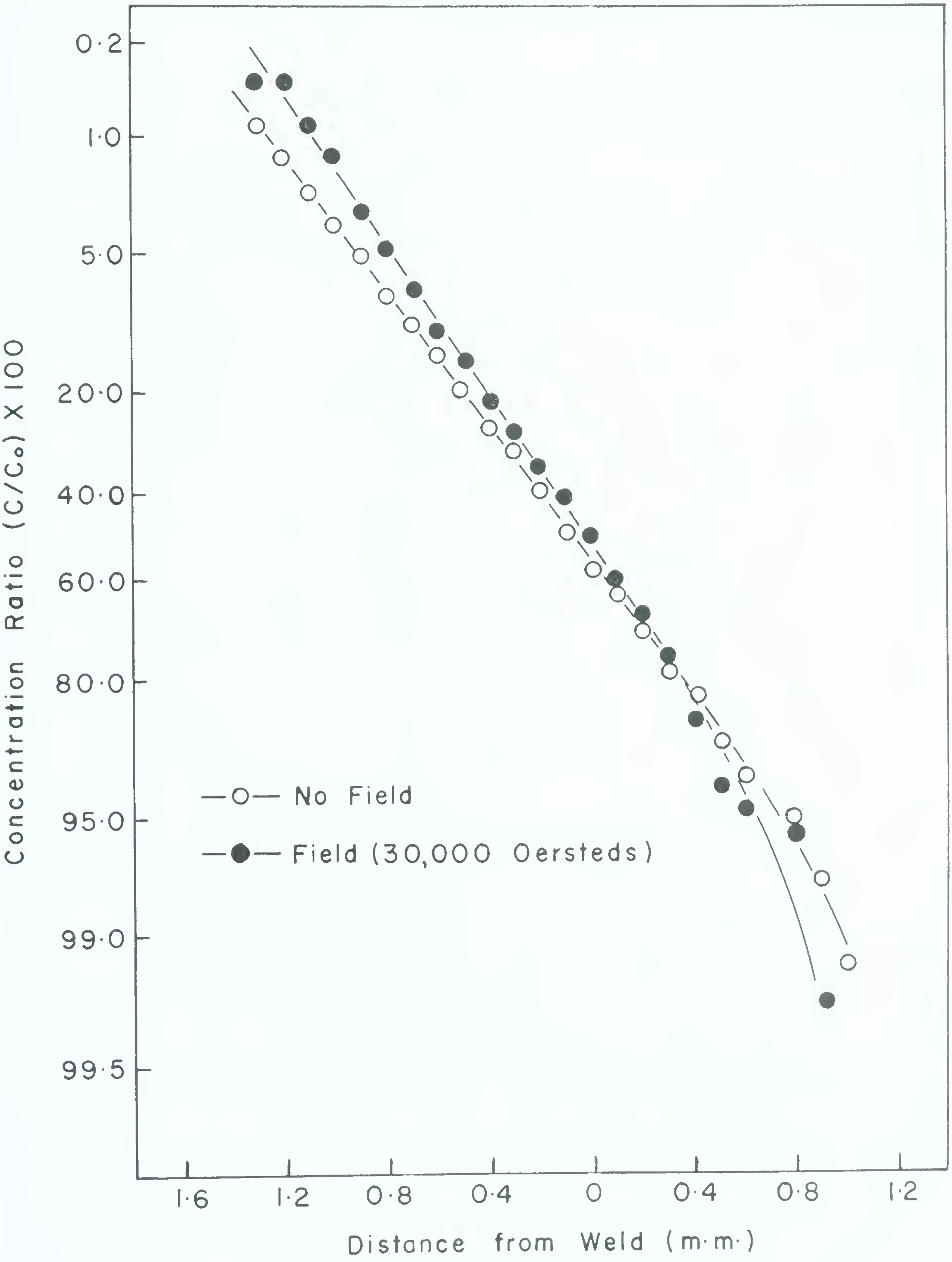

Figure 11 - Comparison of probability plots for cylindrical couples C-1 (field) and C-2 (no-field) annealed for nine days at 540°C.

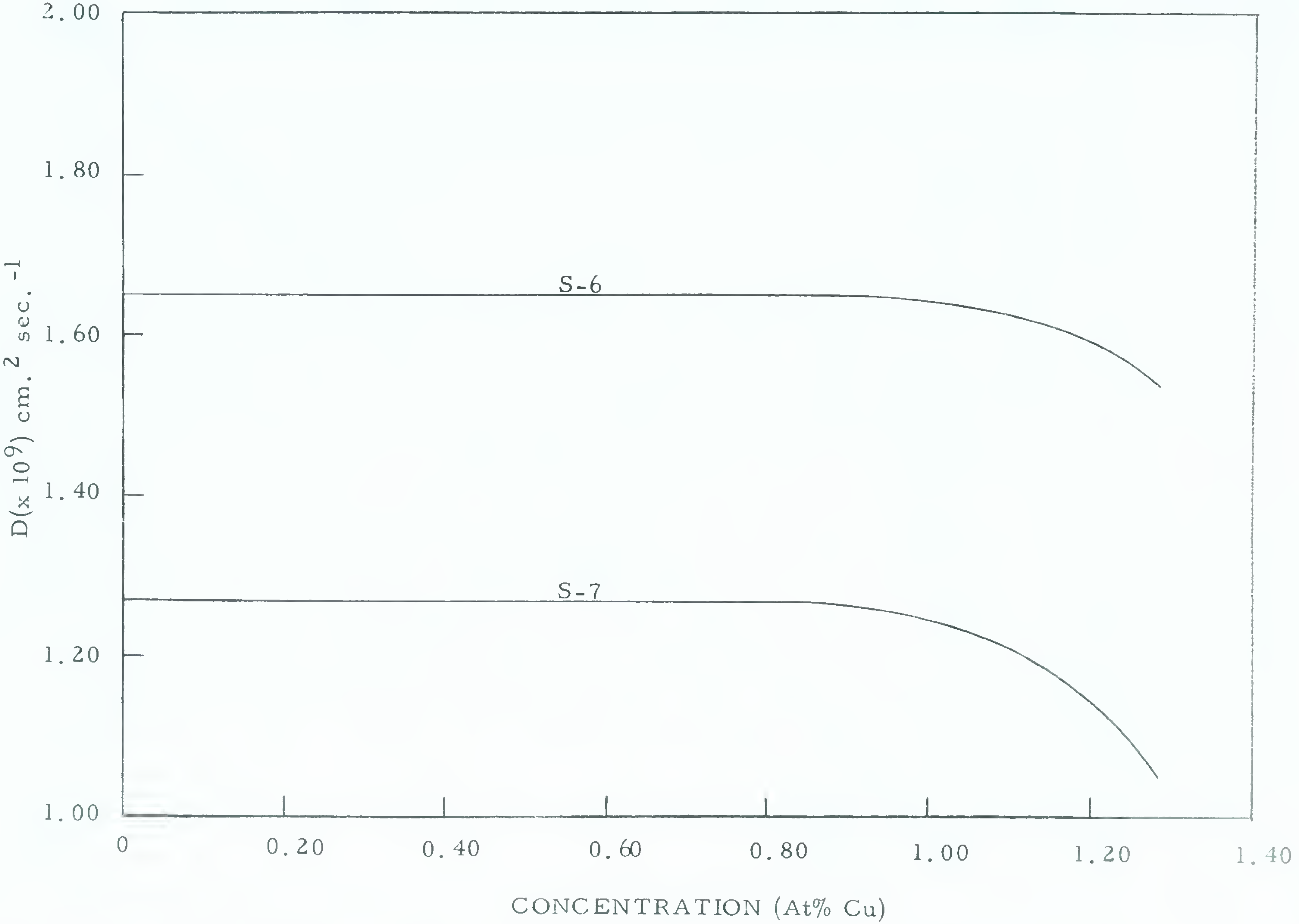

Figure 12. Variation of the interdiffusion coefficients with concentration.

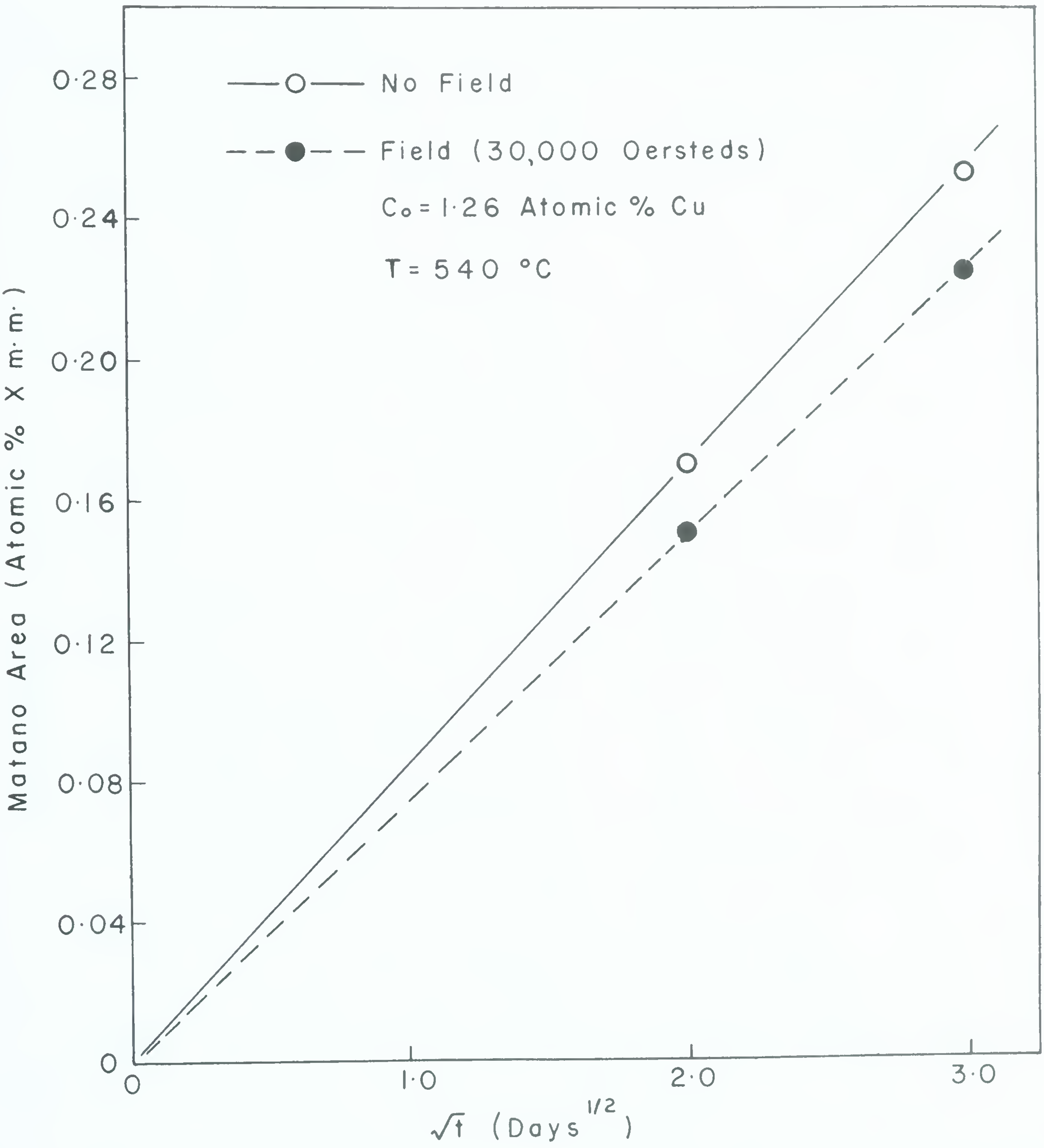

Figure 13 - Matano area versus $(\text{time})^{1/2}$.

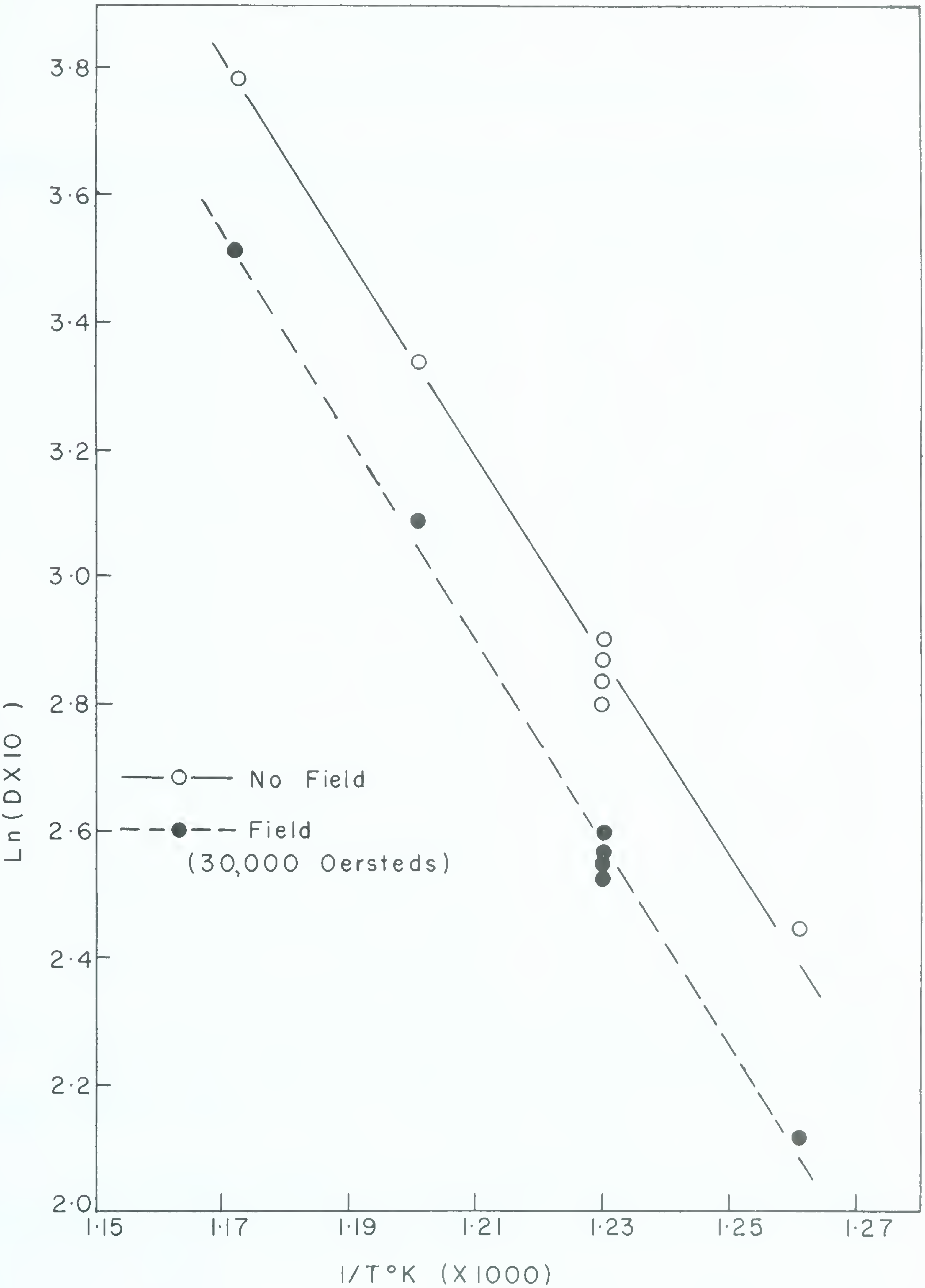

Figure 14 - Variation of field and no-field interdiffusion coefficients with temperature.

TABLE III

KIRKENDALL SHIFTS AND DIMENSIONAL CHANGES

Couple No.	Kirkendall Shift[*] (cm. x 2 x 10^3)	ΔL[‡] (cm. x 10^3)	ΔW[‡] (cm. x 10^3)
C-4	0.1		+0.8
C-7	0.4		+0.3
S-6	-2.5	+0.8	-1.2
S-7	-0.3	-1.0	+2.1
S-18	-0.3	-1.2	-0.3
S-19	-1.8	-2.5	-0.8
S-20	-0.3	-3.6	-2.0
S-21	-0.3	+4.1	-1.5
S-24	-1.1	+0.3	-0.3
S-25	-2.1	+2.0	0.0
S-28	-0.3	-0.3	-0.3
S-29	-0.3	-3.8	-2.8

[*] The shift represents the change in interweld distance across the pure aluminum core of the cylindrical couples and across the alloy core of the sandwich couples.

[‡] The sandwich couples were approximately 2.5 cm. long and 2.0 cm. wide. For the cylindrical couples, which were 2.0 cm. in diameter, ΔW represents the change in diameter.

TABLE IV

CONCENTRATION-DISTANCE DATA

Distance from Weld (mm)	Concentration (At. % Cu.) C-1	C-2	F-1	F-2
1.20	1.39	1.41	1.25	1.27
1.15	1.42	1.40	1.26	1.26
1.10	1.41	1.44	1.26	1.28
1.05	1.43	1.40	1.23	1.25
1.00	1.40	1.41	1.27	1.26
0.95	1.40	1.39	1.26	1.25
0.90	1.38	1.38	1.26	1.24
0.85	1.37	1.36	1.26	1.24
0.80	1.35	1.35	1.26	1.24
0.75	1.34	1.35	1.25	1.22
0.70	1.33	1.36	1.24	1.22
0.65	1.33	1.34	1.22	1.16
0.60	1.33	1.31	1.20	1.14
0.55	1.35	1.29	1.18	1.12
0.50	1.31	1.27	1.16	1.09
0.45	1.28	1.27	1.14	1.05
0.40	1.21	1.20	1.10	1.02
0.35	1.16	1.15	1.05	0.97
0.30	1.07	1.10	0.99	0.92
0.25	0.99	1.06	0.97	0.91
0.20	0.94	1.00	0.95	0.85
0.15	0.89	0.93	0.88	0.82
0.10	0.86	0.88	0.80	0.77
0.05	0.75	0.85	0.73	0.73
0.00	0.72	0.81	0.69	0.69
0.05	0.64	0.76	0.73	0.73
0.10	0.59	0.69	0.60	0.61
0.15	0.54	0.63	0.53	0.56
0.20	0.48	0.56	0.48	0.52
0.25	0.43	0.50	0.44	0.46
0.30	0.39	0.44	0.39	0.40
0.35	0.35	0.41	0.35	0.38
0.40	0.30	0.36	0.31	0.33
0.45	0.26	0.32	0.26	0.29
0.50	0.22	0.27	0.23	0.26
0.55	0.20	0.24	0.20	0.22

TABLE IV (continuted)

CONCENTRATION-DISTANCE DATA

Distance from Weld	Concentration (At. % Cu.)			
(mm)	C-1	C-2	F-1	F-2
0.60	0.16	0.21	0.17	0.19
0.65	0.14	0.18	0.14	0.17
0.70	0.11	0.15	0.12	0.13
0.75	0.09	0.13	0.10	0.11
0.80	0.07	0.11	0.08	0.09
0.85	0.06	0.09	0.05	0.08
0.90	0.04	0.07	0.04	0.06
0.95	0.03	0.06	0.04	0.05
1.00	0.02	0.05	0.03	0.04
1.05	0.02	0.03	0.02	0.04
1.10	0.01	0.03	0.01	0.03
1.15	0.01	0.02	0.01	0.03
1.20	0.01	0.02	0.01	0.02
1.25	0.01	0.01	0.00	0.02
1.30	0.00	0.01	0.00	0.01
1.35	0.00	0.01	0.00	0.01
1.40	0.00	0.01	0.00	0.01
1.45	0.00	0.00	0.00	0.00
1.50	0.00	0.00	0.00	0.00

TABLE V

CONCENTRATION-DISTANCE DATA

Distance from Weld (mm)	Concentration (At. % Cu.)			
	C-4	C-7	S-6	S-7
1.00	1.18	1.26	1.31	1.30
0.95	1.20	1.26	1.30	1.31
0.90	1.18	1.26	1.28	1.27
0.85	1.17	1.24	1.30	1.29
0.80	1.18	1.25	1.33	1.34
0.75	1.20	1.27	1.29	1.30
0.70	1.18	1.26	1.28	1.30
0.65	1.19	1.25	1.28	1.32
0.60	1.18	1.25	1.27	1.30
0.55	1.17	1.23	1.24	1.29
0.50	1.15	1.21	1.23	1.28
0.45	1.12	1.18	1.19	1.26
0.40	1.09	1.14	1.15	1.21
0.35	1.04	1.11	1.12	1.16
0.30	1.01	1.07	1.08	1.10
0.25	0.94	1.01	1.04	1.03
0.20	0.90	0.94	0.99	0.97
0.15	0.84	0.89	0.91	0.89
0.10	0.78	0.82	0.85	0.82
0.05	0.70	0.79	0.78	0.74
0.00	0.62	0.69	0.69	0.65
0.05	0.55	0.64	0.61	0.56
0.10	0.48	0.55	0.52	0.48
0.15	0.41	0.47	0.48	0.41
0.20	0.35	0.41	0.41	0.34
0.25	0.28	0.35	0.35	0.28
0.30	0.23	0.30	0.28	0.23
0.35	0.18	0.24	0.23	0.19
0.40	0.14	0.19	0.17	0.15
0.45	0.11	0.15	0.14	0.11
0.50	0.07	0.12	0.11	0.08
0.55	0.05	0.09	0.09	0.05
0.60	0.04	0.07	0.06	0.04
0.65	0.03	0.05	0.05	0.03
0.70	0.02	0.04	0.03	0.02
0.75	0.01	0.03	0.02	0.01

TABLE V (continued)

CONCENTRATION-DISTANCE DATA

Distance from Weld (mm)	Concentration (At. % Cu.)			
	C-4	C-7	S-6	S-7
0.80	0.01	0.02	0.01	0.01
0.85	0.01	0.01	0.01	0.00
0.90	0.00	0.01	0.01	0.00
0.95	0.00	0.00	0.00	0.00
1.00	0.00	0.00	0.00	0.00
1.05	0.00	0.00	0.00	0.00
1.10	0.00	0.00	0.00	0.00
1.15	0.00	0.00	0.00	0.00
1.20	0.00	0.00	0.00	0.00

TABLE VI

CONCENTRATION-DISTANCE DATA

Distance from Weld (mm)	Concentration (At.% Cu.)			
	S-18	S-19	S-20	S-21
1.00	1.26	1.28	1.26	1.24
0.95	1.28	1.25	1.26	1.26
0.90	1.27	1.25	1.27	1.26
0.85	1.26	1.27	1.28	1.23
0.80	1.25	1.28	1.27	1.24
0.75	1.25	1.27	1.26	1.26
0.70	1.24	1.25	1.26	1.26
0.65	1.23	1.27	1.26	1.23
0.60	1.19	1.22	1.28	1.20
0.55	1.20	1.20	1.26	1.20
0.50	1.17	1.20	1.22	1.18
0.45	1.13	1.15	1.18	1.15
0.40	1.08	1.11	1.14	1.11
0.35	1.05	1.07	1.10	1.09
0.30	1.02	1.04	1.05	1.04
0.25	0.97	1.00	1.03	0.98
0.20	0.93	0.94	0.97	0.94
0.15	0.85	0.86	0.92	0.87
0.10	0.83	0.81	0.85	0.84
0.05	0.78	0.75	0.78	0.75
0.00	0.66	0.68	0.70	0.68
0.05	0.59	0.62	0.62	0.61
0.10	0.51	0.55	0.54	0.56
0.15	0.44	0.48	0.46	0.47
0.20	0.40	0.40	0.38	0.43
0.25	0.35	0.36	0.31	0.35
0.30	0.29	0.30	0.26	0.30
0.35	0.24	0.25	0.21	0.25
0.40	0.20	0.20	0.17	0.22
0.45	0.15	0.18	0.13	0.17
0.50	0.12	0.12	0.07	0.13
0.55	0.10	0.09	0.05	0.09
0.60	0.07	0.06	0.05	0.08
0.65	0.06	0.05	0.03	0.05
0.70	0.04	0.04	0.02	0.03
0.75	0.04	0.03	0.02	0.04

TABLE VI (continued)

CONCENTRATION-DISTANCE DATA

Distance from Weld (mm)	Concentration (At.% Cu.) S-18	S-19	S-20	S-21
0.80	0.02	0.02	0.01	0.02
0.85	0.02	0.02	0.01	0.02
0.90	0.01	0.01	0.01	0.01
0.95	0.01	0.01	0.00	0.01
1.00	0.01	0.01	0.00	0.01
1.05	0.00	0.00	0.00	0.00
1.10	0.00	0.00	0.00	0.00
1.15	0.00	0.00	0.00	0.00
1.20	0.00	0.00	0.00	0.00

TABLE VII

CONCENTRATION-DISTANCE DATA

Distance from Weld (mm)	Concentration (At.% Cu.)			
	S-24	S-25	S-28	S-29
1.00	1.24	1.29	1.23	1.23
0.95	1.27	1.26	1.26	1.26
0.90	1.28	1.26	1.25	1.27
0.85	1.24	1.25	1.28	1.26
0.80	1.25	1.26	1.26	1.24
0.75	1.26	1.24	1.26	1.26
0.70	1.25	1.25	1.26	1.24
0.65	1.26	1.24	1.25	1.22
0.60	1.24	1.23	1.25	1.22
0.55	1.21	1.20	1.23	1.18
0.50	1.19	1.22	1.21	1.20
0.45	1.19	1.17	1.19	1.15
0.40	1.14	1.14	1.15	1.11
0.35	1.10	1.11	1.11	1.06
0.30	1.05	1.06	1.06	1.04
0.25	1.00	0.99	1.01	1.00
0.20	0.95	0.99	0.94	0.93
0.15	0.90	0.93	0.91	0.86
0.10	0.83	0.88	0.83	0.82
0.05	0.74	0.81	0.77	0.77
0.00	0.68	0.73	0.67	0.68
0.05	0.57	0.65	0.59	0.61
0.10	0.52	0.60	0.52	0.55
0.15	0.45	0.53	0.46	0.47
0.20	0.36	0.45	0.39	0.42
0.25	0.29	0.39	0.32	0.37
0.30	0.24	0.35	0.26	0.30
0.35	0.19	0.27	0.22	0.24
0.40	0.14	0.21	0.16	0.20
0.45	0.11	0.19	0.12	0.15
0.50	0.10	0.15	0.09	0.12
0.55	0.06	0.12	0.06	0.11
0.60	0.05	0.09	0.05	0.07
0.65	0.02	0.08	0.03	0.06
0.70	0.02	0.04	0.02	0.05
0.75	0.02	0.04	0.01	0.03

TABLE VII (continued)

CONCENTRATION-DISTANCE DATA

Distance from Weld (mm)	Concentration (At%. Cu.)			
	S-24	S-25	S-28	S-29
0.80	0.01	0.03	0.01	0.02
0.85	0.00	0.02	0.01	0.02
0.90	0.01	0.02	0.00	0.00
0.95	0.00	0.01	0.00	0.01
1.00	0.00	0.01	0.00	0.01
1.05	0.00	0.01	0.00	0.00
1.10	0.00	0.00	0.00	0.01
1.15	0.00	0.00	0.00	0.00
1.20	0.00	0.00	0.00	0.00

TABLE VIII

CONCENTRATION-DISTANCE DATA

Distance from Weld (mm)	Concentration (At.% Cu.) S-32
1.00	1.25
0.95	1.27
0.90	1.22
0.85	1.25
0.80	1.23
0.75	1.25
0.70	1.24
0.65	1.23
0,60	1.22
0.55	1.20
0.50	1.18
0.45	1.15
0.40	1.13
0.35	1.07
0.30	1.05
0.25	1.00
0.20	0.96
0.15	0.87
0.10	0.83
0.05	0.76
0.00	0.68
0.05	0.61
0.10	0.54
0.15	0.47
0.20	0.41
0.25	0.34
0.30	0.28
0.35	0.23
0.40	0.17
0.45	0.13
0.50	0.12
0.55	0.09
0.60	0.06
0.65	0.04
0.70	0.02
0.75	0.01

TABLE VIII (continued)

CONCENTRATION-DISTANCE DATA

Distance from Weld (mm)	Concentration (At. % Cu.) S-32
0.80	0.01
0.85	0.01
0.90	0.01
0.95	0.00
1.00	0.00
1.05	0.00
1.10	0.00
1.15	0.00
1.20	0.00

DISCUSSION

A. DISCUSSION OF ERRORS

It is difficult to estimate the overall error in the measurement of diffusion because of the large number of operations involved and the extent to which the error involved in each may depend on the skill and judgement of the individual worker. It is possible, however, to list the various sources of error and assess their effect on the measured diffusion parameters. The sources of error may be divided into experimental errors (measurement and control of temperature, analysis, inhomogeneity of base alloys, grain boundary diffusion) and computational errors (fitting of diffusion curves to experimental data and measurement of slopes). In the present work it is the precision of measurement that is of importance, that is, the degree to which errors have been eliminated between the field and no-field determinations, and the errors will be discussed in this regard.

1. Measurement and Control of Temperature

It is clear that the precision of diffusion measurement is very sensitive to errors in the measurement of temperature because temperature appears as an exponential factor in the Arrhenius expression for the diffusion coefficient. For example, at 540°C, an error of two degrees in temperature measurement will produce an error in the diffusion coefficient of five per cent. Chromel-P-Alumel thermocouples

were used for both control and measurement of temperature in the present work. Some of the factors which may lead to erroneous results when using these thermocouples will now be considered.

(a) Inhomogeneities - one of the more important properties of good thermocouple wires is uniformity of composition and physical condition throughout. Errors will arise when a region of chemical or physical inhomogeneity in the thermocouple wire lies in a temperature gradient. The as-received wires contain mechanical inhomogeneities produced by cold work which are removed to a certain extent by short time heating above 400°C. Potts and McElroy[67] found that heating for half an hour at 400°C results in a positive shift of Chromel-P wire with respect to the as-received material by about 120 μV; the Alumel shifts positive with respect to the as-received Alumel by about 20 μV. The net result is a positive drift of the thermocouple by half a degree. No results were given for higher temperatures but it would be safe to assume that a thermocouple made up from the as-received materials and used at a higher temperature would undergo a positive shift of at least 1/2°C. The wires also contain chemical inhomogeneities which will lead to appreciable errors if the inhomogeneous sections are located in temperature gradients. These sources of error may be largely overcome by calibrating the thermocouples installed in the position in which they are to be used. The measuring thermocouples used in

the present study were calibrated in situ against a laboratory standard platinum-platinum-rhodium thermocouple both before and after they were used to measure the temperature of a couple during the diffusion anneal.

(b) Oxidation - no appreciable oxidation of Chromel-P-Alumel thermocouples takes place in an inert or slightly oxidizing atmosphere such as the argon atmosphere used for the diffusion anneals in the present work.

(c) Chromium depletion - Potts and McElroy report that a third effect, the precipitation of chromium carbide and subsequent depletion of the solid solution of chromium, has been stated as the reason for certain observed performances by personnel in the thermocouple industry. The implication was that carbide precipitated during exposure of 2 - 8 hours in the temperature range 425 to 650°C with a 6° to 9°C positive drift of the thermocouple during this period. Drift studies were conducted by Potts and McElroy at temperatures of 300, 390, 550 and 700°C for times in excess of 500 hours and none of these tests showed the above mentioned positive drift. They concluded that carbide precipitation can occur and cause large changes in thermal e.m.f. only if some form of carbon is externally available to the thermocouple. However, if an inert or oxidizing atmosphere is used there is not sufficient carbon present in the as-received Chromel-P thermocouple wire to cause a detectable change in thermal e.m.f.

The argon atmosphere used in the present work was inert or only slightly oxidizing. No source of carbon was externally available to the thermocouples. One would not therefore expect an error to occur due to carbide precipitation in the Chromel-P leg of the thermocouple wires.

Bennett and Rainey[68] have conducted experiments in stagnant helium atmospheres that show a rapid negative drift even without contaminants at 1000°C. The principle mechanism involved is the selective oxidation of chromium in the 800° - 900°C region of the Chromel-P wire. Their results indicate that selective intergranular oxidation of the chromium can occur only in a limited temperature range and within rather critical limits of atmospheric oxidizing potential. The most conducive atmosphere was unpurged, stagnant helium.

There are two reasons why the selective intergranular oxidation of chromium would not be expected to occur in the Chromel-P wires of the thermocouples used in the present work. First, the maximum temperature of the diffusion anneals, 580°C, was considerably below the minimum temperature of 800°C given by Bennett and Rainey for the selective oxidation of chromium. Second, the diffusion furnace was thoroughly purged with flowing argon before it was turned on, during the heating-up period and also for half hour periods at 24 hour intervals during the diffusion anneals. This procedure would probably reduce the oxygen content of the atmosphere used in the present anneals to a much lower value than that of the unpurged helium atmosphere used by Bennett

and Rainey. One would not expect, therefore, that the conditions used in the present work would lead to a large negative e.m.f. deviation in the Chromel-P leg of the measuring thermocouples due to preferential oxidation of chromium.

(d) Loscoe and Mette[69] have reported that a magnetic field has an effect on the e.m.f. of Chromel-P-Alumel thermocouples at ambient temperatures. Their investigation showed that magnetovoltages were produced not in the thermocouple junction but rather in the portions of the thermocouple wires subjected to temperature gradients. Two magnetovoltages were identified, one independent of the direction of the field (called the IDF magnetovoltage) and the other dependent on the direction of the field (the DDF magnetovoltage).

In the IDF effect the magnetized and unmagnetized portions of the wire act as two different materials occupying two different places in the thermoelectric series. The output voltage of this effect does not depend on the temperature gradient in the wire but rather on the temperature difference between the hottest and coldest parts of the wire in the field. For a field of 9,000 gauss and a temperature differential of 100°C between the magnetized and unmagnetized portions of the wire, the effect reaches a maximum of 32 μV at a temperature of 140°C and then falls with increasing temperature to approximately 2μV at 210°C, which is the highest temperature at which the effect was investigated by Loscoe and Mette. The magnetovoltage of 32μV corresponds to a positive

error of nearly 1°C at 140°C.

The DDF effect is caused by temperature gradients along the diameter of the wire. This is the Nernst effect with the magnetovoltage given by:

$$E_y = Q_N B_z \, dT/dx$$

where Q_N = Nernst coefficient, $cm^2 \, sec.^{-1} \, (^{\circ}K)^{-1}$

B = magnetic induction, gauss

dT/dx = the temperature gradient

In minimizing this effect the length of the wire in the field should be kept as small as possible, the wire should be protected from radiant heat by means of insulators and wire used should have a low ratio of Nernst coefficient to heat conductivity.

Loscoe and Mette found that Alumel exhibited a much larger DDF magnetovoltage than did Chromel-P. For a temperature gradient across the Alumel leg of the thermocouple of 10°C/cm., magnetic field of 9,000 gauss and temperature of 300°K they found an error in temperature due to the DDF magnetovoltage of approximately 1/4°C The sign of the effect depends on the direction of the magnetic field and of the temperature gradient.

The experiments were not extended to the 500 to 600°C temperature range which is of interest to the present work. Accordingly, tests were performed in which the magnetic field was repeatedly turned on and off while measuring the temperature of a trial sample (at 540°C). No effect

of the magnetic field on the output of the Chromel-P-Alumel thermocouple was detected. It would appear from the results of Loscoe and Mette that there are two possible reasons for a negative result. First, their results show that the IDF magnetovoltage has fallen to a negligible 2 μV by the time a temperature of 210°C is reached. Second, the thermocouple wires were protected with alumina insulators so that it is unlikely that a temperature gradient of the order of 10°C/cm. could occur across the Alumel wire to produce an appreciable DDF magnetovoltage.

In summary it can be stated that a systematic error in temperature measurement of sufficient magnitude (10°C) to explain the difference between the field and no-field diffusion results is very unlikely to have occurred without detection.

2. Analysis by Microhardness Measurement

Bückle[61] has recently given a comprehensive review of the whole field of microhardness, including a full discussion of sources of error, in which it is repeatedly emphasized that errors in microhardness determinations are best eliminated by the method of comparison. That is the principle which was adopted for this work. To obtain concentration-distance data the microhardness readings obtained at intervals across the diffusion zones were compared with the readings determined in the pure aluminum and alloy sections of the couples. All experimental conditions involved with preparation of the surfaces of the samples, and in making and reading the microhardness indentations,

were kept as constant as possible by following a rigorously systematic procedure. The procedure was considered to be successful since good agreement was always obtained (within the 95 per cent confidence limits calculated from the scatter observed on individual measurements) between the microhardness readings for the base alloy and pure aluminum sections of the couples and the readings that would be expected from the calibration curve. The errors that remained in the measurements were then considered to be random rather than systematic and amenable to treatment by statistical methods.

The standard deviation observed on over one thousand hardness measurements on alloys containing approximately 1.30 atomic per cent copper was 2.64 filar units on the diagonal which is equivalent to 0.42 microns. In terms of concentration, this is equivalent to a standard deviation of 0.05 atomic per cent copper. On samples of pure aluminum the standard deviation of the individual diagonal measurements was somewhat less, amounting to 2.38 filar units or 0.38 microns. This again represents the deviation calculated from the results of over one thousand measurements. For an alloy containing very little copper (0.10 atomic per cent) a standard deviation of 0.38 microns of the diagonal is equivalent to 0.01 atomic per cent copper. Three hardness measurements were taken for each position (at 0.05 mm intervals) across the diffusion zone of a couple. For each position on a diffusion curve the standard deviation of the concentration measurements would then vary

from 0.03 atomic per cent copper at the alloy end to 0.006 atomic per cent copper toward the pure aluminum end of the couple.

To estimate the effect of errors in the individual measurements of concentration on the confidence which could be placed in the difference observed between the field and no-field diffusion curves, couple C-1 and C-2 (nine day field and no-field cylindrical couples respectively) were selected as typical examples and linear regression coefficients were calculated by the method of least squares[66] for the probability plots of the couples over the concentration range where the plots were linear. The points included in the calculation covered over 80 per cent of the concentration range of the couples. Values of the argument of the error function corresponding to function values ($2c/c_o-1$) were tabulated as y data for each value of the position coordinate x. Regression lines ($y = mx + b$) were then calculated for y upon x with the values of the independent variable x considered to have negligible error of measurement. Confidence limits for the difference between the two regression coefficients m_1 and m_2, were then calculated and it was found that even at the 99 per cent confidence level the two coefficients were significantly different. It was concluded that there was a statistically significant difference between the slopes of the probability plots of the field and no-field couples and, since the diffusion curves are directly related to the probability plots, that the difference observed between the two diffusion curves was also statistically significant and could not reasonably be

expected to occur due to random scatter of the individual measurements.

3. Inhomogeneity of Base Alloys

The concentration distribution along the length of undirectionally solidified ingots of dilute aluminum-copper alloys has been studied both theoretically and experimentally.[58] Information obtained from the reports of these studies was used to cast and crop ingots of macroscopically uniform composition. No variation in composition could be detected along the lengths of the cropped sections by chemical analysis or by microhardness traverses.

Kirkaldy, Mason and Slater[16] experienced difficulty in obtaining alloys of uniform composition for studies of diffusion in dilute aluminum-copper alloys. In referring to this difficulty Kirkaldy _et al_ state:

> This points up the necessity for extreme care in selection and preparation of alloys for accurate chemical diffusion studies. It is necessary that the standard materials be selected from the same discs as used in a given couple, and preferably at a position just outside the diffusion zone.

It is also apparent from the diffusion curve which is presented that inhomogeneities were present in the base alloys used by Murphy. The curve exhibits anomolous behavior as it approaches the alloy side of the diffusion zone in that it reaches a maximum concentration and then falls again. It is believed that the present technique of producing alloys of uniform composition represents a significant improvement over previous methods.

4. Bonding

It has been shown that aluminum, in dry air at room temperature, forms an amorphous oxide film 20A° thick in less than one hour.[65] The film forms very rapidly in the first few minutes of exposure reaching a thickness of about 15A° in less than 15 minutes. Thus it is likely that all of the measurements made on interdiffusion in dilute aluminum-copper alloys have incurred some error due to the presence of an oxide layer at the weld interface. In the present work an attempt was made to minimize the oxide layer by clamping the discs in an inert atmosphere as soon as possible after they were faced on the lathe. For the preparation time involved in the present work, which was approximately 5 to 10 minutes, oxide layers of approximately 10 - 15A° would have formed, and their thicknesses should be very nearly the same for all the couples as they were all welded by the same technique. For the field and no-field couples (designated 'pair') bonding differences should be eliminated, since the field and no-field couples were cut from the same weld composite.

The weld in the couples used in the present work were judged sound if they did not reveal any defect after a vigorous chemical polish. It was found that ordinary mechanical polishing and etching methods did not reveal the welds, and this was taken as evidence that the welds were of very good quality.

5. Grain Boundary Diffusion

The effects of grain boundary diffusion would be minimal due to the relatively large grain size and high annealing temperatures used in the present work. The grain size of all the couples was of the order of 2000 μ for the alloy sections and 5000 μ for the pure aluminum. The annealing temperatures used were greater than 0.75 Tm °K where Tm is the melting temperature.

6. Computational Errors

The concentration ratios c/c_o were plotted on probability paper and the best fit lines drawn through the points. The scatter of the data was not large and it is believed that the best fit lines represented the data quite accurately. For example, for couples C_1 and C_2, the best fit lines obtained by the method of least squares did not differ perceptibly from the lines originally drawn through the points by eye. The curves from the probability plots were used to draw the concentration-penetration curves from which the diffusion coefficients were calculated by the Boltzmann-Matano method. In comparing the field and no-field results the Matano areas were used as the principle criterion to avoid errors due to the measurement of slopes.

The effect of the combined errors in the determination of the diffusion coefficients upon the difference observed between the field and no-field results may be estimated by a consideration of the mean values

obtained on couples annealed at 540°C. Confidence limits for the difference between the means for small samples[70] were calculated for the 5 no-field and 4 field couples annealed at 540°C and it was found that even at the 99 per cent confidence level the observed difference was statistically significant.

B. DISCUSSION OF DIFFUSION RESULTS

A comparison between the present no-field results and those of previous workers is shown in Figure 15 which gives the relationship between interdiffusion coefficient and reciprocal temperature. It is apparent that the present results are somewhat higher than those of previous workers. For example, the coefficients obtained for the 540°C no-field anneals vary from 1.65 to 1.80 ($\times 10^{-9}$ cm.^{2} sec.$^{-1}$) with the mean at 1.70($\times 10^{-9}$ cm.^{2} sec.$^{-1}$). This is in contrast to the values reported by other investigators (cf. Table I and Figure 15) which vary from 0.9 to 1.4 ($\times 10^{-9}$ cm.^{2} sec.$^{-1}$) for approximately the same copper concentration as used in the present investigation. The consistently high results obtained for the interdiffusion coefficient in the present case can probably be attributed to efficient bonding. Some evidence for this is presented in Figure 16 where it can be seen that the weld does not exhibit any defects even after a severe chemical polish. An oxide barrier at the couple interface can drastically reduce diffusion rates of alloying components in aluminum. Lundy and Murdoch[17] have shown that diffusion of ^{54}Mn in

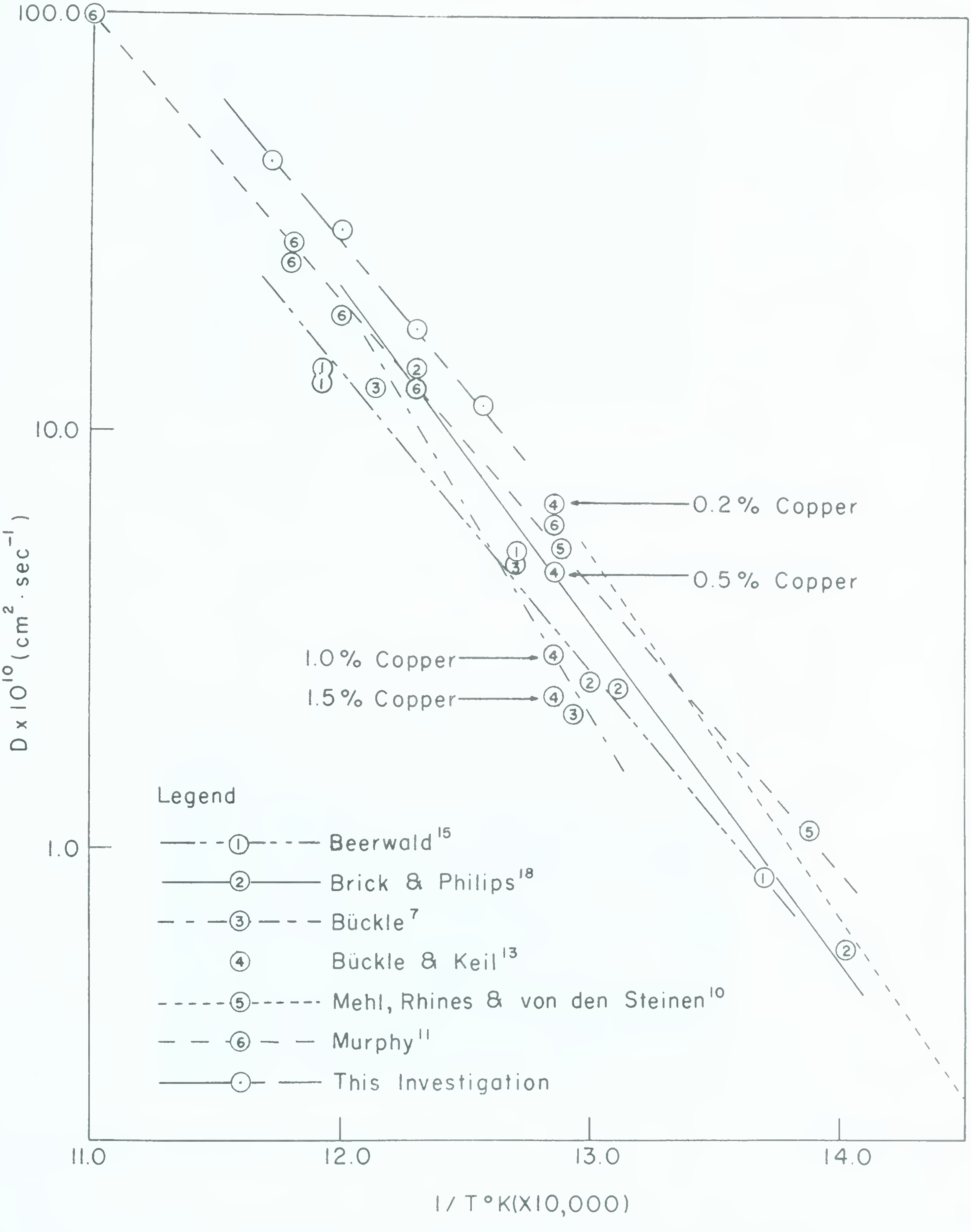

Figure 15 - Comparison of previous data with present no-field results.

Figure 16 - Photomicrograph of a weld in diffusion couple S-6. 3 minute chemical polish. Mfg. 500X.

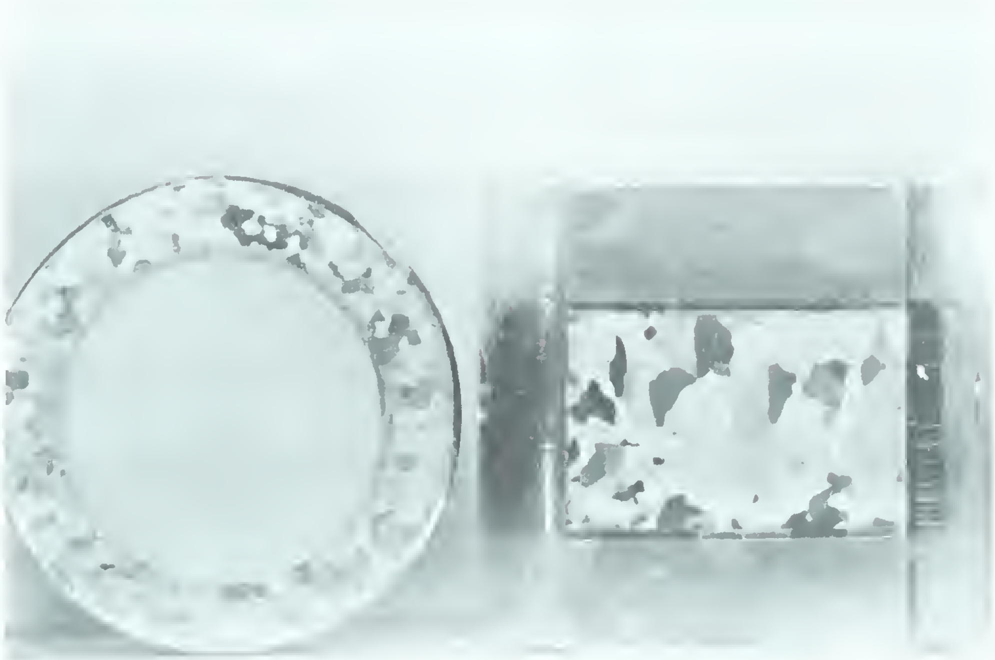

Figure 17 - Photograph of a cylindrical and a sandwich couple.

aluminum is greatly affected by the presence of an Al_2O_3 barrier between the two parts of the diffusion couple, and that this barrier is of little importance in the self diffusion of aluminum. In any case it is the difference in the field and no-field results that is of significance, for it may be assumed that errors inherent in the procedure will be common to both field and no-field couples and will cancel out in the comparison of the diffusivities.

The linear plots of Matano area versus the square root of time (cf. Figure 13) indicates that the diffusion process obeys the classical phenomenological laws of diffusion, and that the field effect is not a function of time (and hence the concentration gradient). The Kirkendall shifts (distance between the weld and the Matano interface) were found to be the same, within experimental error, for the no-field and corresponding field couples. For example, the mean values for the Kirkendall shifts for the 4 day, 540°C anneals, were 0.0045 cm. and 0.0040 cm. for the no-field and field couples respectively. For the 9 day, 540°C anneal, the mean shifts were 0.007 cm. and 0.008 cm. respectively for the no-field and field diffusion couples. Although a Kirkendall shift is observed from the penetration curves for each of the couples, direct measurements to find the shift proved unsuccessful. Two sandwich couples, S-3 and S-4, had three tungsten wires, 0.003 inches in diameter, welded into the interfaces. 'Direct measurements' were made between opposite pairs of wires. It was observed that the wires remained at

the weld interfaces, and this was considered as evidence that the position of the weld interface accurately determines the extent of the Kirkendall shift in each of the couples. Direct measurements of the distances between the weld interfaces gave scattered results, (cf. Table III) with the average shift observed equal to about one-tenth that obtained by the diffusion curve method, which therefore was not considered to be significant. One effect that would contribute to cancelling any shift observed by direct measurement (and at the same time affect the result obtained from the diffusion penetration curves) is the change in lattice parameter with concentration in dilute aluminum copper solid solutions.[80] Copper atoms diffusing toward the aluminum side of a couple produce a contraction of the lattice while at the same time aluminum atoms diffusing into the alloy cause an expansion of the lattice on the other side of the interface. Also, anisotropic grain growth was observed in several couples. This would further tend to mask the Kirkendall shift obtained by direct measurement. The important point here is that the Kirkendall shifts obtained from the diffusion penetration curves (distance from the Matano interface to the weld interface) were consistent, and were equal for both the field and no-field couples. This would support the hypothesis that it is the interdiffusion process that is inhibited by the field and not the intrinsic diffusion rates of either

the copper or aluminum ions. This would be expected if the effect of the field is via the plasma-magnetohydrodynamic forces as proposed in the theory.

The cylindrical couples gave the same calculated diffusivities (within experimental error) as those calculated from the flat or sandwich couples. The original intention for the cylindrical couples was to prevent the build-up of a Hall field in the sample which would have cancelled out the Lorentz force acting on the diffusing ions and electrons. The cylindrical couples were of such diameter as to make negligible any effect of the circular geometry on the value of D obtained.[72] It is obvious from the interdiffusion coefficients from both the flat and cylindrical couples that no Hall field was present in the non-cylindrical couples. This is to be expected considering the effect of specimen size on the Hall field. It has been shown that the Hall field in a specimen will not be affected if the length to width ratio is greater than three (see Putley[73]). In the present investigation the length (diffusion zone $\simeq$1 mm.) to width (specimen diameter $\simeq$25 mm.) ratio is of the order of 10^{-2}, for which it is shown that the Hall field is virtually cancelled out.

The diffusivities obtained for the diffusion couples annealed in a magnetic field of 30,000 oersteds applied perpendicular to the direction of diffusion are 22 to 27 per cent lower than the diffusivities for the corresponding no-field couples. In a statistical analysis of the results

using linear regression theory, linear regression coefficients were calculated by the method of least squares for the linear portions (0 - 1.0 atomic per cent copper) of the probability plots for couples C_1 and C_2. It was found that even for 99 per cent confidence the regression coefficients for the field and corresponding no field probability plots were significantly different.

The Arrhenius plots of the diffusivities (Figure 14) for the field and no-field results give activation energies of 32,000 ± 1,200 and 31,300 ± 1,500 calories/g. atom respectively, where the limits given are standard deviations (again calculated using linear regression theory). The mean values compare well with the activation energies of 31,200 ± 1,500 and 32,600 calories/g. atom reported by Murphy[11] (0.5 wt. per cent copper core) and Beerwald[15] (2 wt. per cent copper core) respectively. The limits quoted by Murphy are the 95 per cent confidence limits. The standard deviations of Q are given for the present work because the limited number of determinations of the interdiffusion coefficients and the relatively short temperature range, mitigates against the relevancy of placing high confidence limits on the values obtained. The frequency factors were found to be $0.50\begin{pmatrix}+0.55\\-0.26\end{pmatrix}$ cm.^{2} sec.$^{-1}$ and $0.45\begin{pmatrix}+0.65\\-0.26\end{pmatrix}$ cm.^{2} sec.$^{-1}$, for the field and no-field results respectively, where the limits given are again standard deviations. Murphy gives for the frequency factor $0.29\begin{pmatrix}+0.43\\-0.17\end{pmatrix}$ cm.^{2} sec.$^{-1}$ where again the limits quoted are for 95 per cent confidence. It is clear from the standard

deviations obtained for the Q and D values that the uncertainty involved in the measurements makes it impossible to decide from the experimental evidence whether the field effect on D is through the activation energy, the frequency factor or through a change in both. Hence it is necessary to rely on theoretical arguments alone to determine whether the field effect is on Q or D_o. In view of the arguments presented in the theory on charge screening, it is suggested that the decreased D occurs through a change in the frequency factor D_o. Further evidence supporting this hypothesis is the absence of any effect of the parallel field on the diffusivity obtained for couple S-19. If the field had affected the screening parameter then the activation energy must also necessarily change.

The magnitude of the field effect on diffusion is calculable provided the effective mass and collision frequency of the transported electron is known. From conductivity data, assuming a semi-classical kinetic model for the electron transport process, the collision frequency of the electron is calculated to be in the range 10^{12} to 10^{14} per second.[74] The collision frequency will in fact be a function of the wave vector of the electron, and it is clear that there will exist a collision frequency spectrum for electrons in a metal. The effective mass of the electron in aluminum (and presumably in aluminum alloys of low concentration), determined from measurements of the de Haas van Alphen effect,[32] is approximately 1/2 the true mass (high frequency, 100 plane). If it is

assumed that at least some of the free electrons in the alloy have collision frequencies of the order of 10^{12} per second, which is a reasonable assertion, then these will effectively control the diffusion rate since they will be the slowest to move in the direction of the gradient. A calculation of the factor $1/(1+\omega_{ce}^2/\nu_e^2)$ gives for 30,000 oersteds, $\nu_e \sim 10^{12}$ per second, and $m^* \sim m$, a 25 per cent decrease in D, which is approximately the observed decrease in D for the field couples. For $m \sim 0.5\ m$ the decrease would be even greater, however for lack of experimental data on the variation of m with crystallographic direction, we assume $m^* \sim m$. The diffusivity obtained for the S-32 couple diffusion annealed in a field of 20,000 oersteds is $1.5(\mathrm{x}\ 10^{-9}\ \mathrm{cm.}^2\ \mathrm{sec.}^{-1})$, which compares well with the calculated D, assuming $m^* \sim m$, and $\nu_e \sim 10^{12}$ per second.

Finally, it is necessary to discuss the results of the present investigation in relation to the "magnetic diffusion effect" observed in ferromagnetic metals and alloys (see "Historical Review"). It is clear that the "magnetic diffusion effect" observed in the ferromagnetic metals and alloys arises from the onset of spin alignment in the partially filled 3d shell of the ion cores. The interaction of the spins with the internal magnetic field (Weiss) is transmitted via the spin-orbit coupling to the crystal lattice, which increases the formation energy of the vacancies. The coupling of the spins to the phonon system (and hence the crystal lattice) is more strikingly manifested in the phenomenon of paramagnetic

resonance (see Rosenberg[75]).

The above situation does not occur in metals having closed inner shells such as aluminum and aluminum-copper alloys. The magnetic properties are determined almost entirely by the diamagnetic contribution of the ion cores, and the paramagnetic and diamagnetic contributions of the free or conduction electrons; hence the spin-phonon interaction is absent or negligibly small and will not influence the diffusivity as in the case of ferromagnetic metals and alloys. Furthermore, it is suggested that the decrease in D_o in the ferromagnetic metals may be attributed in part to the plasma-magnetohydrodynamic effects reported in this work. For the magnetic diffusion inhibition effect observed in dilute aluminum-copper solid solutions, it is proposed that D_o is decreased through a decrease in the atom-vacancy jump frequency or interchange. This decrease in jump frequency due to the magnetic field cannot be associated with an activation energy increase for the jump process or by a change in the entropy factor of diffusion, as is generally done when considering the magnitudes of diffusion constants. The decreased value of D_o arises through the decreased free electron diffusion flux which controls the diffusion rate of the ions, and this mechanism cannot be related to the diffusion parameters in the usual way.

SUMMARY AND CONCLUSIONS

1. A magnetic field of 30,000 oersteds applied perpendicular to the direction of diffusion has the effect of reducing the interdiffusion coefficient in dilute aluminum copper solid solutions by approximately 25 per cent. No effect was found for a magnetic field applied parallel to the direction of diffusion.

2. A theory based on the plasma-magnetohydrodynamic properties of the alloy system was developed to explain the results. It is proposed that the diffusivity is decreased by the factor $1/(1+\omega_{ce}^2/\nu_e^2)$ where ω_{ce} and ν_e are the cyclotron and collision frequencies of the diffusion transported electrons.

3. The experimental data are not sufficiently precise to show whether the effect of the magnetic field on the interdiffusion coefficient is through the activation energy, the frequency factor, or through a change in both.

4. On the basis of theoretical arguments it is concluded that the effect of the field on charge screening is not of sufficient magnitude to have a significant effect on diffusion. This conclusion is supported experimentally by the lack of any effect on the interdiffusion coefficient when the magnetic field is applied parallel to the direction of diffusion. It is therefore proposed that the interdiffusion coefficient is decreased through the frequency factor D_o by the plasma-magnetohydrodynamic forces and not through the activation energy of the jump process by a

change in the screening parameters of the solute and solvent ions.

5. The decrease in the frequency factor D_o associated with the magnetic diffusion effect in ferromagnetic metals and alloys can probably be attributed in part to the plasma-magnetohydrodynamic effects reported in this work.

6. The theory (based on the diffusion inhibition effect of the field) which has been used to explain the effect of a magnetic field on solidification phenomena, is supported.

BIBLIOGRAPHY

BIBLIOGRAPHY

1. Golant, V. E., Soviet Physics USPEKHI, 6 (2), 161-197 (1963).

2. Glicksman, M.G. and Steele, M.C., Phys. Rev. Letters, 2 (11), 461-3(1959).

3. Bowers, R., Legendy, C., and Rose F., Phys. Rev. Letters, 7(9), 339-41 (1961).

4. Colton, D.R., Masters Thesis, Univ. of Alberta (1960).

5. Cahoon, J.R., Masters Thesis, Univ. of Alberta (1963).

6. Dorward, R.C., Masters Thesis, Univ. of Alberta (1964).

7. Bückle, H., Z. Metallkunde, 34, 130-3 (1942).

8. Cournot, J., and Perot, E., Compt. rend., 183, 1289 (1926).

9. Grube, G., and Haefner, R., Z. Elektrochem., 835-42 (1932).

10. Mehl, F., Rhines, F.N., and von den Steinen, K.A., Metals and Alloys, 13, 41-3 (1941).

11. Murphy, J.B., Acta. Met., 563-9 (1961).

12. Burkhardt, A. and Sachs, G., Metallwirtschaft, 14, 1-3 (1935).

13. Bückle, H. and Keil, A., Metaux et Corrosion, 24, 59-64 (1949).

14. Krusensjen, A.V. and Hentschel, F., Metallober flache, 263-6 (1962).

15. Beerwald, A., Z. Elecktrochem, 45, 789-95 (1939).

16. Kirkaldy, J.S., Mason, G.R. and Slater, W.J., C.I.M. Bulletin 54, 59-67 (1961).

17. Lundy, T.S. and Murdoch, J.F., J. Appl. Phys., 33, 1671-3 (1962).

18. Brick, R.M. and Phillips, A., A.I.M.E. Trans., 124, 331-47 (1937).

19. Bailey, G.L.J. in "Physical Examination of Metals" (2nd edition, E. Arnold Ltd., London, 1960) p. 484.

20. Wells, C., in "Atom Movements" (American Society for Metals, Cleveland, 1960) p. 28.

21. Borg, R. J. and Birchenall, C. E., A. I. M. E. Trans., 218, 980-4 (1960).

22. Birchenall, C. E., Metals Rev., 3, 235 (1958).

23. Stanley, J. and Wert, C., J. Appl. Phys., 32, 267-73 (1961).

24. Zener, C., in "Imperfections in Nearly Perfect Crystals" (J. Wiley, New York, 1952) p. 289.

25. Alers, G. A., Neighbours, J. R. and Sato, H., Phys. and Chem. Solids, 13, 40 (1960).

26. Buffington, F. S., Hirano, K. and Cohen, M., Acta. Met. 9, 434-9 (1961).

27. Hirano, K., Cohen, M. and Averbach, B. L., Acta Met. 9, 440-5 (1961).

28. Hirano, K., Agarwala, R. P., Averbach, B. F. and Cohen, M., J. Appl. Phys., 33, 3049-54 (1962)

29. Borg, R. S., J. Appl. Phys., 34, 1562-3 (1963).

30. Metcalfe, A. G., Acta. Met., 1, 609-10 (1953).

31. Hendricks, S. B., Jefferson, M. E., and Schultz, J. E., Z. Krist., 73, 376 (1930).

32. Fiks, V. B., Soviet Physics - Solid State, 1, 14-28 (1959).

33. Miller, Yu. G., Soviet Physics,- Solid State, 3, (8), 1728-32 (1962).

34. Miller, Yu. G. and Gurov, K. P., Soviet Physics - Solid State, 3 (3), 2096-7 (1962).

35. Angus, J., Verhoeven, J. and Hucke, E. E., "Physical Chemisty of Process Metallurgy", Part I (Interscience Pub. Inc., New York, 1961) p. 429.

37. Fiks, V. B., Soviet Physics - Solid State, 3 (3), 2094-5 (1962).

38. Knof, H., Z. Naturforschg., 15 (a), 745-6 (1960).

39. Cowling, T.G., "Magnetohydrodynamics" (Interscience Pub. Inc., New York, 1957) p.3.

40. Spitzer, L., "Physics of Fully Ionized Gases" (Interscience Pub. Inc., New York, 1956) p. 94.

41. Mangelsdorf, P.C., "Physical Chemistry of Process Metallurgy", Part I (Interscience Pub. Inc., New York, 1961) p. 429.

42. Longmire, C.L., and Rosenbluth, M.N., Phys. Rev., 103, 507 (1956).

43. Ziman, J.M., Electrons and Phonons (Oxford University Press, 1962) p. 494.

44. Kapitza, P., Proc. Roy. Soc., A, 123, 292 (1929).

45. Alfred, L.C.R., and March, N.H., Phil. Mag., 2, 985 (1957).

46. Le Claire, A.D., Phil. Mag., 7, 141 (1962).

47. Bohm, D. and Pines, D., Phys. Rev., 82, 625 (1951).

48. ibid, 85, 338 (1952).

49. ibid, 92, 609 (1953).

50. Pines, D., Phys. Rev., 92, 626 (1953).

51. Landau, L.D., Soviet Phys. JETP, 16, 574 (1946).

52. Bonch-Bruevich, V.L. and Mironov, A.G., Soviet Physics - Solid State, 2, 454 (1960).

53. Seitz, F., "Modern Theory of Solids" (McGraw Hill, 1940) p.585.

54. Stephen, M.J., Phys. Rev., 129, 997 (1963).

55. Gross, E.P., Phys. Rev., 82, 232 (1951).

56. Saltpeter, E.E., Phys. Rev., 122, 1663 (1961).

57. Zyranov, P.S., Soviet Phys. JETP, 13, 751 (1961).

58. Kirkaldy, J. S. and Youdelis, W. V., A. I. M. E. Trans., 833, (1958).

59. W. W. Scott, "Standard Methods of Chemical Analysis", Vol. 1 (D. Van Nostrand Inc., New York, 1939) p. 40, 368.

60. "Microhardness, Its Theory and Practice with the Reichert Microhardness Tester", (an instruction manual issued by C. Reichert Optische Werke, Wien, Austria. 43 ref.) p. 9.

61. H. Bückle, Met. Rev., 4, 49-100 (1959).

62. Jost, W., "Diffusion in Solids, Liquids, Gases" (Academic Press Inc., New York, 1952), p. 32.

63. Shewmon, P. G., "Diffusion in Solids" (McGraw Hill, New York, 1963), p. 32.

65. Cabrera, N. and Mott, N. F., Rep. Progr. Phys. 12, 163-84 (1948-1949).

66. Davies, E. O. "Statistical Methods in Research and Production" (Oliver and Boyd, London, 1957) p. 157.

67. Potts, J. F. and McElroy, D. L. in "Temperature, Its Measurement and Control in Science and Industry" Volume Three, Part II (New York, Reinhold Publishing Co. 1962) p. 253.

68. ibid, Bennett, R. L. and Rainey, W. T., p. 289.

69. ibid, Loscoe, C. and Mette, H., p. 283.

70. Kenney, J. F. and Keeping, E. S., "Mathematics of Statistics, Part I (D. Van Nostrand Co. Inc., New York, 1960) p. 184.

71. da Silva, L. C. C. and Mehl, R. F., A. I. M. E. Trans., 191, 155-73 (1951).

72. Rhines, F. N. and Mehl, R. F., A. I. M. E. Trans, 128, 185 (1938).

73. Putley, E. H., "The Hall Effect and Related Phenomena" (Butterworths, London, 1960), p. 45.

74. Kittel, C., "Introduction to Solid State Physics" (John Wiley and Sons, Inc., 2nd ed., 1956) p. 239.

75. Rosenberg, H. M., "Low Temperature Solid State Physics" (Clarendon Press, Oxford, 1963) p. 285.

76. Snellman, O. and Burge, E. J., J. Sci. Instr., 26, 331-5 (1949).

77. Bitter, F. and Read, F. E., Rev. Sci. Instr., 22 (3), 171-3 (1951).

78. Bowen, L. O., J. Sci. Instr., 34, 265-8 (1957).

79. Hyung Sup Choi, Personal communication.

80. Pearson, W. B. "Handbook of Lattice Spacings and Structure of Metal and Alloys" (Pergammon Press, New York, 1958) p. 327, 353.

APPENDICES

APPENDIX A

Introduction

The major factors required in the performance of laboratory electromagnets, namely, high field intensity and good field homogeneity over accessible working volumes, have been achieved with moderate power consumption in iron-clad magnets.[77, 78] The high power efficiencies available from this type of design together with modest copper and iron requirements gives it some advantage over other types of laboratory electromagnets.

Construction

A photograph of the magnet is given in Figure 17. The magnetic circuit is formed from two low carbon steel castings with central cores on which pole pieces of high permeability alloy may be mounted (c.f. Figure 18). The pole-pieces and cores conform to the optimum angles of 120° and 90°, respectively, specified by Dreyfus[76] to obtain the maximum air gap intensity. The working area may be reached by means of four diametrically opposite holes, each having a width of 3 inches and length of 5 inches. The yokes are mounted on sleeves which slide on pipe rails so that the magnet may be opened for installation of apparatus in the working area.

The coils are made of 0.140 inch copper strap, 1 inch wide, which is uniformly wound (10 turns to the inch) with 0.010 inch diameter nylon

monofilament. The nylon wound strap is formed into pancake coils which are bound with resin-impregnated glass tape. Three pancake coils, connected in series, provide a total of approximately 80 turns in each half of the magnet.

The magnet is cooled by pumping demineralized water directly through the coils. Aluminum retaining plates, which bolt to flanges on the inner and outer periphery of the winding spaces, form these spaces into water tight compartments. (All surfaces in contact with water were well coated with epoxy resin). The inlet and outlet holes, which were drilled through the yokes, are well distributed to provide a uniform flow of cooling water through the coils. After passing through the magnet the demineralized water is led to a heat exchanger where it is cooled by a flow of tap water. The cooling water is pumped through the magnet at a pressure of 40 pounds per square inch and at a rate of 15 gallons per minute. With a power input of 30 kilowatts the temperature differential between the tap water entering the heat exchanger and the demineralized water leaving the magnet is 25°C. This may be compared to a temperature rise of 70°C through the coils of the Bitter magnet,[77] which is of comparable size, at a power input of 20 kilowatts.

Accessory Equipment

Power is supplied to the magnet from the Hobart MCV-900-S constant voltage direct current generator. The generator is capable of

continuous operation at 900 amperes and 40 volts. The ripple in the output from the generator at full load is 2 per cent.

The magnet is fitted with various safety devices, controls, and instruments designed for convenience in operation. Relays activated when the tap water pressure or demineralized water pressure fall below safe minimums are provided. Safety switches are also provided to prevent the inadvertent application of power to the magnet coils when the two halves are separated. Speed and convenience in opening and closing the magnet are accomplished by the use of an air cylinder. In addition, all of the controls are mounted for convenience on a movable control panel.

Performance

The field produced by the magnet with 4 inch conical pole pieces separated by a 1.5 inch air gap is shown as a function of the current input in Figure 19. The field was measured with a fluxmeter and flip coil. The performance of the magnet compares favorably with other magnets of similar size and construction. It has the advantage that efficient cooling permits operation at higher power levels, and hence at higher field strengths.

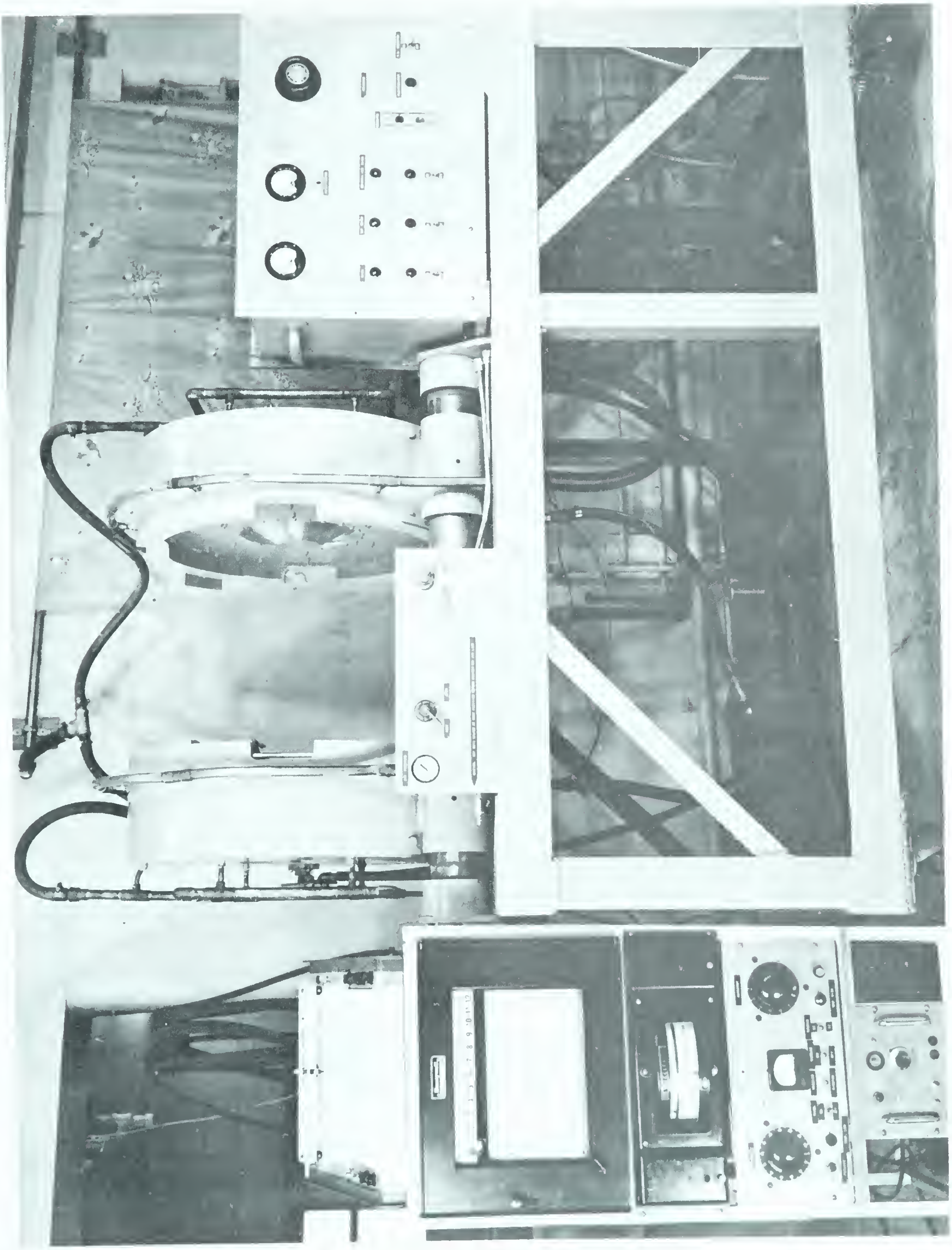

Figure 18 - Photograph of the electromagnet.

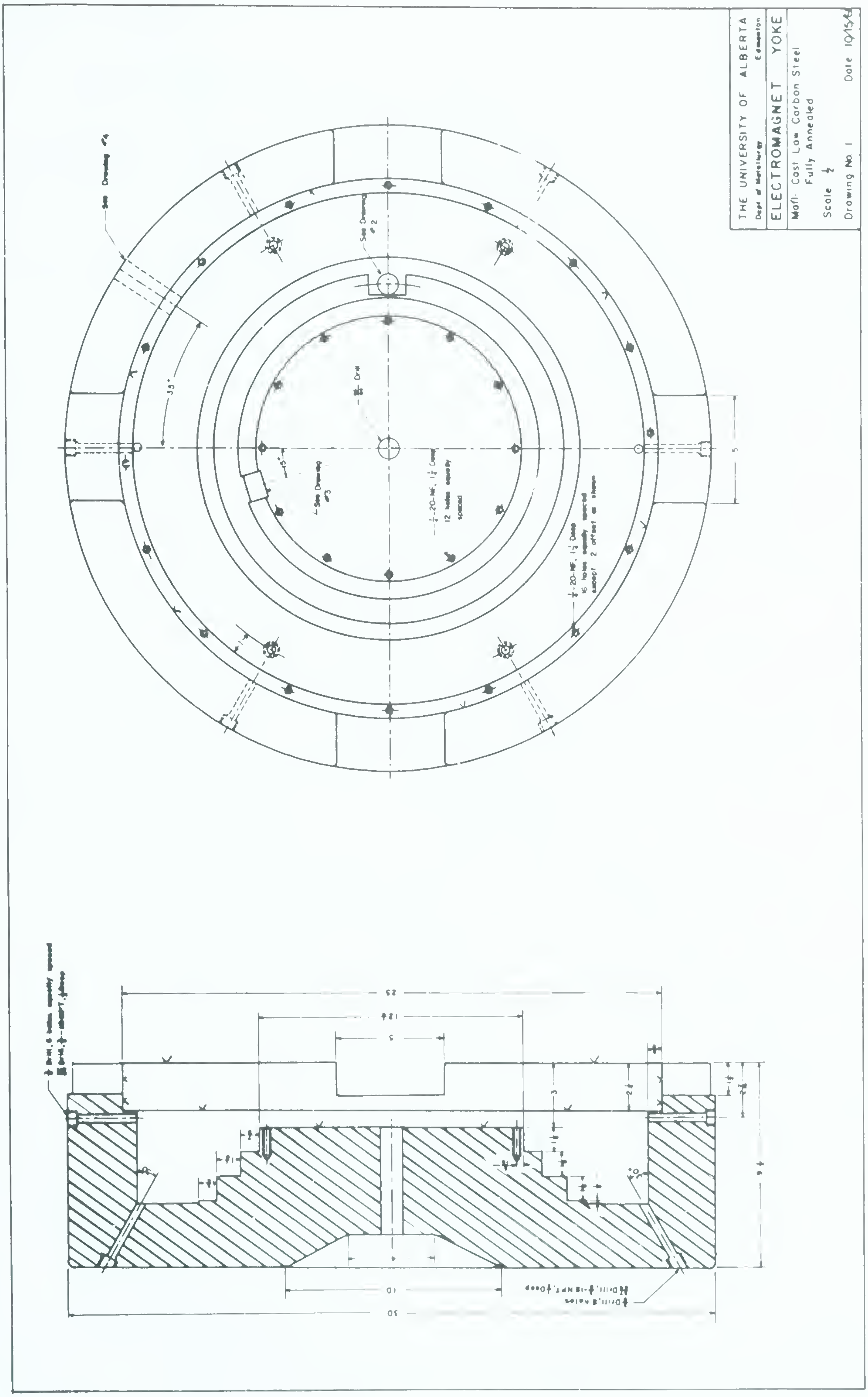

Figure 19 - Diagram of the electromagnet yoke.

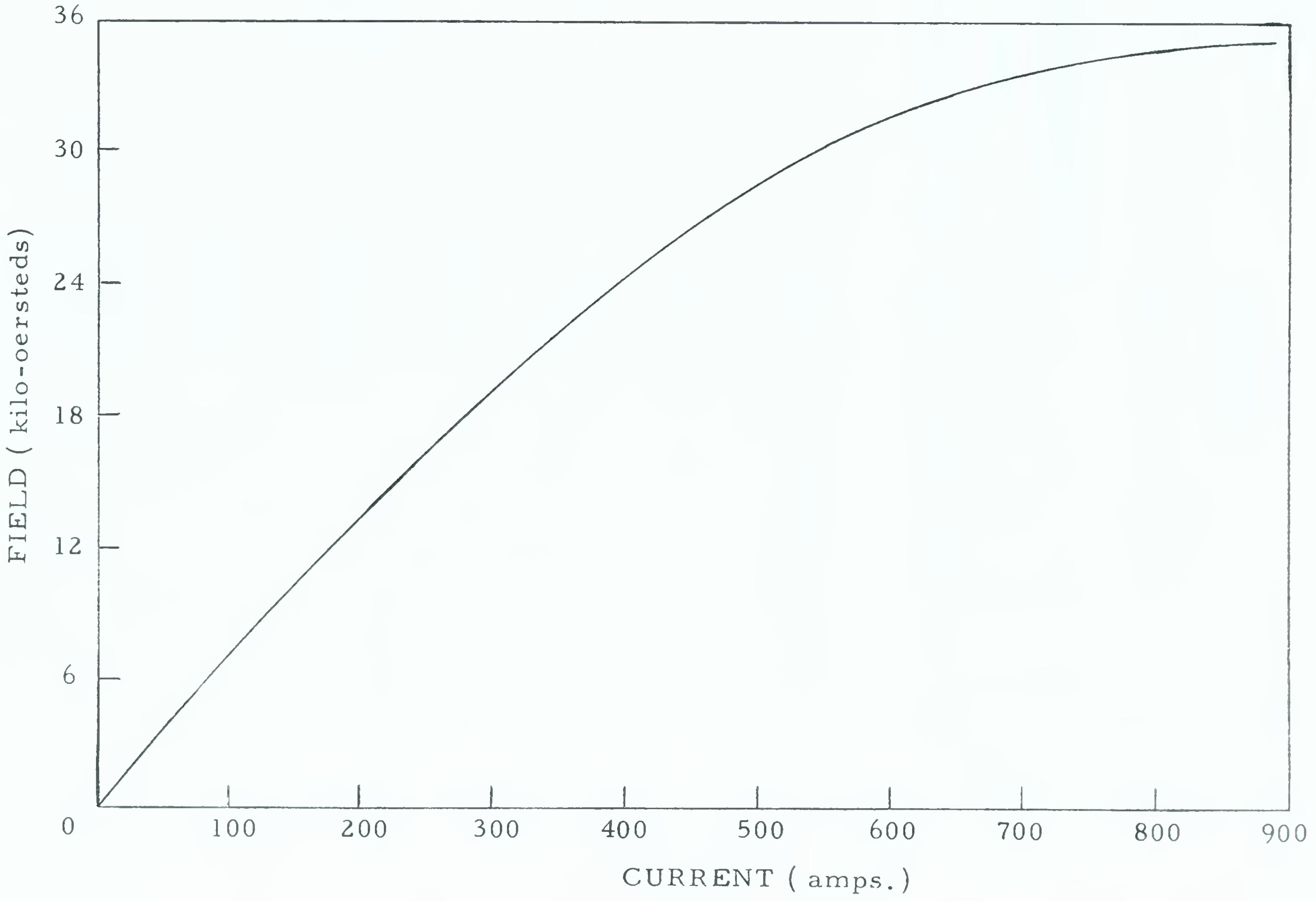

Figure 20. Field produced by the electromagnet.

APPENDIX B

ANALYSIS OF MATERIALS

SUPER-PURITY ALUMINUM

The following analysis was obtained on a sample of the super-purity aluminum by Chicago Spectro Service Laboratory, Inc.

Sample	Estimate of Quantity Present
Silicon	0.005 %
Copper	0.0025 %
Magnesium	0.004 %
Iron	0.005 %
Titanium	<0.002 %
Zinc	< 0.01 %
Manganese	<0.002 %
Lead	<0.01 %
Tin	<0.01 %
Nickel	<0.001 %
Chromium	<0.001 %
Hydrogen	Not detected
Oxygen	0.005 %
Nitrogen	Not detected <0.002 %

HIGH-PURITY COPPER

The following spectrographic analysis was furnished for the copper rods by the supplier, Johnson, Matthey & Co., Ltd.

Element	Estimate of Quantity Present parts per million
Iron	2
Silicon	1
Silver	1
Magnesium	less than 1

The following elements were specifically sought but not detected, i.e. either they are not present or they were below the limits of detection:

Al, As, Au, B, Ba, Be, Bi, Ca, Cd, Ce, Cr, Cs, Ga, Ge, Hf, Hg, In, Ir, K, Li, Mn, Mo, Na, Nb, O, P, Pb, Pd, Pt, Rb, Re, Rh, Sb, Se, Sn, S, Ta, Te, Ti, Tl, V, W, Zn, Zr.

B29819